STRUCTURAL DETERMINANTS OF $GABA_A$ RECEPTOR BIOGENESIS

By

Wen-yi Lo

Dissertation

Submitted to the Faculty of the

Graduate School of Vanderbilt University

in partial fulfillment of the requirements

for the degree of

DOCTOR OF PHILOSOPHY

in

Neuroscience

December, 2008

Nashville, Tennessee

Approved:

Professor Danny G. Winder

Professor Robert L. Macdonald

Professor Roger J. Colbran

Professor Jerod Scott Denton

This work is dedicated to my parents, whose love and wisdom encouraged and guided me through tough times.

ACKNOWLEDGMENTS

This dissertation would not have been possible without help from mentors and educators. I am indebted to my advisor, Dr. Robert Macdonald, for his financial support and academic guidance. Furthermore, I sincerely thank my dissertation committee, Drs. Danny Winder, Roger Colbran, and Jerod Denton, for their advice. I am also grateful to the support provided by the neuroscience graduate program at Vanderbilt University. Particularly, the continuous concerns and suggestions from Drs. Lou DeFelice, Elaine Sanders-Bush and Mary Early-Zald have been kept me on track during my graduate studies. I would also like to express my appreciation to the generous hearts of Drs. Michael Cooper, Andrew Link and Martin Gallagher. They have allowed me free access to their lab equipment, which has been helpful for my experiments.

I am thankful to those whom I have had the pleasure to work with. Learning flow cytometry analysis from Emmanuel Botzolakis and Dr. Aleksandar Stanic, analytical centrifugation from Adam Farley, electrophysiological recording from Drs. David Hinkle and Matt Bianchi, and confocal microscopy from Drs. Shawn Goodwin and Anne Kenworthy were wonderful experiences. I would also like to extend my thanks to Katharine Gurba, Drs. Dorothy Jones-Davis and Emily Schwartz, and various people working in the Neurology department, the Neuroscience graduate program and the Vanderbilt University for enriching my culture-learning adventure. Mostly, I am grateful to Emmanuel Botzolakis, Katharine Gurba and Adam Farley for spending their time improving my writing skills.

TABLE OF CONTENTS

LIST OF TABLES

LIST OF FIGURES

LIST OF ABBREVIATIONS

5-HT_3 receptor	5- hydroxytryptamine (serotonin) type 3 receptor
7-AAD	7-amino-actinomycine D
ACh	acetylcholine
AChBP	acetylcholine binding protein
AP2	adaptor protein 2
BIG2	brefeldin A-inhibited GDP/GTP exchange factor 2
BiP	immunoglobulin heavy-chain binding protein
cDNA	complementary DNA
CMS	congenital myasthenic syndrome
COP	coat protein complex
C-terminal	carboxy-terminal; carboxyl-terminal; COOH-terminal
endo H	endoglycosidase H
ER	endoplasmic reticulum
ERAD	endoplasmic reticulum associated degradation
FI	fluorescence index
GABA	γ-aminobutyric acid
$GABA_A$ receptor	GABA type A receptor
$GABA_C$ receptor	GABA type C receptor
GABARAP	$GABA_A$ receptor associated protein
GODZ	Golgi-specific DHHC zinc finger protein
GRIF-1	$GABA_A$ receptor interacting factor-1

HEK cells	human embryonic kidney cells
IGE	idiopathic generalized epilepsy
IDV	integrated density volume
LGIC	ligand-gated ion channel
M1, 2, 3 and 4	transmembrane domain 1, 2, 3 and 4
M3-M4 loop	cytoplasmic loop linking the transmembrane domain 3 and 4
MAP	microtubule-associated protein
mRAN	messenger ribonucleic acid
nACh receptor	nicotinic acetylcholine receptor
N-linked	asparagines-linked
N-terminal	amine-terminal; amino-terminal; NH_2-terminal
PBS	phosphate buffered saline
PCR	polymerase chain reaction
PDI	protein disulfide isomerase
Plic-1	protein linking IAP to the cytoskeleton
PNGaseF	peptide N-glycosidase-F
PVDF membrane	polyvinylidene fluoride membrane
RIPA buffer	radio-immuno-precipitation assay buffer
SDS-PAGE	sodium dodecyl sulfate-polyacrylamide gel electrophoresis
UPS	ubiquitin-proteasome system
UGGT	UDP-glucose: glycoprotein glucosyltransferase

CHAPTER I

BIOGENESIS AND HETEROGENEITY OF CYS-LOOP RECEPTORS

Introduction

The human brain is a complex network of approximate 10^{11} neurons, each forming about 1,000 synapses (Greengard, 2001). The resulting communication between neurons gives rise to consciousness and controls voluntary behavior. More than 99% of synapses relay signals using chemical neurotransmitters, which include amino acids (γ-aminobutyric acid, glutamate and glycine), monoamines (acetylcholine, 5-hydroxytryptamine, dopamine, epinephrine, norepinephrine, melatonin and histamine), and neuropeptides (vasopressin, somatostatin and etc.) (Iversen, 1984;Greengard, 2001). The release of neurotransmitters from presynaptic vesicles into the synaptic cleft is induced by an action potential, which propagates down the axon to the nerve terminal. Neurotransmitter receptors on the cell surface of the postsynaptic neuron then convert the chemical signals into electrical and/or secondary chemical signals.

Depending on how fast the receptors in postsynaptic neurons transduce signals, communication across synapses is classified as either fast or slow neurotransmission. Fast neurotransmission is mediated mainly by ligand-gated ion channels (LGICs). Once activated by neurotransmitters, LGICs go through a series of conformational changes that lead to their opening and initiation of action potential propagation within one millisecond. Half of the receptors mediating fast neurotransmission are excitatory and mainly activated by glutatmate; the other half of receptors in fast synapses are inhibitory and are

responsive to γ-aminobutyric acid (GABA) (Greengard, 2001). In contrast, slow neurotransmission takes hundreds of milliseconds to minutes to achieve its effects, because it is primarily mediated by guanine nucleotide binding protein (G protein)-coupled receptors (GPCRs), which accomplish signal transmission by activating coupled G-proteins and then downstream effectors. It is worth noting that some neurotransmitters such as GABA, acetylcholine (ACh) and 5-hydroxytryptamine (5-HT) activate both LGICs and GPCRs. For instance, GABA can activate GABA type A and C ($GABA_A$ and $GABA_C$) LGICs as well as GABA type B ($GABA_B$) GPCRs.

Cys-loop superfamily receptors, which include $GABA_A$ and $GABA_C$, glycine, nicotinic ACh (nACh) and 5-HT type 3 ($5\text{-}HT_3$) receptors, are members of LGICs (Macdonald and Olsen, 1994;Lynch, 2004;Kalamida et al., 2007;Reeves and Lummis, 2002). Thus, functional surface expression of Cys-loop receptors regulates neuronal excitability and shapes neuronal plasticity (Biggio et al., 2001). Expression of Cys-loop receptors with diverse electrophysiological and pharmacological properties, and with distinct temporal and spatial distributions is primarily regulated by receptor biogenesis. Indeed, mutations in Cys-loop receptors, which affect receptor biogenesis and thus alter receptor surface density, have been associated with idiopathic generalized epilepsies (IGEs) (Macdonald et al., 2006;Frugier et al., 2007;Gallagher et al., 2005;Harkin et al., 2002;Kang and Macdonald, 2004), startle syndromes (Bakker et al., 2006), congenital myasthenic syndromes (CMSs) (Shen et al., 2005), and psychiatric disorders (Niesler et al., 2001a). To develop effective treatment strategies, the biogenesis of Cys-loop receptors was investigated in the present studies. In particular, the studies focused on structural determinants of $GABA_A$ receptor biogenesis.

Archetypal Cys-loop receptor structure and biogenesis

Cys-loop receptor topology has been deduced by studying the muscle-type nACh receptor and the ACh binding protein (AChBP)

Taking advantage of the enrichment of muscle-type nACh receptors in the post-synaptic membrane preparation from the marine ray (*Torpedo marmorata*) electric organ (which is anatomically similar to skeletal muscle), the receptor structure and subunit topology have been determined at a 4 Å resolution using cryoelectron microscopy (Unwin, 2005) (Figure 1A). The *Torpedo* nACh receptor is composed of five homologous subunits that are arranged pseudo-symmetrically around a central axis in an order of β-α-γ-α-δ, counterclockwise as viewed from the synaptic cleft. The tertiary structure of each subunit consists of an extracellular N-terminal domain that contains binding sites for ligands and drugs (Blount and Merlie, 1988) (Figure 1B). This domain also has the signature Cys-loop, an absolutely conserved 15 amino acid-long region with the two terminal residues forming a disulfide bond (Ortells and Lunt, 1995). Consistent with previous predictions, which were based on hydrophobicity analysis (Noda et al., 1982), four transmembrane domains (named M1, M2, M3 and M4) were resolved with the M2 domain lining the ion channel (Figure 1E). The cytoplasmic loop linking the M3 and M4 domains, which is named the M3-M4 loop here after, is the longest of the three loops connecting the four transmembrane domains and is the major site for cellular regulation (Figure 1B). Based on the similarity of their primary sequences and secondary structures (such as the conserved Cys loop and the predicted 4 transmembrane domains), all Cys-loop receptor subunits are believed to share a similar topology.

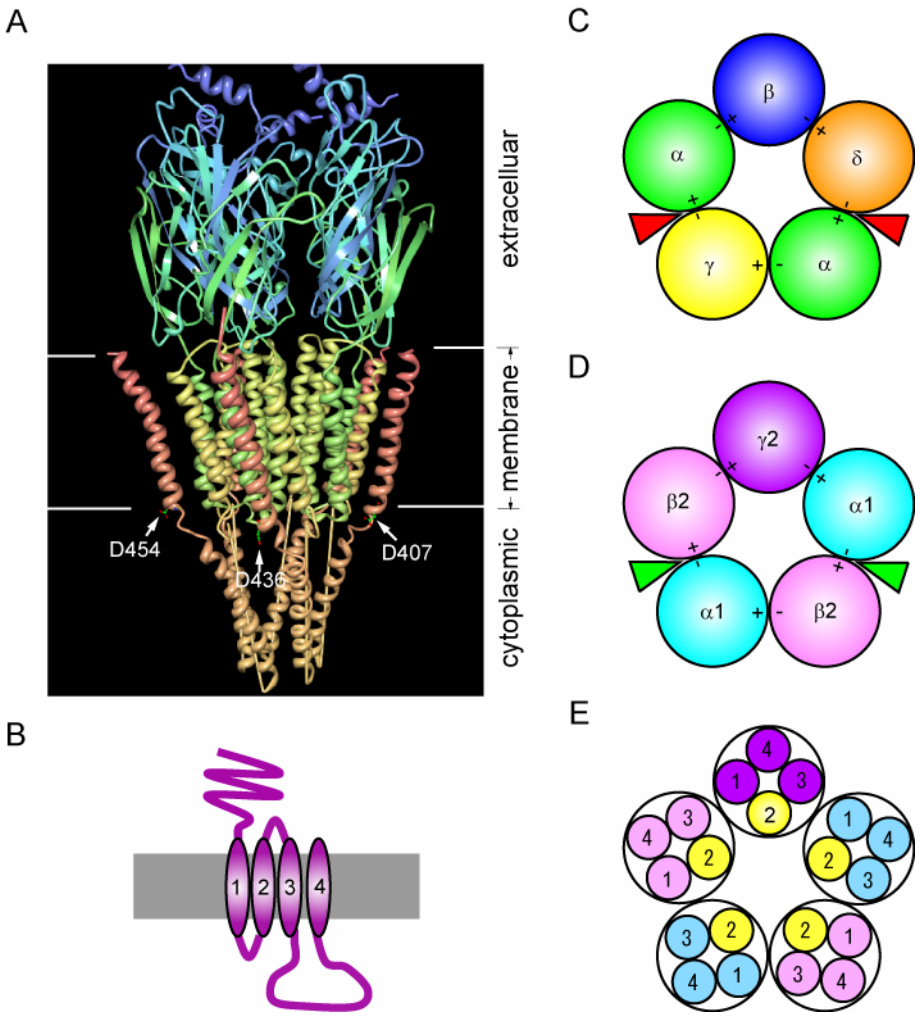

Figure 1. Structures of Cys-loop receptors

A, The three-dimensional structure of a *Torpedo* muscle-type nACh receptor was adopted from the RCSB protein data bank (http://www.pdb.org/pdb/explore.do?structureId=2BG9) (lateral view). The conserved aspartate residues (D407, D436, and D454 in α, β, and δ subunits, respectively) are labeled in white. Note that large portions of the major cytoplasmic loops were omitted here. **B**, A schematic presentation of a Cys-loop receptor subunit is presented (lateral view). **C** and **D**, Schematic presentations of the N-terminal domain arrangements of the *Torpedo* nACh receptor and an inferred $GABA_A$ receptor, respectively, are presented (top view from synaptic cleft). The triangles represent the ligands binding to the interfaces of subunits. **E**, A schematic presentation of the arrangement of transmembrane domains of the $GABA_A$ receptor is shown (top view after removing the N-terminal domains).

The crystal structure of the soluble AChBP from the *Lymnaea stagnalis*, the fresh water snail, has been resolved at 2.7 Å (Brejc et al., 2001). The AChBP homo-pentamer resembles the extracellular portions of homomeric α7 and α9 nACh receptors, and advances our understanding of Cys-loop receptor functions in ligand binding and interactions between subunit N-terminal domains. Based on the homology to the AChBP, the interacting surface of the N-terminal domain of a $GABA_A$ receptor subunit is divided into plus (+) and minus (-) sides. Portions of the loops (named L1, 2, 4, 5, 7, 8 and 10), which link α-helixes and/or β-sheets, constitute the (+) side, while portions of α-helix 1, β-sheet 1, 2, 3, 5, 6, and L9 constitute the (-) side (Brejc et al., 2001). The GABA binding pocket is located at the α-β subunit interface, which is constituted by portions of the β subunit (+) side and the α subunit (-) side (Akabas, 2004) (Figure 1D).

Cys-loop receptor biogenesis has been deduced from study of the muscle-type nACh receptor

It is also believed that the essential biogenic steps of all Cys-loop receptors are similar since Cys-loop receptor subunits are similar, and all receptors are assembled from multiple homologous subunits (Keller and Taylor, 1999). Given that the muscle-type nACh receptor is by far the best characterized Cys-loop receptor, it is considered the prototype for biogenesis of other Cys-loop receptors.

Nascent polypeptides of transmembrane proteins have been demonstrated to be translated simultaneously by endoplasmic reticulum (ER)-associated ribosomes and inserted through translocons into the membrane of the ER (Alder and Johnson, 2004;White and von Heijne, 2005). Nascent nACh receptor subunit polypeptides have been shown to undergo several co- and post-translational modifications including

cleavage of signal peptides, glycosylation and formation of the signature disulfide bond in the Cys-loop (Blount and Merlie, 1990). Subunit folding is facilitated by glycosylation of certain asparagine residues in a consensus sequence in the subunit N-terminal domain (Blount and Merlie, 1990) and by association with ER-resident chaperones such as immunoglobulin heavy-chain binding protein (BiP) (Paulson et al., 1991), calreticulin, and calnexin (Gelman et al., 1995). The assembly of pentamers leads to dissociation of ER-associated chaperones (Wanamaker et al., 2003;Wanamaker and Green, 2007) (Figure 2). Consequently, only fully assembled pentamers are allowed to be trafficked to the cell surface.

Two ER-associated protein machineries act complimentarily to perform ER quality control. First, coat protein complex II (COPII) specifically sorts only fully assembled pentameric receptors into forward trafficking vesicles (Aridor and Traub, 2002). Second, COPI retrieves incompletely assembled intermediates with exposed ER retention signals (Keller et al., 2001;Wang et al., 2002). Assembled intermediates and misfolded proteins that are retained or retrieved then go through refolding, oligomerization, and assembly cycles (Wanamaker and Green, 2007). Subunits that undergo several cycles in the ER but fail to incorporate into a fully assembled pentamer are than transferred to the cytoplasm via translocons for ER associated degradation (ERAD), which is executed by the ubiquitin-proteasome system (UPS) (Christianson and Green, 2004;Wanamaker and Green, 2007) (Figure 2).

Fully assembled Cys-loop receptors, which are released from the ER, pass the Golgi compartment and finally reach the cell surface. Receptors then either

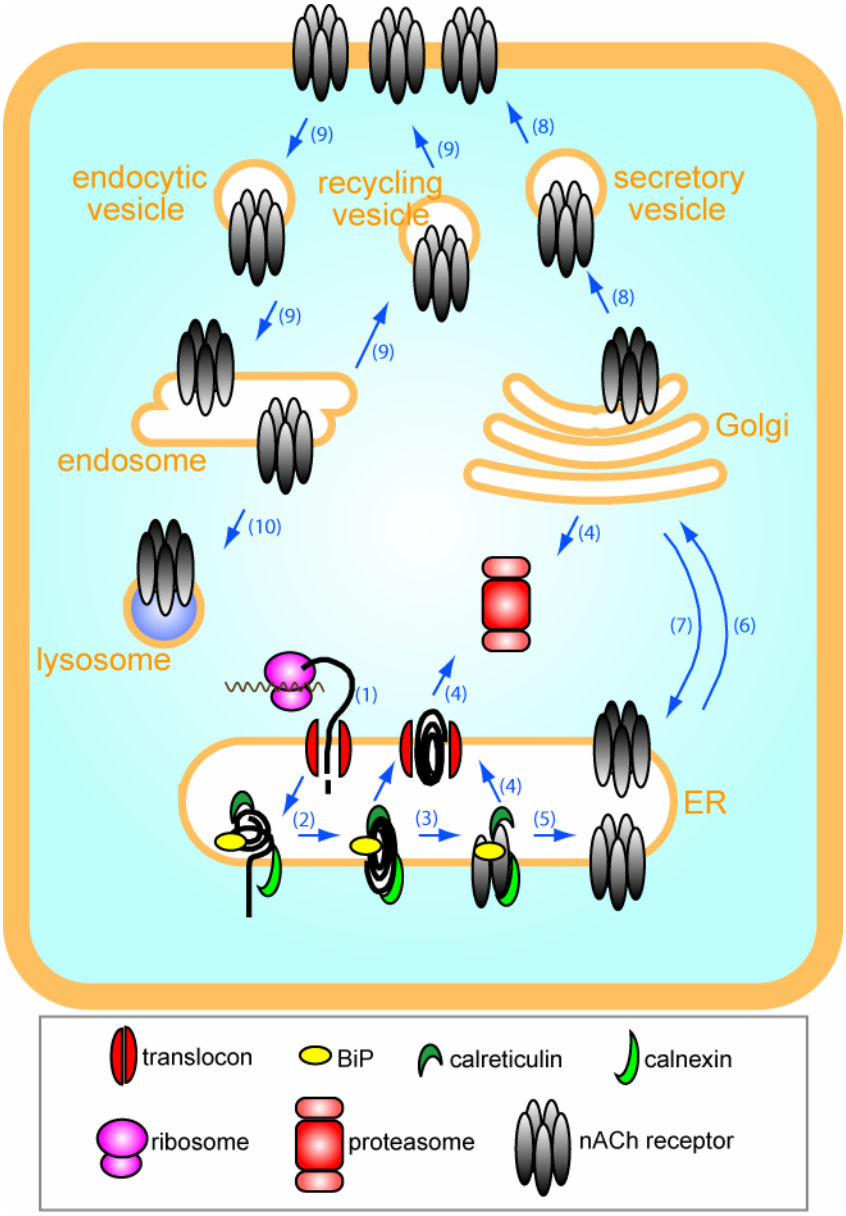

Figure 2. Biogenesis of the muscle-type nACh receptor

The identities of some interacting proteins and protein complexes are shown in the box. The biogenesis processes includes (1) insertion of a nascent-receptor-subunit polypeptide via the translocon to the ER, (2) folding of a polypeptide with the help of chaperones, (3) oligomerization of subunits, (4) degradation of a subunit polypeptide by the proteasomal system, (5) assembly of a receptor pentamer, (6) releasing of a receptor from the ER, (7) retrieval of a receptor from the Golgi apparatus, (8) forward trafficking from Golgi apparatus to the cell surface, (9) recycling of receptors, and (10) degradation of a receptor by the lysosomal system.

continuously recycle between the surface and intracellular pools (Bruneau et al., 2005), or are directed to the lysosomal degradation pathway (Fumagalli et al., 1982) (Figure 2). These trafficking processes are under regulation by cellular proteins, which mainly interact with the receptor subunit M3-M4 loops. Since the M3-M4 loops are the most diverse portions of Cys-loop receptor subunits, these interactions between subunits and cellular proteins are predicted to be specific to individual subunits and receptor isoforms. Given the focus of this dissertation, the proteins involved in nACh receptor forward trafficking and surface stability will not be discussed further, and those involved in $GABA_A$ receptor trafficking will be discussed later.

Cys-loop receptor biogenesis and functions

Receptor assembly being the basis for receptor heterogeneity

An early step of Cys-loop receptor biogenesis, multiple-subunit assembly, confers receptors with great diversity. A Cys-loop receptor can be composed of five identical subunits (i.e. homo-pentamer) or different subunits (i.e. hetero-pentamer). While the homologous subunits are believed to share a similar topology, they have different primary sequences with about 70-80%, 30-40%, and 20-30% of amino acid residues are identical among the same type of subunits, among different types of subunits within the same family, and among different families, respectively (Macdonald and Olsen, 1994). Consequently, specific combinations of subunit subtypes produce different receptor isoforms with diverse electrophysiological and pharmacological properties, and with distinct temporal and spatial distributions.

Table 1. Subunits of Cys-loop receptors

Anionic receptors	Subtypes	Cationic receptors	Subtypes
$GABA_A$ receptors	α1-6, β1-3, γ1-3, δ, ε, θ and π	**nACh receptors**	α1-10*, β1-4, γ, δ and ε
$GABA_C$ receptors	ρ1-3	**5-HT_3 receptors**	5-$HT_{3A, 3B, 3C, 3D}$ and $_{3E}$
Glycine receptors	α1-4 and β		

* α8 subunit of nACh receptor family is absent from human (Millar and Harkness, 2008).

To date, 16, 3, 5, 16 and 5 subunit subtypes of $GABA_A$, $GABA_C$, glycine, nACh and 5-HT_3 receptor subunits, respectively, have been identified in humans (Table 1) (Darlison et al., 2005;Chebib, 2004;Kirsch, 2006;Millar, 2003;Niesler et al., 2008). Furthermore, some subunit subtypes have alternative spicing variants, which further increase subunit diversity. Mathematically, the number of possible receptor isoforms for a given Cys-loop receptor family is 5^{N-1} (where N equals number of subunit subtypes including splicing variants that have been identified for a given family of Cys-loop receptors). However, because of additional-assembly constraints, actual pentameric isoforms are fewer. In past decades, investigations using heterologous expression systems, in which a specific combination of a recombinant Cys-loop receptor can be expressed, have revealed several possible-subunit combinations of functional-surface Cys-loop receptors. However, not all these possible receptor isoforms are present in the nervous system, suggesting that some factors limit the diversity of endogenous Cys-loop receptors.

Constraints on receptor heterogeneity

Several lines of evidence suggest that an early step in receptor biogenesis, inter-subunit interactions, could favor some assembly intermediates, and thus, play a role in determining receptor stoichiometry. First, although $GABA_A$ receptor α1 and β1 subunits are sufficient for functional binary receptor surface expression, the presence of γ2 subunits results in preferential surface expression of ternary receptors, which show higher conductance and have benzodiazepine sensitivity (Angelotti and Macdonald, 1993). Second, while 5-HT_{3A} single subunit expression results in functional surface receptors, 5-HT_{3A} and 5-HT_{3B} subunit coexpression leads to favored assembly of binary receptors (Boyd et al., 2002). Third, glycine receptor α1 and β subunit coexpression generates receptors with fixed stoichiometry ($\alpha1_3\beta_2$), whereas α1 and α2 subunit coexpression produces several isoform combinations that are randomly assembled (Kuhse et al., 1993).

The temporal and spatial availability of subunits, which is regulated by regionally-specific-transcriptional regulation of receptor subunit genes, is another important factor determining which receptor isoforms are present in the nervous system. For instance, only five subtypes of nACh receptor subunits, α1, β1, γ, δ and ε, are expressed at the neuromuscular junction, where γ and ε subunit expression is developmentally regulated. Consequently, the embryonic muscle only expresses the $\alpha1_2\beta1\gamma\delta$ nACh receptor isoform, while the adult muscle exclusively expresses the $\alpha1_2\beta1\varepsilon\delta$ isoform (Mishina et al., 1986). Similarly, the cessation of glycine receptor α2 subunit expression and the initiation of glycine receptor α1 and β subunit expression after birth leads to the replacement of α2 homomeric receptors by α1β receptors (Lynch, 2004;Malosio et al., 1991).

Receptor biogenesis resulting in functional and distributional heterogeneity

Receptor assembly confers Cys-loop channels with distinct properties, such as gating behaviors, pharmacological profiles, and ion selectivity. These unique properties have been use for their classification. As revealed in their names, although both glycine and GABA can activate glycine receptors, potencies of the two ligands are very different (Lu et al., 2008). Likewise, although taurine activates both $GABA_A$ and glycine receptors, a higher concentration of taurine is required to activate $GABA_A$ receptors than to activate glycine receptors (Wu et al., 2008). The distinct pharmacological profiles could then differentiate receptors activated by the same ligands. For instance, the bicuculline insensitivity of $GABA_C$ receptors distinguishes them from $GABA_A$ receptors (Rabow et al., 1995). Finally, based on their ion selectivity, Cys-loop receptors can be classified as anionic or cationic channels (Table 1). The former includes $GABA_A$, $GABA_C$ and glycine receptors, which are permeable to Cl^- and HCO_3^- ions, and the latter contains nACh and 5-HT_3 receptors, which are permeable to Na^+, K^+ and Ca^{2+} ions.

Activation of a Cys-loop receptor by ligand binding leads to opening of the receptor channel pore and passive diffusion of permeable ions between the intracellular cytoplasm and the extracellular environment. The net flux of permeable ions is determined by the difference between the intracellular and extracellular concentration of the specific permeable ions. Due to their passive ion permeability, Cys-loop receptor functions are affected by environmental conditions. In adult nervous system, the cationic nACh and 5-HT_3 receptors mediate excitatory neuronal transmission by allowing the net influx of cations to depolarize postsynaptic membranes or to induce release of neurotransmitters. In contrast, the $GABA_A$ and glycine receptors mediate inhibitory

neuronal transmission since the net influx of permeable Cl^- hyper-polarizes the cells. However, the anionic receptors are excitatory right after birth, when the openings of channels lead to the net efflux of Cl^- ions and depolarization of neurons due to the higher intracellular Cl^- concentration. The decline of inward $Na^+/K^+/2Cl^-$ cotransporter expression and the increase of K^+/Cl^- co-transporter expression during the first two weeks after birth is responsible for the transition of intracellular chloride concentration from higher to lower (Delpire and Mount, 2002;Stein and Nicoll, 2003).

The expression patterns of Cys-loop receptors are also temporally and spatially regulated. Since Cys-loop receptors are mediators of neuronal transmission, environments of Cys-loop receptors, where upstream messengers and downstream effectors of receptors vary, can profoundly affect Cys-loop receptor functions. The combination of this distribution diversity with different environmental contexts thus confers even greater functional heterogeneity. Consequently, $GABA_C$ receptors are involved in vision transmission due to their high expression levels in the retina (Boue-Grabot et al., 1998). Similarly, glycine receptors regulate motor function and pain transmission because they are mainly distributed in spinal cord (Kirsch, 2006). Finally, 5-HT_3 receptors, which are highly expressed in the areas of the brain stem such as the area postrema and the nucleus tractus solitarius, play a role in emesis (Miquel et al., 2002). It is worth noting that some Cys-loop receptor families are widely distributed and have broad spectrum of functions. For example, $GABA_A$ receptors, the principal mediators of the most abundant neurotransmitter in the brain (Somogyi et al., 1998), are involved in neural excitability, circadian rhythm, and neural plasticity (Collinson et al., 2002). Thus, they are associated with epilepsy (Sperk et al., 2004), sleeping disorders

(Ning et al., 2004), anxiety, and alcoholism (Follesa et al., 2006;Mohler, 2007). Likewise, neuronal nACh receptors are involved in cognition, learning and memory, arousal, nicotine abuse, Alzheimer's disease, Parkinson's disease and schizophrenia (Paterson and Nordberg, 2000).

Disturbances of receptor biogenesis cause congenital diseases

Several congenital human diseases have been associated with mutations of Cys-loop-receptor subunits, which cause disturbances of receptor biogenesis. First, bipolar affective disorders and schizophrenia have been, respectively, associated with a mutation that increases the 5-HT_{3A} subunit mRNA level (Niesler et al., 2001a), and a polymorphism in the 5-HT_{3A} subunit that decreases 5-$HT_{3A/B}$ receptor surface levels (Niesler et al., 2001b;Krzywkowski et al., 2007). Second, CMSs, a group of genetic disorders showing weak ocular, cranial, and/or limb muscles, are commonly caused by insufficient levels of surface-muscle-type nACh receptors. Several mutations have been identified in receptors and shown to affect different biogenic steps. Some of these mutations result in premature termination of translation by introducing a stop codon or inducing a frame-shift (Ohno et al., 1997), thus reducing available subunits for receptor assembly. The other mutations hinder subunit assembly by removing the biogenic structural determinants for receptor oligomerization, such as *N*-glycosylation site consensus sequences (Ohno et al., 1996), or Cys-loop cysteines (Milone et al., 1998). Third, hyperekplexia or startle syndrome, which is characterized by sudden involuntary-bilateral movements of the body induced by surprise, alarm and acute pain, has been linked to mutations of glycine receptor α1 subunits. A set of these mutations disturb

glycine receptor biogenesis by affecting the availability of subunits, transmembrane insertion of a subunit, oligomerization of subunits, assembly of a pentameric receptor, and/or trafficking of receptors (Bakker et al., 2006;Castaldo et al., 2004;Humeny et al., 2002). Finally, IGEs, including childhood absence, juvenile myoclonic, or generalized tonic-clonic epilepsy, have been associated with several $GABA_A$ receptor subunit mutations that decrease surface receptor levels (Macdonald et al., 2004). These mutations are discussed together with other experimental mutations in following sections as they reveal some of the structural determinants of $GABA_A$ receptor biogenesis.

Structural determinants of $GABA_A$ receptor biogenesis

As the prototype-nACh receptor and the AChBP provide structural and biogenic information about Cys-loop receptors, it is clear that cellular proteins regulate Cys-loop biogenesis by interacting with specific portions/residues of receptor subunits. Several of these regions, which are described here after as structural determinants of $GABA_A$ receptor biogenesis, have been identified and are discussed based on their position in following sections.

In the N-terminal domains

Studies of natural and artificial mutations, combined with homology modeling have significantly advanced our understanding of $GABA_A$ receptor biogenesis. To date, several motifs or residues that are located in the N-terminal domain of $GABA_A$ receptor subunits have been shown to regulate subunit oligomerization. For instance, a γ2 subunit mutation, which is a conserved residue across all Cys-loop receptor subunits (S171), has

been shown to decrease co-immunoprecipitated partnering α2 and β1 subunits by γ2 subunits. Interestingly, although the mutations abolished the benzodiazepine antagonist binding sites, they had no significant effects on GABA agonist binding sites. This finding suggests that α2β1 binary receptors are assembled and expressed on the cell surface. Based on homology modeling, this residue is predicted to stabilize an exposed loop structure, on the subunit (+) side (Jin et al., 2004).

Similarly, a naturally occurring mutation in the $GABA_A$ receptor γ2 subunit, which changes a superfamily conserved arginine to glutamine at position 43 (R43Q), has been associated with IGEs (Baulac et al., 2001) and causes the ER retention of mutant subunits (Kang and Macdonald, 2004). Homology modeling predicts that the mutation disrupts the inter-subunit contact between the β2 subunit minus side and the γ2 subunit plus side (Sancar and Czajkowski, 2004). Supporting the hypothesis, a γ2 subunit 15 amino-acid-long peptide with the conserved (R43) residue and its surrounding sequences was able to pull-down partnering α1 and β2 subunits. Furthermore, the equivalent regions from α1 and β2 subunits were also capable of pulling-down partnering subunits, suggesting that the region is sufficient for mediating subunit oligomerization (Hales et al., 2005). Controversially, despite significantly decreased surface expression of mutant γ2(R43Q) subunits, oligomerization of γ2(R43Q) subunits with α3 and β2 subunits was not impaired as shown by an immunoprecipitation assay (Frugier et al., 2007). This inconsistency may originate from heterogeneity of subunits and/or from the involvement of other regions of the full-length subunits.

Another mutation in γ2 subunits substituting the arginine at position 139 with glycine has also been associated with IGEs (Audenaert et al., 2006). An in depth study

revealed that the mutation caused reduction of surface α1β2γ2 receptor levels due to ER retention of γ2(R139G) subunits. Impaired oligomerization/assembly was predicted as surface and α1 and β2 subunit levels were not decreased suggesting surface expression of normally disfavored α1β2 receptors (Schwartz et al., unpublished).

It is worthwhile pointing out that some of these oligomerization motifs in $GABA_A$ receptors are unique for one type or subtype of subunits and mediate interactions with specific partnering subunits. Oligomerization signals in this category are suggested to constrain possible combinations and regulate the stoichiometry of receptors. For instance, the β3 subunit sequence from residue 76 to 89, G-I-P-L-N-L-T-L-D-N-R-V-A-D, on the minus side of the N-terminal domain mediates the subunit interaction with the α1 but not the γ2 subunit, implying that other oligomerization signals on the minus side of the β3 subunit are involved in β3 and γ2 subunit interactions (Ehya et al., 2003). The presence of more than one oligomerization signal on the same contacting side of the subunit N-terminal domain suggests that interactions among different types of partnering subunits are distinguishable. In turn, these interactions regulate assembly order and receptor stoichiometry. Supporting the argument, a residue conserved among all α subunit subtypes, α1(R66), is specifically required for oligomerization with β2 but not β1 or β3 subunits (Bollan et al., 2003). Different affinities of those signals for members of one subunit type are potential mechanisms for preferential incorporation of one subunit over other subunits within the same subunit type.

Post-translational modifications in the N-terminal domain also play a crucial role in receptor biogenesis. Blocking N-linked glycosylation of proteins using tunicamycin caused the absence of $GABA_A$ receptor surface expression (Connolly et al., 1996). The

two functional glycosylation sites, N10 and N110 (N38 and N138 if the signal peptide is included), in the α1 subunit have been identified (Buller et al., 1994). In human embryonic kidney (HEK) cells, but not *Xenopus* oocytes, removal of either one of the two glycosylation sites by N to Q mutation caused a significant decrease of ligand binding, which suggested reduction of surface receptor density. Furthermore, the temperature-dependence of the effect of the mutation indicated that glycosylation was important for subunit folding (Buller et al., 1994). Potential glycosylation sites in other $GABA_A$ receptor subunits are predicted based on their location in a consensus sequence, N-X-S/T, where X can be any amino acid except proline. Whether these predicted glycosylation sites are functional or not remains to be determined.

Some point-mutations associated with IGEs and located in the subunit N-terminal domains also cause decrease of surface-receptor-functional expression (Feng et al., 2006). However, how these mutations affect receptor biogenesis is less clear. Given the importance of the N-terminal domain in receptor assembly, these mutations may affect early steps of receptor biogenesis. Particularly, the δ(E177A) mutation is right before the absolutely conserved cysteine δ(C178), which forms a disulfide bond with δ(C164). Cys-loop disulfide-bond formation has been shown to be essential for receptor assembly (Green and Wanamaker, 1997). Thus, it is possible that the δ(E177A) mutation affects this essential post-translational modification.

In the M3 transmembrane domain

Insertion of transmembrane helices is essential for establishing the topology of transmembrane proteins. Therefore, residues that are involved in maintaining the helical

structure or in interacting with the lipid bilayer play a role in receptor subunit folding (Popot and Engelman, 2000). Recently, an alanine to aspartate mutation in M3 domain of $GABA_A$ receptor α1 subunit, α1(A322D) has been associated with autosomal dominant juvenile myoclonic epilepsy (Cossette et al., 2002). This mutation exemplifies the importance of transmembrane domain structure in $GABA_A$ receptor biogenesis, as it impaired the biogenesis of $GABA_A$ receptors by causing protein misfolding and reducing the availability of subunits for receptor assembly (Gallagher et al., 2004;Gallagher et al., 2005;Gallagher et al., 2007;Bradley et al., 2008). Few α1(A322D) subunits manage to fold correctly, assemble into pentamer, and be expressed on the cell surface. In this case, the α1(A322D) mutation has an additional effect and results in a faster endocytosis rate of receptors containing the mutant subunits (Bradley et al., 2008).

In the M2-M3 extracellular loop

The γ2 subunit mutation, K289M, a residue that is conserved across $GABA_A$ and glycine receptors, has been associated with IGE (Baulac et al., 2001) and shown to cause reduction of mutant and partnering subunits in HEK cells (Kang et al., 2006). Interestingly, a systematic investigation of the residue equivalents in α1, β2 and γ2L subunits demonstrated that the conserved residues were differentially required for receptor surface expression. Supporting the importance of this residue in receptor biogenesis, the equivalent β2(K274M) mutation profoundly reduced α1β2(K274M) and α1β2(K274M)γ2L receptor surface levels to 4% and 13%, respectively, of wild type α1β2 and α1β2γ2L receptor levels, respectively. Controversially, the α1(K278M) and γ2L(K289) mutations caused no effects on receptor surface levels (Hales et al., 2006).

The inconsistent effects of γ2S(K289M) and γ2L(K289M) mutations may originate from the difference between the γ2S and γ2L splice variants, which have different trafficking properties (Hales et al., 2006).

In the M3-M4 cytoplasmic loops

The intracellular loop between the M3 and M4 domains is the major site for intracellular regulation. Several proteins and posttranslational modifications have been demonstrated to directly interact with subunit M3-M4 loops and to regulate surface density of $GABA_A$ receptors.

Table 2. Proteins directly associating with M3-M4 cytoplasmic loops of α, β, and γ subunits

	Plic-1	BIG2	GRIF-1	AP2	GODZ	GABARAP
α subunits	1-3, 6	-	-	-	-	-
β subunits	1-3	1-3	2	1-3	-	-
γ subunits	-	-	-	2	1-3	1-3
↑/↓surface expression	↑	↑	↑	↓	↑	↑

First, the ubiquitin-like protein, Plic-1 (protein linking IAP to the cytoskeleton) directly interacts with α1-3, α6, and β1-3 subunit M3-M4 loops. It increases receptor surface density by increasing the stability of receptor subunits in the ER and plasma-membrane insertion of receptors in the secretory vesicles (Bedford et al., 2001;Saliba et al., 2008). Second, the brefeldin A-inhibited GDP/GTP exchange factor 2 (BIG2) binds

to all β subunits. It functions as a guanine nucleotide exchange factor which can activate small G-protein ADP-ribosylation factor 1 and 3. Thus, BIG2 promotes anterograde trafficking from the trans-Golgi network (Charych et al., 2004). Third, the adaptor protein 2 (AP2) complex directly associates with β1-3, γ2 and δ subunits (Kittler et al., 2005). It facilitates clathrin-dependent endocytosis, and therefore, decreases the surface level of receptors. Fourth, gephyrin directly and indirectly interacts with α2 and γ2 subunits, respectively, and facilitates receptor synaptic clustering (Tretter et al., 2008;Alldred et al., 2005;Essrich et al., 1998;Jacob et al., 2005;Kneussel et al., 1999). Fifth, GABARAP binds to γ1-3 subunits. Its interactions with gephyrin, the *N*-ethylmaleimide-sensitive factor, and tubulin suggest that it regulates the intracellular trafficking of γ subunit-containing $GABA_A$ receptors (Wang et al., 1999). Sixth, the $GABA_A$ receptor interacting factor-1 (GRIF-1) binds to β2 subunits. It may regulate receptor trafficking via its interaction with GABARAP (Beck et al., 2002). Seventh, protein kinase C and the receptor for activated C kinase-1 directly associates with β1-3 subunits (Brandon et al., 1999;Brandon et al., 2002). Phosphorylation regulates receptor surface levels possibly by affecting receptor turn-over (Connolly et al., 1999a;Kanematsu et al., 2006). Last, the Golgi-specific DHHC zinc finger protein (GODZ) directly interacts with γ2 subunit M3-M4 loops (Keller et al., 2004) and plays a role in synaptic clustering of $GABA_A$ receptors (Fang et al., 2006) (Figure 3).

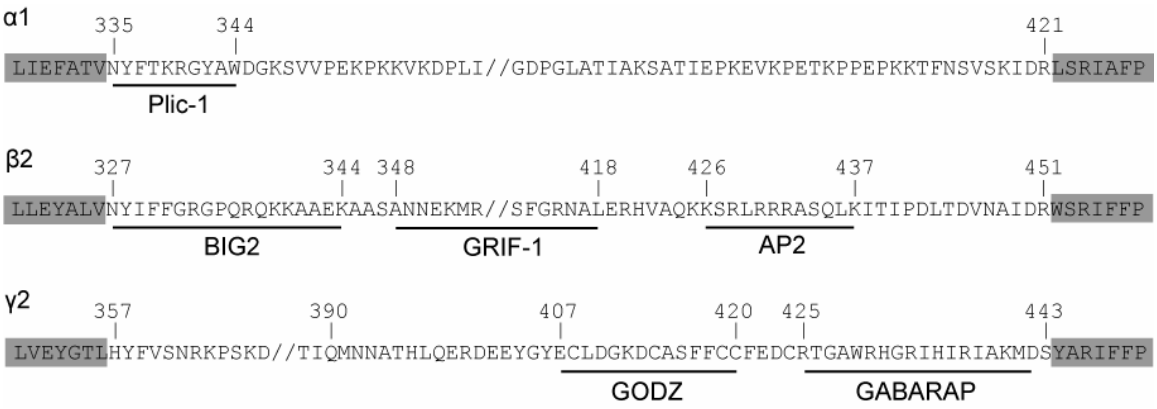

Figure 3. The M3-M4 loops of α1, β2 and γ2S subunits contain multiple protein binding motifs

C- and N-terminal portions of M3 and M4 domains, respectively, of individual subunits are highlighted in grey. Numbers above the sequences indicate the start and finish of the M3-M4 loop and its protein binding motifs (underlined). The numbering is relative to the first amino acid of the immature polypeptide. Thus, the residue Q351 mentioned in text was indicated as Q390 here. Note that slashes (//) indicate omitted regions.

The γ2S subunit mutation, Q351X, which has also been associated with an IGE, causes truncation of a γ2 subunit polypeptide C-terminal to residue Q351. As a result, the mutant subunit, which lacks the GABARAP binding motif, the following M4 domain, and the C-terminal tail, is retained in the ER (Harkin et al., 2002). The underlying mechanism for the absence of surface expression of the γ2S(Q351X) subunits could be similar to the α1 subunit mutation, A322D, ,which reduced availability of subunits due to subunit misfolding and ERAD. Alternatively, the γ2S(Q351X) subunits could result in less incorporation of subunits in $GABA_A$ receptor complexes, and/or inefficient delivery of α1β2γ2S(Q351X) receptors to the cell surface. Whether the lack of the GABARAP binding motif results in the significantly lower surface expression of γ2S(Q351X) subunits remains to be elucidated. Furthermore, it remains to be determined whether or

not the decrease of γ2S(Q351X) subunit surface expression changed the population and profiles of receptor isoforms expressed on cell surface.

Specific aims

Since Cys-loop receptor channels operate on the cell surface, fluctuations of receptor surface levels are accompanied with changes of channel functionalities. For this reason, biogenesis of Cys-loop receptors is the primary determinant that sets the synaptic strength of neuronal transmission. As mentioned above, several intracellular proteins interact directly with motifs in $GABA_A$ receptor subunits and regulate receptor assembly (e.g. the ER chaperones), anterograde trafficking (e.g. the BIG2, GRIF-1 and GABARAP), endocytosis (e.g. the AP2), and degradation (e.g. the Plic-1). Some of these proteins cross talk with one another (e.g. gephyrin, GABARAP and GRIF-1), suggesting the possibility that they co-exist in a higher order protein complex. It is predictable that removal of motifs involved in receptor anterograde trafficking and recycling processes would result in significant alterations in receptor surface expression. However, considering that at least two subunits, such as α1 and β2, are required for efficient surface expression, it remains to be determined if there is a subunit specificity of the M3-M4 loop. Furthermore, whether there are novel motifs in subunit M3-M4 loops regulating receptor surface expression is an open question. Additionally, whether these structural motif binding proteins cross talk to one another and then impose some effects on structural motifs where they are not directly bound remains to be elucidated. Therefore, the specific aims of my dissertation are as follows:

1. To determine the requirements of individual α1, β2, and γ2 subunit M3-M4 loops for $GABA_A$ receptor surface expression and to narrow down the critical structural motifs in the M3-M4 loops for $GABA_A$ receptor biogenesis.
2. To determine the roles of the critical structural motifs in $GABA_A$ receptor biogenesis.
3. To determine the functional glycosylation sites of the human $GABA_A$ receptor β2 subunits and to determine if there is cross-talk between the N-terminal domain of β2 subunits and the M3-M4 loop of the same subunit.

CHAPTER II

STRUCTURAL DETERMINANTS IN α1, β2 AND γ2S SUBUNIT M3-M4 CYTOPLASMIC LOOPS AND THE α1 SUBUNIT EXTRACELLULAR TAIL FOR SURFACE EXPRESSION OF $GABA_A$ RECEPTORS

Introduction

$GABA_A$ receptors, members of the Cys-loop superfamily of ligand-gated ion channels, mediate fast inhibitory synaptic transmission in the central nervous system. $GABA_A$ receptor surface density regulates neuronal excitably and is involved in neuronal plasticity (Biggio et al., 2001), epilepsy (Frugier et al., 2007;Gallagher et al., 2005;Gallagher et al., 2007;Kang and Macdonald, 2004;Kang et al., 2006), and anxiety (Malizia et al., 1998). $GABA_A$ receptors are pseudosymmetrical pentamers assembled from combinations of sixteen subunit subtypes (α1-6, β1-3, γ1-3, δ, ε, θ and π) (Macdonald and Olsen, 1994). *De novo* synthesized $GABA_A$ receptor subunits should undergo proper folding (Gallagher et al., 2007;Green and Claudio, 1993), post-translational modification such as glycosylation (Connolly et al., 1996), oligomerization, and assembly in the ER (Blount and Merlie, 1990;Green and Claudio, 1993;Klausberger et al., 2001a). The ER is the frontline of quality control where improperly assembled subunits are retained and degraded by ERAD (Gallagher et al., 2007;Christianson and Green, 2004;Meusser et al., 2005). Successfully assembled pentamers are sorted into COPII vesicles for forward trafficking (Aridor and Traub, 2002) and monitored by COPI complexes that retrieve receptors that expose ER retention signals in the case of improper assembly (Wang et al., 2002;Keller et al., 2001;Michelsen et al., 2005). Receptors that

reach the cell surface are then under the regulation of the endosomal system that internalizes receptors, sorts them into lysosomes for degradation, or recycles them back to the plasma membrane (Kittler and Moss, 2003).

All $GABA_A$ receptor subunits share a similar topology that includes an extracellular N-terminal domain, four transmembrane domains, and loops linking the transmembrane domains (Macdonald and Olsen, 1994). The N-terminal portions of subunits that precede the major cytoplasmic loop linking the third and fourth transmembrane domains (M3-M4 loop) are conserved among subunit types (Thompson et al., 1994) and are thought to mediate inter-subunit oligomerization (Hales et al., 2005;Jin et al., 2004;Sancar and Czajkowski, 2004). In contrast, M3-M4 loops vary in length and sequence among different $GABA_A$ receptor subunit types and contain several protein binding motifs that are involved in receptor forward trafficking, endocytosis and degradation that up-regulate (Beck et al., 2002;Bedford et al., 2001;Charych et al., 2004) or down-regulate (Kittler et al., 2000a) receptor surface density (Figure 3). However, M3-M4 loops may not be the only variable distal $GABA_A$ receptor structural regions that regulate receptor surface density. The extracellular C-terminal "tails" distal to the M4 domains are present only in α1-6 subunits and are composed of ten to thirteen amino acids. Other subunit types, in contrast, have less than two amino-acid "stumps" distal to M4 domains (Figure 12). It has been suggested that this extracellular C-terminal region affects receptor assembly, and thus forward trafficking, since addition of C-terminal epitope tags results in failure of receptor surface expression (Kittler et al., 2000b).

To understand better how $GABA_A$ receptor surface density is regulated, the roles of the α1, β2 and γ2 subunit M3-M4 loops and the α1 subunit C-terminal tail in regulating

receptor surface expression were investigated. A shared signal at the distal end of the M3-M4 loops and the long α1 subunit C-terminal tail were shown to be crucial for receptor surface expression, as they may affect $GABA_A$ receptor assembly or forward trafficking.

Materials and methods

DNA constructs

Complementary DNAs (cDNAs) encoding human α1, β2 and γ2S subunit polypeptides, which include the signal peptides, were inserted into pcDNA3.1(+) plasmids as described previously. The cDNA sequences encoding the FLAG-tag amino acid sequence, D-Y-K-D-D-D-D-K, were introduced into the α1 subunit (between the 8th and 9th amino acids of the mature polypeptide) and β2 and γ2S subunits (between the 4th and 5th amino acids of mature polypeptides). In addition, the HA-tag sequence, Y-P-Y-D-V-P-D-Y-A, was introduced into the γ2S subunit at the same position as that of the FLAG-tags. Deletions of portions of $GABA_A$ receptor subunits and insertions of restriction enzyme sites were conducted using the QuikChange Site-Directed Mutagenesis Kit (Stratagene). The forward sequences of the primer pairs for mutagenesis are listed below (Table 3). The γ2(loopΔ), $\gamma2(\text{loop}\Delta)^{FLAG}$, $\gamma2(\text{GABARAP}\Delta)^{FLAG}$, and $\gamma2(\text{GABARAP+})^{FLAG}$ constructs were kindly provided by Dr. Kang (Vanderbilt University).

Table 3. Forward sequences of primer pairs for Site-Directed mutagenesis I

Mutation	Forward primer sequence (5' to 3')
Deleting major portions of M3-M4 loop	
α1(loopΔ)[§]	GT TAT GCA TGG GAT GGC CTG[†] TCA AGA AA GCC T
β2(loopΔ)	G AGG GGG CCC CAA CGC CAA TGG TCC CGC ATA TTC T
Loop swaps	
Introducing Age I site to M3 domain and M3-M4 loop junction	
α1(Age I+)	G ATT GAG TTT GCC ACA GTA **ACCGGT*** AAC TAT TTC ACT AAG AGA GG
β2(Age I+)	CTG GAA TAT GCT TTG GTC **ACCGGT** AAC TAC ATC TTC TTT GGG
γ2(Age I+)	GTG GAG TAT GGC ACC TTG **ACCGGT** CAT TAT TTT GTC AGC AAC CGG
Introducing Asc I site to M4 domain and M3-M4 loop junction	
α1(Asc I+)	GTC AGC AAA ATT GAC CGA **GGCGCGCC** CTG TCA AGA ATA GCC TTC
β2(Asc I+)	GTG AAC GCC ATT GAT CGG **GGCGCGCC** TGG TCC CGC ATT TTC TTC
γ2(Asc I+)	C ATT GCC AAA ATG GAC TCC **GGCGCGCC** TAT GCT CGG ATC TTC TTC
Deleting Age I site	
$\alpha1_{\beta2}$(Age IΔ)	CTG ATT GAG TTT GCC ACA GTA AAC TAC ATC TTC TTT GGG AGA GG
$\beta2_{\alpha1}$(Age IΔ)	CTG GAA TAT GCT TTG GTC AAC TAT TTC ACT AAG AGA GGT TAT GC
$\beta2_{\gamma2}$(Age IΔ)	CTG GAA TAT GCT TTG GTC CAT TAT TTT GTC AGC AAC CGG
$\gamma2_{\alpha1}$(Age IΔ)	GTG GAG TAT GGC ACC TTG AAC TAT TTC ACT AAG AGA GGT TAT GC
$\gamma2_{\beta2}$(Age IΔ)	GTG GAG TAT GGC ACC TTG AAC TAC ATC TTC TTT GGG
Deleting Asc I site	
$\alpha1_{\beta2}$(Asc IΔ)	GTG AAC GCC ATT GAT CGG CTG TCA AGA ATA GCC TTC CCG
$\beta2_{\alpha1}$(Asc IΔ)	C AGT GTC AGC AAA ATT GAC CGA TGG TCC CGC ATT TTC TTC CC
$\beta2_{\gamma2}$(Asc IΔ)	CGC ATT GCC AAA ATG GAC TCC TGG TCC CGC ATT TTC TTC CC
$\gamma2_{\alpha1}$(Asc IΔ)	C AGT GTC AGC AAA ATT GAC CGA TAT GCT CGG ATC TTC TTC CCC
$\gamma2_{\beta2}$(Asc IΔ)	GTG AAC GCC ATT GAT CGG TAT GCT CGG ATC TTC TTC CCC
Regional deletion	
β2(BIG2Δ)	GAA TAT GCT TTG GTC GCT GCT AGC GCC
β2(GRIF-1Δ)	GAG AAA GCT GCT AGC GAA CGA CAT GTG
β2(postGRIF-1Δ)	C GCC CTG GAA TGG TCC CGC ATT TTC
β2(postGRIF-1+)	G GAA TAT GCT TTG GTC CGA CAT GTG GCA C
β2(postGRIF-1+; preAP2Δ)	G GAA TAT GCT TTG GTC AAA AGT CGC CTG AGG
β2(postGRIF-1+; AP2Δ)	CAT GTG GCA CAA AAG ATC ACC ATC CCC GAC
β2(postGRIF-1+; postAP2Δ)	GCC TCC CAA CTG AAA TGG TCC CGC ATT TTC
β2(postAP2Δ)	GCC TCC CAA CTG AAA TGG TCC CGC ATT TTC
β2(postAP2+)	CTG GAA TAT GCT TTG GTC ATC ACC ATC CCC GAC

§ primer pairs for making α1(loopΔ) and β2(loopΔ) constructs were from Dr. Kang (Vanderbilt University).
† sequences underlined are new junction formed after mutagenesis.
* sequences marked in red indicate restriction enzyme sites.

To swap M3-M4 loops among α1, β2 and γ2S subunits, AgeI and AscI restriction enzyme sites were introduced into individual subunit cDNAs before the codons encoding the N-terminal beginnings of the M3-M4 loop and of the M4 domain, respectively. The boundaries of the M3-M4 loops were predicted based on the UniProt database (http://www.expasy.org/sprot/; GBRA1_HUMAN for the α1 subunit, GBRB2_HUMAN for the β2 subunit and GBRG2_HUMAN for the γ2S subunit). It is worth noting that the prediction of the boundaries of the M3-M4 loops was based on the Uniprot knowledgebase, which predicts longer lengths of the loop than those predicted by the homology alignment to nACh receptors (Unwin, 2005). Since both predictions are equally possible due to lack of experimental data, we chose to investigate larger ranges. M3-M4 loops of individual type of subunits were excised by double digestion with AgeI and AscI and ligated into the other two types of subunits double digested with the same enzymes. Finally, the restriction enzyme sites were deleted. The mutant constructs were confirmed using polymerase chain reactions (PCR).

To introduce the α1 subunit C-terminal tail into β2 subunits, an overlapping PCR strategy was used. Briefly, the DNA sequence encoding the α1 subunit tail (sequence underlined) was embedded in the primer pairs (forward TL+: GG CTT TAC TAT GTG AAC <u>AGA GAG CCT CAG CTA AAA GCC CCC ACA CCA CAT CAA</u> TAA GGA ACC ACT AGT CCA GTG TGG; reverse TL+: CCA CAC TGG ACT AGT GGT TCC TTA <u>TTG ATG TGG TGT GGG GGC TTT TAG CTG AGG CTC TCT</u> GTT CAC ATA GTA AAG CC) that were used to amplify two double-stranded DNA segments from β2 subunit templates. By pairing the upstream T7 primer with the reverse TL+ primer and by pairing the forward TL+ primer with the downstream reverse BGH primer, two β2

subunit segments of double-stranded DNA with overlapping sequence (sequence of the primer pair) were generated. These two segments were then used as templates, and double-stranded DNA with the inserted α1 subunit tail sequence was amplified using T7 and BGH primers. The PCR products were then sub-cloned into pcDNA3.1(+) vectors. The FLAG- and HA-tags were inserted using the same strategy.

Cell culture and transfection

HEK293T cells (ATCC (CRL-11268)) were incubated at 37°C in humidified 5% CO_2/95% air and grown in Dulbecco's Modified Eagle Medium (Invitrogen) supplemented with 10% fetal bovine serum (Invitrogen) plus 100 IU/mL each of penicillin and streptomycin (Invitrogen). Cells were transfected using the FuGene6 transfection reagent (Roche) using 9 μL of reagent per 3 μg of cDNA. For transfection in a 60 mm diameter culture dish, a total of 3 μg of cDNA was used. The cDNA-FuGene6 mixture volumes were scaled up or down proportionally to the surface areas of cell culture dishes. The cDNA mixtures contained α1 and β2 subunits and either empty vector or γ2S subunit in a 1:1:1 ratio. Cells were used for experiments forty-eight hours after transfection.

Flow cytometry

To collect single cells for flow cytometry analysis, monolayer cultures of HEK293 cells were dissociated by trypsin (Invitrogen) for 2 minutes. Trypsinization then was stopped in 4°C FACS buffer, phosphate buffered saline (PBS) with 2% fetal bovine serum and 0.05% sodium azide. Given that trypsin may cleave the extracellular

N-terminal domain and remove the FLAG epitope, the relative surface expression profile of FLAG-tagged subunits from cells dissociated by trypsin was compared with that from cells dissociated by protease free cell detaching solution, (2 mM EDTA in PBS). The two methods generated similar profiles (Gurba and Macdonald, unpublished). Following washes with FACS buffer, cells were incubated with anti-FLAG IgG directly conjugated with R-Phycoerythrin (PE, 1:50 dilution, Martek) for 1 hour. Cells were then washed with FACS buffer again and fixed with 2% paraformaldehyde. The surface fluorescence intensity of each cell was measured using a FacsCalibur (Becton, Dickinson and Company). Data were acquired using Cell Quest (BD Biosciences) and analyzed offline using FlowJo (Treestar, Inc.).

To exclude non-specific surface staining, viable cells were selected based on 7-amino-actinomycin D (7-AAD) exclusion (Figure 4A). On the frequency histogram of fluorescence intensity of viable cells with mock transfection, a gate for specific fluorescence signals was set such that only the brightest 1-2% of cells were included (Figure 4B). For each experimental condition, the percentage of cells with a sufficiently high fluorescence intensity to be included in the gate and the mean fluorescence intensity of those included cells were obtained (Figure 4C). By multiplying these two numbers, a fluorescence index was obtained that represented the adjusted surface mean fluorescence for the whole cell population. For comparison among various experimental conditions, the fluorescence indexes with experimental subunit coexpression were normalized to those of control subunit coexpression. Unless otherwise specified, a one-way ANOVA with Tukey's post test was used to determine if there were significant differences in surface levels among transfection conditions.

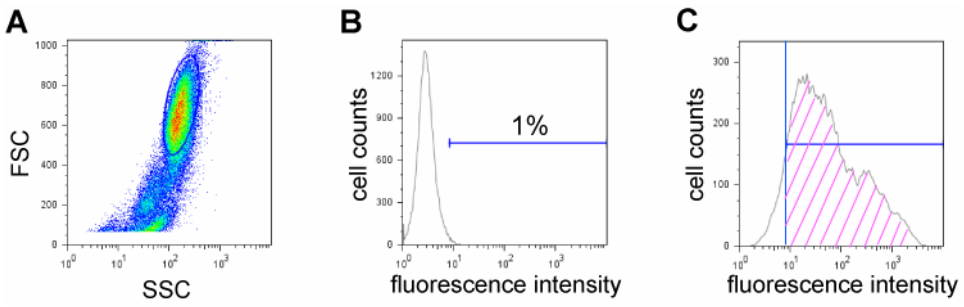

Figure 4. Selections of viable and positively transfected cells

A, A scatter dot plot distinguished individual cells based on their light diffraction properties. Each dot represented a cell which was annotated by two parameters: Y-axis, forward scatter (FSC) is proportional to cell size; the bigger the cell, the higher the detected signal. X-axis, side scatter (SSC) is proportional to cell granularity (e.g. particles and organelles); the more complex the cytoplasmic contents, the higher detected signals. The viable cell population was gated within the pink circle based on 7-amino-actinomycin D (7-AAD) exclusion. **B**, A representative fluorescence histogram of cells in a mock transfection condition is presented. The Y-axis indicates the cell counts and the X-axis indicates the fluorescence intensity (R-Phycoerythrin, PE, in this case, scale is from 1 to 10,000 arbitrary units). The positive-signal gate was set so that only 1% of mock transfected cells were included. **C**, A representative fluorescence histogram of cells with proteins of interests ($\alpha 1^{FLAG}$ subunits coexpressed with β2 subunits in this case) positively expressed on the cell surface is presented.

Western blots

Membrane proteins in transfected cells were extracted in modified radio-immuno-precipitation assay buffers (RIPA buffers), which contained 10-50 mM Tris-HCl (pH 7.4), 150 mM NaCl, 1.0 mM EDTA, 1-2% NP-40, 0.25-0.5% sodium deoxycholate and protease inhibitor cocktail (complete mini, Roche). Cell lysates were cleaned by centrifugation at 10,000X g for 30 minutes. The supernatants were subjected to further experiments or directly to sodium dodecyl sulfate-polyacrylamide gel electrophoresis

(SDS-PAGE). Proteins in gels were transferred to polyvinylidene fluoride (PVDF) membranes (Millipore) or nitrocellulose membrane (Amersham Biosciences).

Monoclonal anti-$GABA_A$ receptor α1 subunit antibodies (final concentration 5 μg/mL, clone: BD24, Chemicon) and monoclonal anti-$GABA_A$ receptor β2/3 antibodies (4 μg/mL, clone: 62-3G1, Upstate) were used to detect the epitopes in wild type or mutant human α1 and β2 subunit N-terminal domains, respectively. In addition, 4 μg/mL monoclonal anti-FLAG antibodies (clone: M2, Sigma) and 1 μg/mL monoclonal anti-HA antibodies (clone: 16B12, Covance) were used to detect FLAG-tagged and HA-tagged γ2 subunits, respectively. Finally, 0.2 μg/mL anti-sodium/potassium ATPase antibodies (clone: ab7671, Abcam) were used to control for loading variations. Following incubation with primary antibodies, secondary goat anti-mouse IgG heavy and light chain antibodies conjugated with horseradish peroxidase were used at a 1:10,000X dilution (Immunoresearch laboratories) for the visualization of specific bands using the enhanced chemiluminescent detection system (Amersham Biosciences). The signals were collected in a digital ChemImager (Alpha Innotech), and the integrated density volumes (IDVs, pixel intensity X mm^2) were calculated using the FluorChem 5500 software. To compare expression levels between the same types of subunits with different mutations, we normalized adjusted IDVs (normalized to loading control Na^+/K^+ ATPase IDVs) to those of control conditions.

Glycosidase digestions

Whole cell lysates extracted using modified RIPA buffer were subjected to endoglycosidase H (endo H) and peptide N-glycosidase-F (PNGaseF) digestion (New

England BioLab) with the supplement of 1X G5 (50 mM sodium citrate, pH5.5) and 1X G7 (50mM sodium phosphate, pH7.5) reaction buffer, respectively. The digestion reactions were carried out at 37°C for 3 hours and were then terminated by addition of sample buffer.

Immunoprecipitation

Protein complexes containing FLAG-tagged $GABA_A$ receptor subunits were immunoprecipitated using EZview Red Anti-FLAG M2 beads (Sigma) at 4°C overnight. After three washes with extracting RIPA buffer, protein complexes were eluted with 100 μg/mL FLAG peptide (Sigma). The presence of $GABA_A$ receptor subunits was determined by Western blotting.

Results

The α1, β2 and γ2S subunit M3-M4 loops were required for maximal surface expression of α1β2 and α1β2γ2 receptors

To determine if there were different requirements for α1, β2 and γ2S subunit M3-M4 loops for $GABA_A$ receptor surface expression, constructs with large portions of their M3-M4 loops deleted (α1(loopΔ), β2(loopΔ) and γ2(loopΔ)) were made. Twelve amino acids, $\alpha1_{N335\text{-}G346}$ and $\beta2_{N327\text{-}Q338}$, and nine amino acids, $\gamma2_{H357\text{-}P365}$, at the N-termini of the loops were retained to link the M3 and M4 domains (Figure 3). To detect surface expression of α1β2 and α1β2γ2S receptors, FLAG-tags were inserted in α1, β2, γ2S, α1(loopΔ), β2(loopΔ) and γ2(loopΔ) subunits and the FLAG-tagged subunits were coexpressed with non-FLAG-tagged partnering subunits such that only one subunit was

FLAG-tagged at a time (e.g. $\alpha1^{FLAG}$ with β2 or α1 with $\beta2^{FLAG}$ subunits when studying coexpressed α1 and β2 subunits). The surface levels of each type of FLAG-tagged subunit using flow cytometry were then measured. Because anti-FLAG antibodies had different affinities for FLAG-tags in different types of subunits, presumably due to the differences of adjacent sequences surrounding the tags located in subunit N-terminal domains (data not shown), comparisons among different types of subunits were not obtained. However, since the subunit N-terminal portions intact and made mutations in only C-terminal portions were kept, anti-FLAG antibodies had the same affinity for FLAG-tags in wild type and mutant subunits were assumed.

For comparison, subunit surface levels in experimental conditions were normalized to those obtained with control α1β2 or α1β2γ2S subunit coexpression (e.g. coexpression of wild type α1 and β2 or α1, β2 and γ2S subunits). Unless otherwise specified, we used "binary" subunit coexpression to indicate coexpression of α1 and β2 subunits and "ternary" subunit coexpression to indicate coexpression of α1, β2 and γ2 subunits, regardless of the wild type or mutant status of each of the subunits. To distinguish wild type partnering subunits coexpressed with mutant subunits from those that were coexpressed with other wild type subunits in control conditions, we used "control subunits" to specify wild type subunits under control conditions.

The $\alpha1^{FLAG}$ or $\beta2^{FLAG}$ subunit surface levels with binary subunit coexpression were first evaluated (Figure 5). Relative to control surface levels, the α1 subunit M3-M4 loop deletion caused significant partial reductions of both α1(loopΔ) and β2 subunit surface levels ($p < 0.001$, $n = 6$). The β2 subunit loop deletion resulted in almost

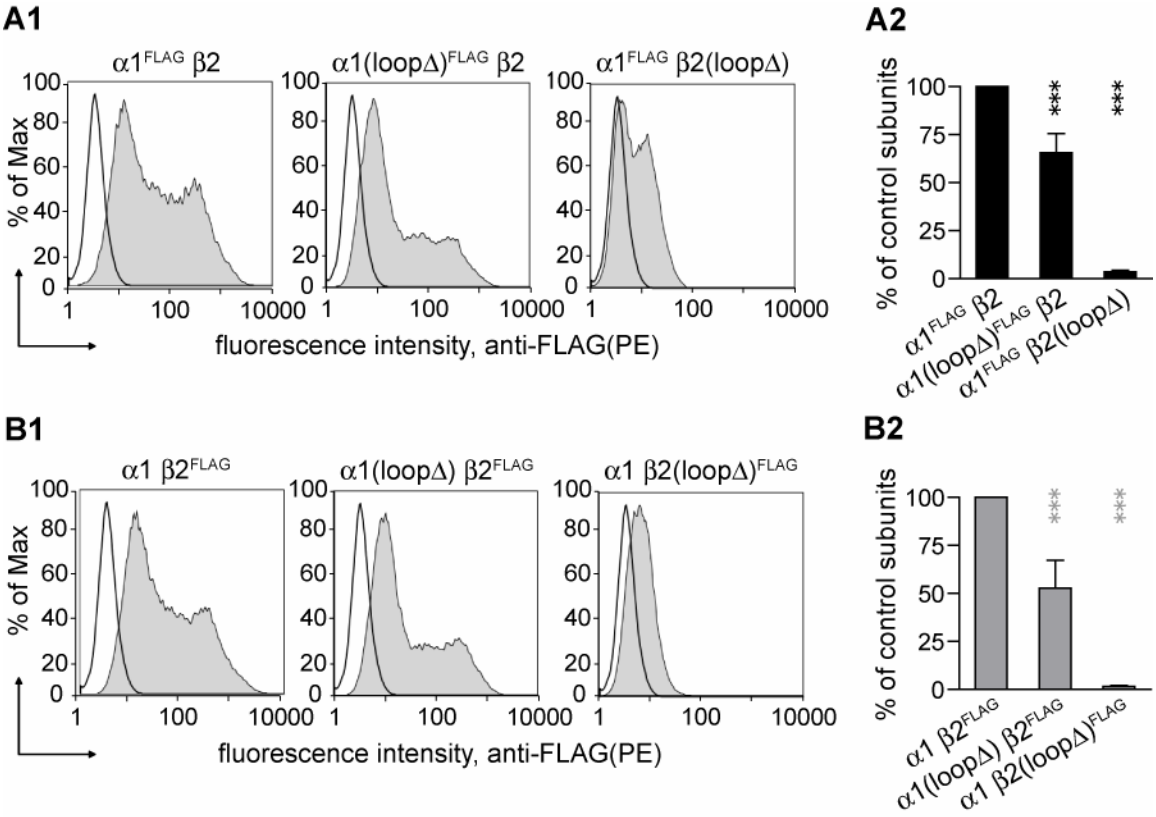

Figure 5. Deletion of the α1 or β2 subunit M3-M4 loop, $\alpha1_{K347\text{-}R421}\Delta$ or $\beta2_{K339\text{-}R451}\Delta$, respectively, substantially reduced α1β2 receptor surface expression

A1, Representative distributions of R-Phycoerythrin (PE) fluorescence intensities for cells coexpressing $\alpha1^{FLAG}\beta2$ (left panel) or $\alpha1^{FLAG}\beta2(loop\Delta)$ (right panel) subunits and stained with a PE-conjugated monoclonal anti-FLAG antibody (M2 clone) were plotted as frequency histograms. The x-axis indicates the fluorescence intensity in arbitrary units (note the log scale) and the y-axis indicates the percentage of the maximum cell count. Representative distributions obtained from mock transfected cells (unfilled histograms) are overlaid with each experimental distribution (filled histograms). **A2**, Surface $\alpha1^{FLAG}$ subunit levels were quantified using the fluorescence index (see Methods) and plotted as a percentage of control $\alpha1^{FLAG}\beta2$ subunit coexpression. **B1**, **B2**, As in Panels A1, A2, except for cells coexpressing $\alpha1\beta2^{FLAG}$ (left panel) or $\alpha1\beta2(loop\Delta)^{FLAG}$ (right panel) subunits. *** corresponds to $p < 0.001$ compared to the control subunit coexpression.

complete loss (>95%) reductions of subunit surface levels of both α1 and β2(loopΔ) subunits such that surface expression of both α1 and β2(loopΔ) subunits were significantly lower than those with α1(loopΔ)β2 subunit coexpression ($p < 0.001$, $n = 4$). Specifically, subunit surface levels with α1(loopΔ)β2 subunit coexpression were 66% and 53%, and subunit surface levels with α1β2(loopΔ) subunit coexpression were only 4% and 2% of control α1 and β2 subunits, respectively.

The α1 and β2 subunit loop deletions caused similar extents of surface level reductions of both themselves and partnering subunits with ternary subunit coexpression ($p < 0.001$ for all types, $n = 10$-14) (Figure 6). Subunit surface levels with α1(loopΔ)β2γ2S subunit coexpression were 79%, 69% and 64%, and subunit surface levels with α1β2(loopΔ)γ2S subunit coexpression were 10%, 5% and 17% of control α1, β2 and γ2S subunit surface levels with α1β2γ2S subunit coexpression, respectively. Interestingly, while the γ2(loopΔ) subunit coexpressed with α1 and β2 subunits had very low surface expression (5% of control γ2S subunits, $p < 0.001$, $n = 10$), surface levels of partnering α1 subunits were much less affected (69% of control α1 subunits, $p < 0.001$, $n = 8$), and surface levels of partnering β2 subunits were not altered ($n = 11$). These observations indicated that γ2S subunit loops were essential for α1β2γ2S receptor surface expression, but possibly not for α1β2 receptor surface expression. An explanation for this finding was that while γ2(loopΔ) subunits had reduced capacity to oligomerize, α1 and β2 subunits remained free to assemble. To determine if the γ2(loopΔ) subunits could still interact with α1 and β2 subunits and decrease surface levels of α1β2 receptors, surface levels of α1 and β2 subunits with α1β2γ2(loopΔ) subunit coexpression were

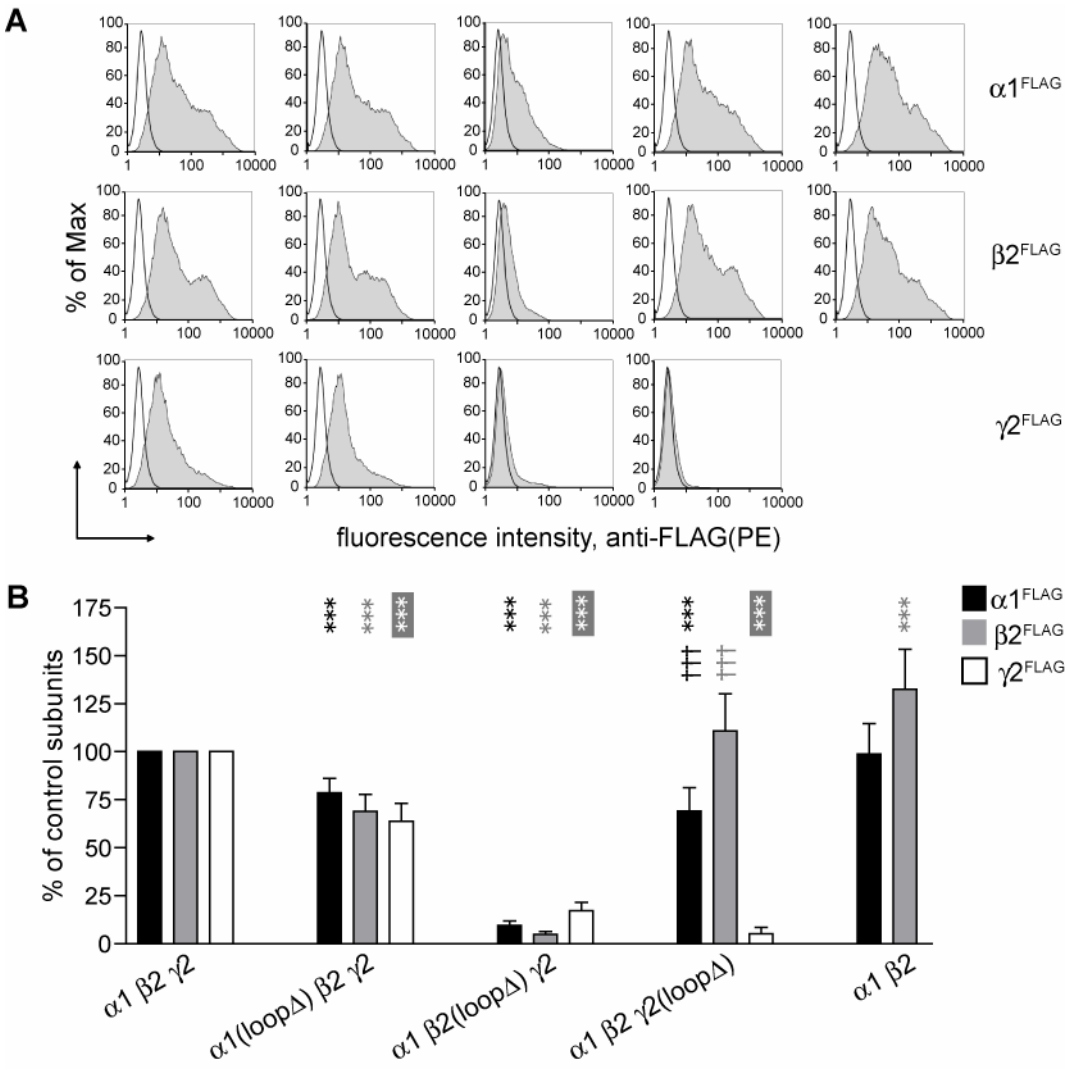

Figure 6. Deletion of the α1, β2 or γ2 subunit M3-M4 loop, $\alpha1_{K347\text{-}R421}\Delta$, $\beta2_{K339\text{-}R451}\Delta$ or $\gamma2_{S366\text{-}S443}\Delta$, respectively, substantially reduced receptor surface expression

A, Representative fluorescence histograms of cells with control α1β2γ2 (first column), α1(loopΔ)β2γ2 (second column), α1β2(loopΔ)γ2 (third column), α1β2γ2(loopΔ) (fourth column), or α1β2 (fifth column) subunit coexpression were generated. Upper panels indicates surface $\alpha1^{FLAG}$ subunit levels; middle panels indicates surface $\beta2^{FLAG}$ subunit levels; lower panels indicates surface $\gamma2^{FLAG}$ subunit levels. **B**, Surface $\alpha1^{FLAG}$ (black bars), $\beta2^{FLAG}$ (grey bars), and $\gamma2^{FLAG}$ (white bars) subunit levels were quantified in each condition as a percentage of control subunit coexpression. *** corresponds to $p < 0.001$ compared to the control subunit coexpression; ††† corresponds to $p < 0.001$ compared to the α1β2 subunit coexpression.

compared to those with α1β2 subunit coexpression. To make a proper comparison between these two expression conditions, empty pcDNA3.1(+) vector was added with α1β2 subunit coexpression to maintain the same amount of total DNA. The surface levels of α1 and β2 subunits with α1β2γ2(loopΔ) subunit coexpression were significantly lower (70% and 84% of those with α1β2 subunit coexpression, respectively ($p < 0.001$ for both α1 and β2 subunits, n = 8-15). Taken together, these data suggested that γ2(loopΔ) subunits could interact with partnering α1 and β2 subunits, but with reduced capacity, and that the resulting oligomers or pentamers could not traffic to the cell surface, thus decreasing the surface levels of both α1 and β2 subunits.

Total cellular loop-deleted subunit protein levels were not reduced to the same extent as surface loop-deleted subunit protein levels

The substantial reductions of $GABA_A$ receptor subunit surface expression resulting from α1, β2 and γ2S subunit loop deletions could have been due, at least in part, to extensive reductions of total cellular protein levels (which includes surface and intracellular subunit protein levels). To examine this hypothesis, the total cellular subunit protein levels of mutant and partnering subunits with α1(loopΔ)β2, α1β2(loopΔ) and $\alpha1\beta2\gamma2(loop\Delta)^{HA}$ subunit coexpression were compared to those of control subunits. The subunit total cellular protein expression profiles with α1(loopΔ)β2γ2S and α1β2(loopΔ)γ2S subunit coexpression were not compared since the surface levels of α1 and β2 subunits with these experimental conditions were similar to those obtained with binary subunit coexpression. In HEK293T whole cell lysates, non-specific proteins were recognized by anti-γ2 subunit and anti-FLAG antibodies, thereby masking the specific γ2S or $\gamma2S^{FLAG}$ subunit signals. Thus, the HA-tag was inserted into the γ2S subunit at the

same position as the FLAG-tag to obtain less ambiguous mobility patterns of γ2S subunits in Western blots.

Relative to control subunits, no significant reductions in total cellular protein levels of α1(loopΔ) or β2(loopΔ) subunits with binary subunit coexpression were observed (n = 5) (Figure 7A1,B1). Since total cellular subunit proteins are generally composed of two thirds surface protein and one third intracellular protein (Botzolakis and Macdonald, unpublished), this suggested that intracellular subunit protein levels were actually increased, not decreased (Figure 5). Surprisingly, significant reductions in total cellular protein levels of the partnering subunits (β2 subunits coexpressed with α1(loopΔ) subunits ($p < 0.001$, n = 5); α1 subunits coexpressed with β2(loopΔ) subunits ($p < 0.001$, n = 5)) (Figure 7A1,B1) were found, consistent with maintained intracellular but reduced surface subunit protein levels.

We compared the surface and total levels of $\gamma2(\text{loop}\Delta)^{HA}$ subunits with $\alpha1\beta2\gamma2(\text{loop}\Delta)^{HA}$ subunit coexpression. Although the subunit-total-protein level was significantly reduced relative to that of the control condition (77 % of control subunits, n = 6, p = 0.0045, paired t-test) (Figure 7A2, B2), its extent was not as severe as that of subunit-surface-level reduction (Figure 6B), consistent with increased, or a least maintained, intracellular subunit protein levels. Similar to α1(loopΔ) and β2(loopΔ) subunits, which caused reduction of partnering subunits with binary subunit coexpression, α1 and β2 partnering subunits were significantly reduced with coexpression of $\gamma2(\text{loop}\Delta)^{HA}$ subunits (55% and 67% of control α1 and β2 subunits, p = 0.001 and 0.0021, respectively, n = 6), again consistent with increased, or a least maintained, intracellular subunit protein levels.

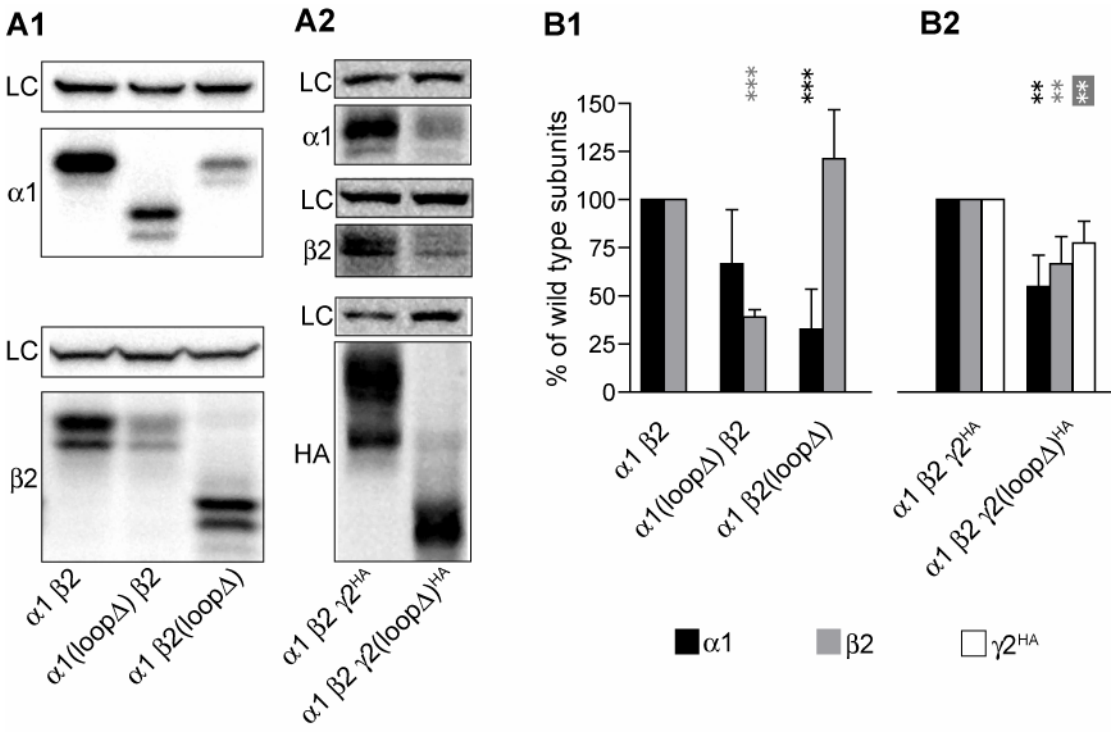

Figure 7. Effects of α1(loopΔ), β2(loopΔ) and γ2(loopΔ) subunits on total cellular protein levels of their own and partnering subunits with α1β2 and/or α1β2γ2 subunit coexpression

A1, Representative Western blots of RIPA buffer-extracted total proteins from cells with α1β2 (first column), α1(loopΔ)β2 (second column) and α1β2(loopΔ) (third column) subunit coexpression are presented. Loading duplicates were stained with monoclonal anti-Na^+/K^+ ATPase (as loading control, LC; the upper panels of both sets), with anit-α1 (upper set) or with anti-β2 (lower set) antibodies. **A2**, Representative Western blots of extracted total proteins from cells with $\alpha1\beta2\gamma2S^{HA}$ (first column) and $\alpha1\beta2\gamma2(loop\Delta)^{HA}$ (second column) subunit coexpression are presented. Loading triplicates were stained with anti-α1 (upper set), anti-β2 (middle set) and anti-HA (low set) antibodies. **B1**, Relative total subunit expression levels were expressed as % of corresponding control α1 or β2 subunits with α1β2 subunit coexpression (e.g. IDVs of α1(loopΔ) subunits with α1(loopΔ)β2 subunit coexpression were normalized to those of control α1 subunits with α1β2 subunit coexpression). **B2**, Relative subunit expression levels of α1, β2 and $\gamma2(loop\Delta)^{HA}$ subunits with $\alpha1\beta2\gamma2(loop\Delta)^{HA}$ subunit coexpression were expressed as % of corresponding control subunits with $\alpha1\beta2\gamma2^{HA}$ subunit coexpression. ** and *** correspond to $p < 0.01$ and 0.001, respectively, compared to the control subunit coexpression.

Mutant loop-deleted and partnering subunits were retained in the ER

The low levels of surface expression of β2(loopΔ) and γ2(loopΔ) subunits suggested a severe alteration in $GABA_A$ receptor biogenesis or turnover that could have been due to either arrest of forward trafficking or to an increased rate of endocytosis. For multimeric subunit protein complexes such as $GABA_A$ receptor pentamers, the ER is the frontline of quality control where improperly assembled subunits are retained. Therefore, to better understand the underlying mechanism for the loss of $GABA_A$ receptor subunit surface expression caused by β2 and γ2 subunit loop deletions, we first determined if the loop deletions caused subunit ER retention. $GABA_A$ receptor subunits are glycosylated proteins and subunit processing in the Golgi apparatus confers resistance to endo H glycosidase digestion. Therefore, endo H digested $GABA_A$ receptor subunits that were not ER retained would keep complex oligosaccharides and would show populations with higher molecular masses than those with all oligosaccharides removed, which could be accomplished by PNGaseF digestion. In contrast, glycosylated subunits that were retained in the ER would keep high-mannose oligosaccharides sensitive to endo H digestion and would therefore have mobility after endo H digestion similar to that after PNGaseF digestion.

Endo H resistance of α1, β2 and γ2 subunits with α1β2, α1(loopΔ)β2, α1β2(loopΔ), $\alpha1\beta2\gamma2S^{HA}$ and $\alpha1\beta2\gamma2(loop\Delta)^{HA}$ subunit coexpression was measured. Approximately 80% of total α1 or β2 subunit proteins with control α1β2 subunit coexpression were endo H resistant as indicated by the presence of bands with molecular masses higher than 46 kDa (for α1 subunits) and 48 kDa (for β2 subunits) following the

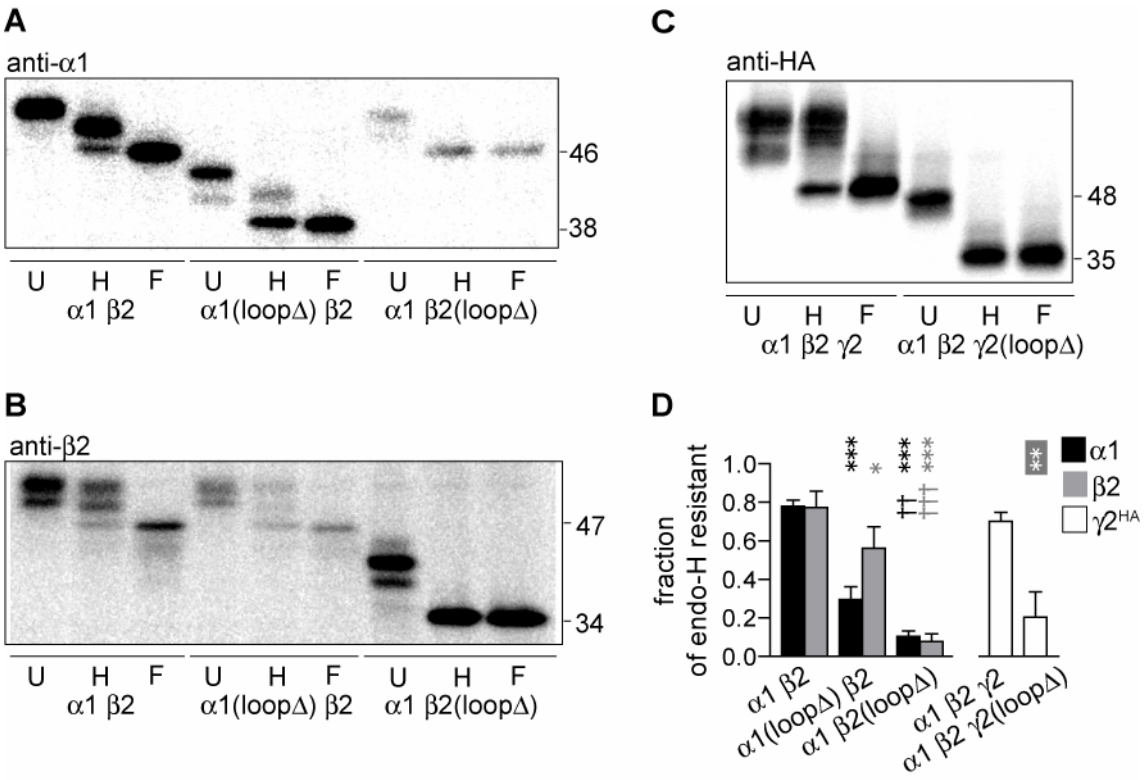

Figure 8. Glycosidase digestions

A, RIPA buffer extracted proteins from cells with α1β2 (first set), α1(loopΔ)β2 (second set) and α1β2(loopΔ) (third set) subunit coexpression were undigested (U), or digested with endo H (H) or PNGaseF (F). Proteins were probed with anti-α1 antibodies. After endo H digestion, these α1 subunits showing molecular mass equal to that of PNGaseF digestion (46 kDa) were considered endo H sensitive; while after endo H digestion, these α1(loopΔ) subunits showing molecular mass equal to that of PNGaseF digestion (38 kDa) were considered endo H sensitive. **B,** A duplicate of the panel A, which was probed with anti-β2 antibodies. β2 and β2(loopΔ) subunits migrating at 47 kDa and 34 kDa, respectively, after endo H digestion were considered endo H sensitive. **C**, Similarly the glycosylation status of $\gamma2^{HA}$ and $\gamma2(loop\Delta)^{HA}$ subunits from cell with $\alpha1\beta2\gamma2^{HA}$ and $\alpha1\beta2\gamma2(loop\Delta)^{HA}$ were analyzed. $\gamma2^{HA}$ and $\gamma2(loop\Delta)^{HA}$ subunits migrating at 48 kDa and 35 kDa, respectively, after endo H digestion were considered endo H sensitive. Four independent experiments were analyzed. **D**, Fractions of endo H resistant populations of total α1, β2 or γ2-HA subunits were quantified. *, ** and *** correspond to $p < 0.05$, 0.01 and 0.001, respectively, compared to the control subunit coexpression; †† and ††† correspond to $p < 0.01$ and 0.001, respectively, compare to α1(loopΔ)β2 subunit coexpression.

endo H digestion (Figure 8A, B). This was consistent with the observation that the majority of control subunit proteins were mature and present on the cell surface. In support of the hypothesis that β2 subunit loop deletion resulted in ER retention of both types of subunits, no more than 10% of α1 or β2(loopΔ) subunit total proteins with α1β2(loopΔ) subunit coexpression were endo H resistant ($p < 0.001$, $n = 3$, Figure 8D). Loop deletion of α1 subunits led to less severe subunit ER retention, with 30% of α1(loopΔ) and 56% of β2 subunits being endo H resistant with α1(loopΔ)β2 subunit coexpression. The α1(loopΔ) subunit endo H resistant fraction was significantly lower than that of the wild type α1 subunit ($p < 0.001$, $n = 3$), but was significantly higher than that of the α1 subunit with α1β2(loopΔ) subunit coexpression ($p < 0.01$, $n = 3$). Similarly, the endo H resistant fraction of the β2 subunit with α1(loopΔ)β2 subunit coexpression was significantly different from that with control α1β2 ($p < 0.05$, $n = 3$) or α1β2(loopΔ) ($p < 0.001$, $n = 3$) subunit coexpression. Likewise, 70% of $\gamma2S^{HA}$ subunits with $\alpha1\beta2\gamma2S^{HA}$ subunit coexpression were endo H resistant, while $\gamma2(loop\Delta)^{HA}$ subunits with $\alpha1\beta2\gamma2(loop\Delta)^{HA}$ subunit coexpression were significantly different from those with wild type coexpression ($p = 0.0037$, paired *t*-test) and only 20% of $\gamma2(loop\Delta)^{HA}$ subunits were endo H resistant (Figure 8 C, D).

Mutant loop-deleted subunits oligomerized with partnering subunits

The retention of mutant and partnering subunits could have been due to lack of the prerequisite assembly of pentameric receptors for $GABA_A$ receptor surface expression. Although previous findings have demonstrated that the N-terminal domains

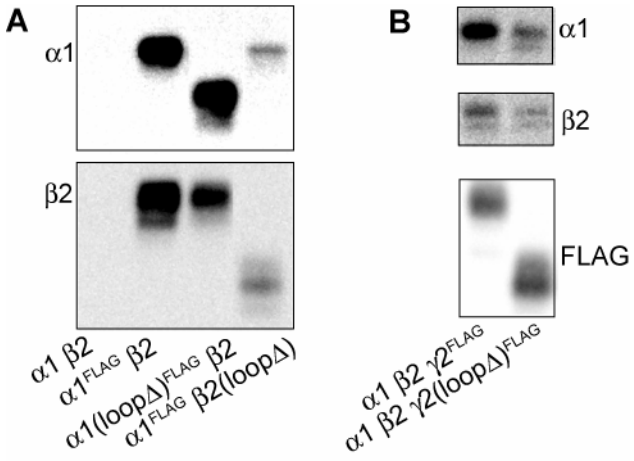

Figure 9. Immunoprecipitation of FLAG-tagged and partnering $GABA_A$ receptor subunits

A, RIPA buffer-extracted proteins from cells with α1β2 (first column), $\alpha1^{FLAG}\beta2$ (second column), $\alpha1(loop\Delta)^{FLAG}\beta2$ (third column) and $\alpha1^{FLAG}\beta2(loop\Delta)$ (fourth column) subunit coexpression, respectively, were immunoprecipitated using M2 beads against FLAG-tagged α1 subunit variants (e.g. $\alpha1^{FLAG}$). Proteins immunoprecipitated were detected using monoclonal anti-α1 (upper panel) or anti-β2 antibodies (lower panel). **B**, Similarly, immunoprecipitated proteins from cells with $\alpha1\beta2\gamma2^{FLAG}$ (first column), and $\alpha1\beta2\gamma2(loop\Delta)^{FLAG}$ (second column) coexpression were detected using monoclonal anti-α1 (upper panel), anti-β2 (middle panel) and anti-FLAG (lower panel) antibodies.

are sufficient to mediate $GABA_A$ receptor oligomerization, these conclusions were derived only from segmental or whole extracellular N-terminal domains (Klausberger et al., 2001b). To exclude the possibility that the absence of subunit M3-M4 loops caused global protein misfolding and thus impaired inter-subunit oligomerization, immunoprecipitation experiments were conducted to determine if partnering subunits still associated with loop-deleted subunits.

With coexpression of partnering and loop-deleted subunits, anti-FLAG M2 beads specifically immunoprecipitated FLAG-tagged α1 subunits whether or not they contained

the loop deletion but did not precipitate non-FLAG-tagged α1 subunits (upper panel of Figure 9A). Furthermore, the immunoprecipitated protein complexes contained associated partnering subunits whether or not they contained the loop deletion (lower panel, Figure 9A). Likewise, with ternary subunit coexpression, M2 beads specifically immunoprecipitated FLAG-tagged control γ2S or mutant γ2(loopΔ) subunits. In addition, partnering α1 and β2 subunits were oligomerized with both control γ2S and mutant γ2(loopΔ) subunits (Figure 9B). Thus, impaired subunit oligomerization was not the main cause of the surface level reductions with α1β2(loopΔ) and α1β2γ2(loopΔ) subunit coexpression.

Replacement of the α1 subunit M3-M4 loop by the β2 subunit M3-M4 loop did not restore α1β2(loopΔ) and α1β2(loopΔ)γ2S " receptor" surface expression

Since inter-subunit oligomerization was retained with loop-deletion, we assumed that pentameric assembly was not abolished. However, it appeared that β2 subunit loop deletion had more profound effects on surface expression than α1 subunit loop deletion. Thus, we further hypothesized that the basis for the absence of surface expression of α1β2(loopΔ) and α1β2(loopΔ)γ2S "receptors" was that the β2, but not the α1, subunit M3-M4 loop was required for $GABA_A$ receptor surface expression. To test this hypothesis, the M3-M4 loops were swapped from β2 to α1 subunits to make $\alpha1_{\beta2}$ subunits (α1 subunits containing the β2 M3-M4 loops, $\beta2_{N327\text{-}R451}$) (Figure 10A). Both types of subunits with $\alpha1_{\beta2}$β2(loopΔ) subunit coexpression showed no significant difference in surface levels from those with α1β2(loopΔ) surface levels (2% of control surface levels for both types, n = 5, Figure 10C). Similarly, surface levels of all three

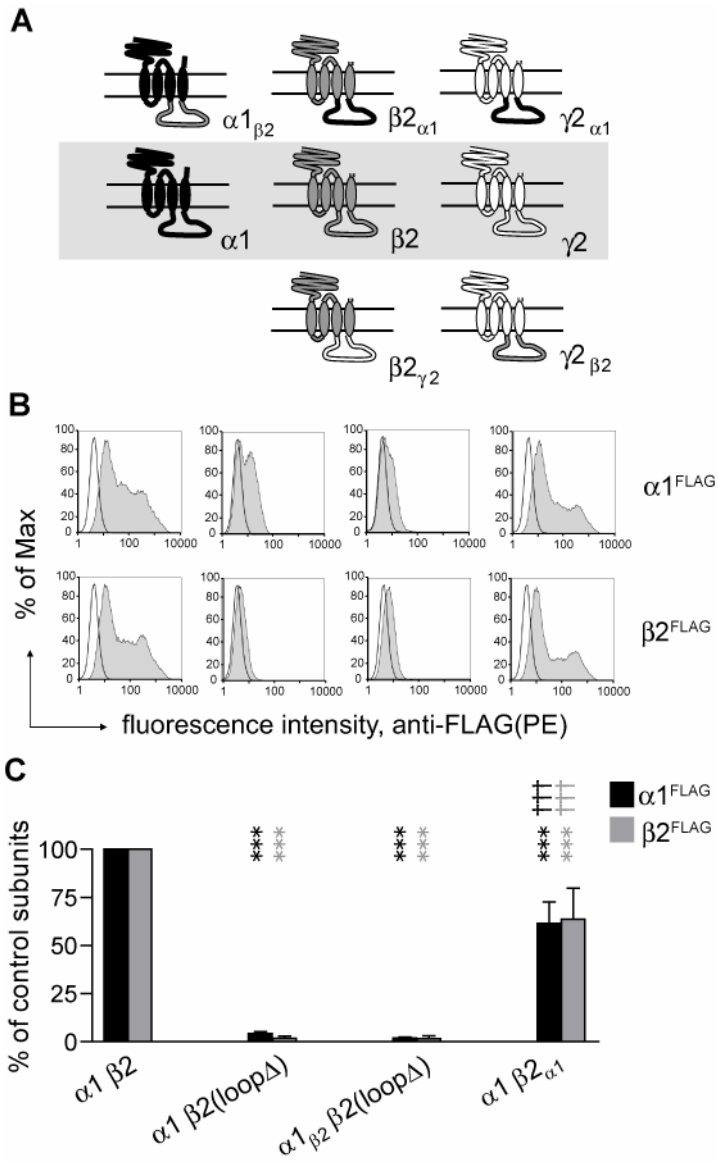

Figure 10. Surface expression of binary $GABA_A$ receptors containing loop-swap subunits

A, Schematic representations of the loop-swap constructs are presented. **B**, Representative fluorescence histograms of cells with control α1β2 (first column), α1β2(loopΔ) (second column), $\alpha1_{\beta2}\beta2$(loopΔ) (third column), or $\alpha1\beta2_{\alpha1}$ (fourth column) subunit coexpression were generated. Upper panels indicates surface $\alpha1^{FLAG}$ subunit levels; lower panels indicates surface $\beta2^{FLAG}$ subunit levels. **C**, Surface $\alpha1^{FLAG}$ (black bars), and $\beta2^{FLAG}$ (grey bars) subunit levels were quantified in each condition as a percentage of control subunit coexpression. *** corresponds to $p < 0.001$ compared to the control subunit coexpression; ††† corresponds to $p < 0.001$ compared to the α1β2(loopΔ) subunit coexpression.

types of subunits with $\alpha1_{\beta2}\beta2(loop\Delta)\gamma2S$ subunit coexpression were not significantly different from those with $\alpha1\beta2(loop\Delta)\gamma2S$ coexpression (for $\alpha1_{\beta2,}$ $\beta2(loop\Delta)$ and $\gamma2S$ subunits, 5%, 5% and 14% of those in control ternary subunit coexpression remained, n = 4, Figure 11B). Therefore, our hypothesis was not supported, as introduction of β2 subunit M3-M4 loops into α1 subunits was not sufficient to restore the loss of receptor surface expression caused by the $\beta2(loop\Delta)$ subunit.

Replacement of β2 or γ2S subunit M3-M4 loops with other subunit M3-M4 loops partially restored surface $GABA_A$ receptor expression

To determine if the presence of M3-M4 loops from other types of subunits could reverse the loss of receptor surface expression caused by β2 or γ2S subunit loop deletion, four constructs ($\beta2_{\alpha1}$, $\beta2_{\gamma2}$, $\gamma2_{\alpha1}$ and $\gamma2_{\beta2}$) from the six possible chimeric loop-swapped subunits were used (Figure 10A). Coexpression of α1 subunits with $\beta2_{\alpha1}$ subunits (β2 subunits containing α1 subunit M3-M4 loops, $\alpha1_{N335\text{-}R421}$) led to chimeric subunit and partnering subunit surface levels that were significantly lower than those with control α1β2 subunit coexpression ($p < 0.001$), but significantly higher than those with $\alpha1\beta2(loop\Delta)$ subunit coexpression ($p < 0.001$, n = 5-8, Figure 10C). Subunit surface levels with $\alpha1\beta2_{\alpha1}$ subunit coexpression were 62% and 64% of control α1 and β2 subunits. These results thus suggested that the presence of the α1 subunit M3-M4 loops alone contained enough information to support receptor surface expression.

Similarly, with ternary subunit coexpression, replacement of the β2 subunit M3-M4 loop with α1 or γ2S subunit M3-M4 loops ($\beta2_{\alpha1}$ or $\beta2_{\gamma2S}$ subunits; Figure 10A) significantly restored the receptor surface expression lost by deleting the β2 subunit M3-

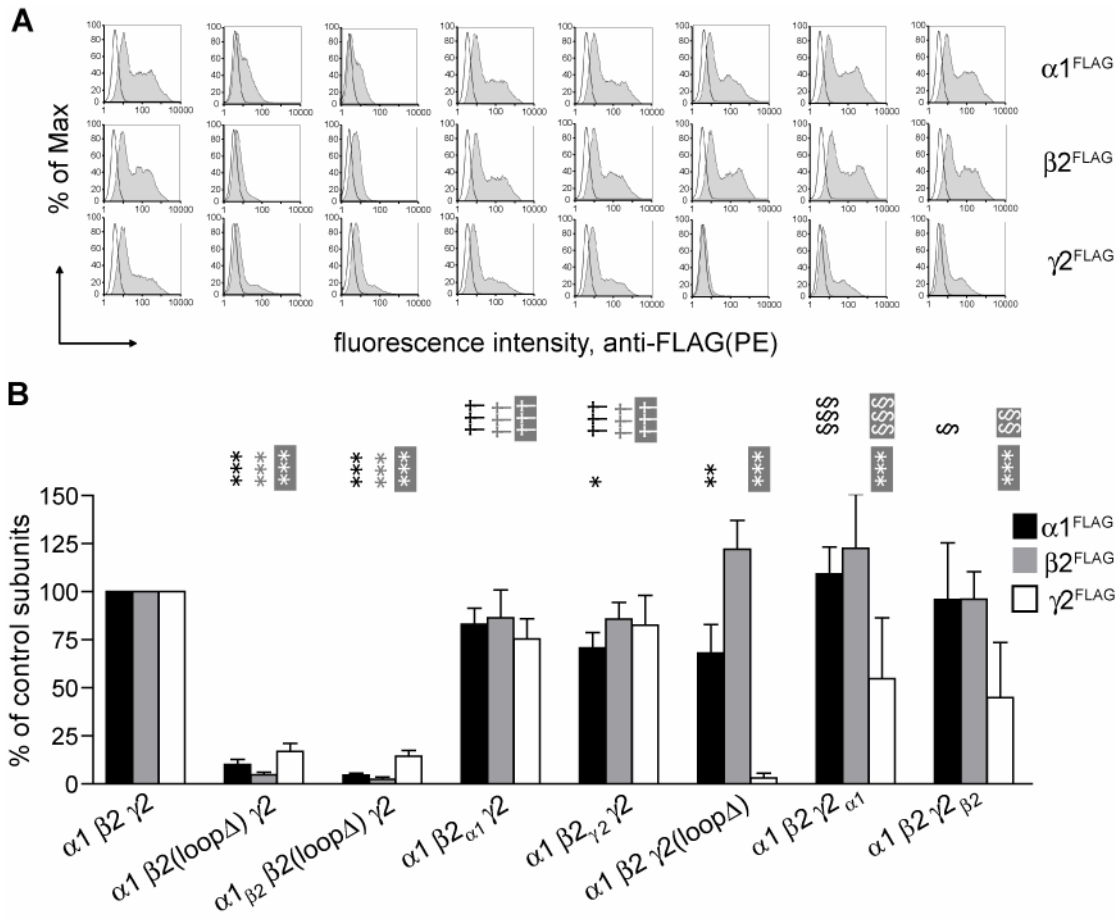

Figure 11. Surface expression of ternary $GABA_A$ receptors containing loop-swap subunits

A, Representative fluorescence histograms of cells with control α1β2γ2 (first column), α1β2(loopΔ)γ2 (second column), $\alpha1_{\beta2}\beta2$(loopΔ)γ2 (third column), $\alpha1\beta2_{\alpha1}\gamma2$ (fourth column), $\alpha1\beta2_{\gamma2}\gamma2$ (fifth column), α1β2γ2(loopΔ) (sixth column), $\alpha1\beta2\gamma2_{\alpha1}$ (seventh column), $\alpha1\beta2\gamma2_{\beta2}$ (eighth column) subunit coexpression were generated. Upper panels indicates surface $\alpha1^{FLAG}$ subunit levels; middle panels indicates surface $\beta2^{FLAG}$ subunit levels; lower panels indicated surface $\gamma2^{FLAG}$ subunit. **B**, Surface $\alpha1^{FLAG}$ (black bars), and $\beta2^{FLAG}$ (grey bars) subunit levels were quantified in each condition as a percentage of control subunit coexpression. *, ** and *** corresponds to $p < 0.05$, 0.01 and 0.001, respectively, compared to the control subunit coexpression; ††† corresponds to $p < 0.001$ compared to the α1β2(loopΔ)γ2 subunit coexpression; §, §§ and §§§ corresponds to $p <$ 0.05, 0.01 and 0.001, respectively, compared to the α1β2γ2(loopΔ) subunit coexpression.

M4 loop ($p < 0.001$ for all types of subunits with $\alpha1\beta2_{\alpha1}\gamma2S$ and $\alpha1\beta2_{\gamma2S}\gamma2S$ subunit coexpression, n = 3-6; Figure 6B). Coexpression of α1, $\beta2_{\alpha1}$ and γ2S subunits resulted in 83%, 86% and 75%, and coexpression of α1, $\beta2_{\gamma2S}$ and γ2S subunits resulted in 71%, 86% and 83% of control α1, β2 and γ2S subunit surface levels, respectively.

We also determined if replacement of the γ2S subunit M3-M4 loop with α1 or β2 subunit M3-M4 loops ($\gamma2_{\alpha1}$ or $\gamma2_{\beta2}$ subunits; Figure 10A) could restore surface expression of γ2 subunits lost by deleting the γ2S subunit M3-M4 loop (γ2(loopΔ)). Although significantly lower than control γ2S subunit surface levels ($p < 0.001$ for $\gamma2_{\alpha1}$ and $\gamma2_{\beta2}$ subunits, n = 5), $\gamma2_{\alpha1}$ and $\gamma2_{\beta2}$ subunit surface levels were 55% and 45% of control γ2S subunit surface levels, respectively, and significantly reversed the γ2 subunit loop-deleted induced loss of subunit surface expression ($p < 0.001$ for γ2α1 subunits and $p < 0.01$ for γ2β2 subunits, n = 5). Furthermore, surface levels of α1 subunits with $\alpha1\beta2\gamma2_{\alpha1}$ and $\alpha1\beta2\gamma2_{\beta2}$ subunit coexpression were significantly higher than those with α1β2γ2(loopΔ) subunits coexpression, and thus, no longer different from those of control α1 subunits. On the other hand, surface levels of β2 subunits were not significantly different with α1β2γ2, α1β2γ2(loopΔ), $\alpha1\beta2\gamma2_{\alpha1}$ and $\alpha1\beta2\gamma2_{\beta2}$ subunit coexpression. Taken together, these results suggested that the presence of M3-M4 loops was required for appreciable receptor surface expression, regardless of the identity of the loop.

The extracellular "tail" of the α1 subunit distal to the M4 domain was involved in regulating receptor surface expression

The exchangeability of M3-M4 loops among α1, β2 and γ2S subunits suggested that specific structures/signals were shared among different types of subunits. However, these specific structures/signals appeared less important for α1(loopΔ) subunit surface

expression with α1(loopΔ)β2 and α1(loopΔ)β2γ2S subunit coexpression. As revealed by subunit sequence alignments, α subunits possess a long extracellular C-terminal "tail" (Figure 12A). Could the 13 amino acid extracellular α1 subunit tails be responsible for the lesser importance of the α1 subunit M3-M4 loop relative to β2 and γ2S subunits for receptor surface expression? To test this hypothesis, the importance of the α1 subunit C-terminal tail for receptor surface expression was systematically investigated (Figure 12B).

Coexpression of C-terminal tail-deleted α1 subunits, α1(tailΔ), with β2 subunits resulted in a small but significant reduction of $GABA_A$ receptors on the cell surface (Figure 12C1). With α1(tailΔ)β2 subunit coexpression, 87% and 75% of control α1 and β2 subunit surface levels were present on the cell surface ($p < 0.001$, $n = 12$). However, deletion of both the α1 subunit M3-M4 loop and C-terminal tail, α1(loopΔtailΔ) led to an additive reduction of α1β2 subunit surface expression. As a result, surface levels with α1(loopΔtailΔ)β2 coexpression were 13% of control α1 subunit surface levels ($n = 9$) and 5% of control β2 subunit surface levels and were no longer different from the respective subunit surface levels with α1β2(loopΔ) subunit coexpression ($n = 10$, Figure 12C1).

Since the α1 subunit C-terminal tail was important for $GABA_A$ receptor surface expression, the α1 subunit C-terminal tail were then introduced into β2 subunits, β2(tail+), as a first step toward determining if α1 subunit C-terminal tails could restore β2(loopΔ)-induced reduction of receptor surface levels (Figure 12C2). Surprisingly, introduction of the α1 subunit C-terminal tail into the β2 subunit resulted in a significant reduction of surface levels of both types of subunits ($p < 0.001$, $n = 8$); 55% and 62% of control α1

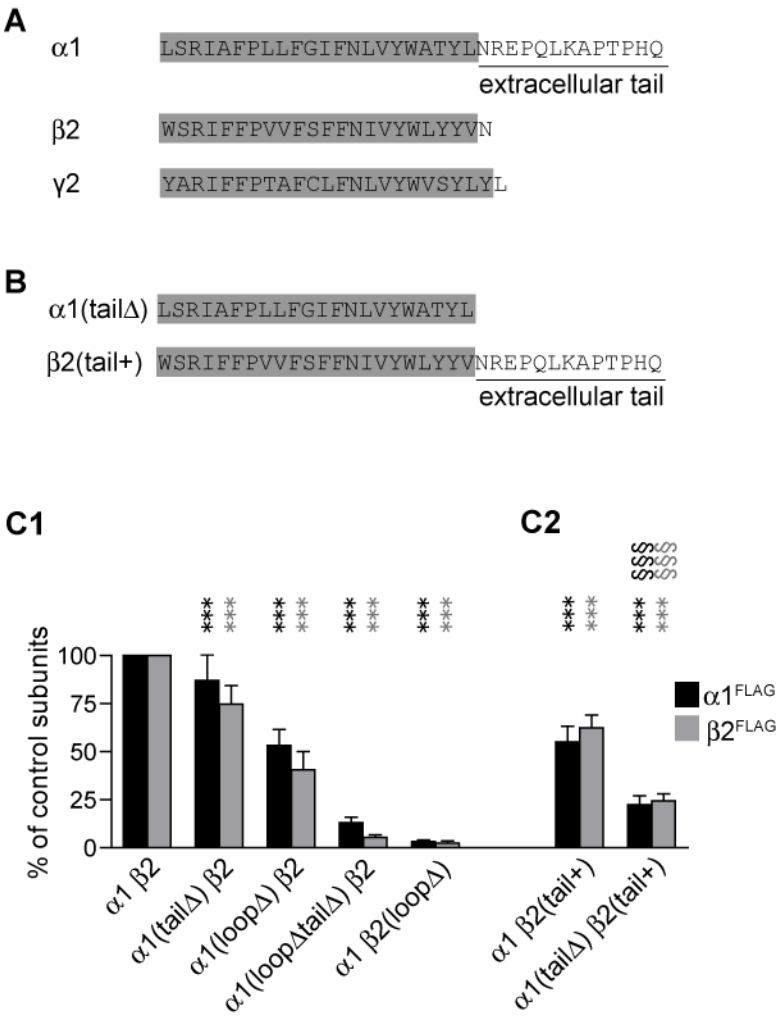

Figure 12. Effects of deletion of α1 subunit C-terminal tails and insertion of the tail into β2 subunits on α1β2 receptor surface levels

A, Comparison of the extracellular C-terminal portions of α1, β2 and γ2 subunits is presented. The preceding M4 domains are highlighted. Note that only the α1 subunit contains a long C-terminal tail. **B**, Schematic representation indicates the region deleted in the α1(tailΔ) and the region inserted in the β2(tail+). **C1-2**, Surface $\alpha1^{FLAG}$ (black bars), and $\beta2^{FLAG}$ (grey bars) subunit levels were quantified in each condition (indicated on the bottom) as a percentage of control subunit coexpression. *** corresponds to $p < 0.001$ compared to the control subunit coexpression; §§§ corresponds to $p < 0.001$ compared to the α1β2(tail+) subunit coexpression.

and β2 subunits were obtained. To determine if only one type of subunit in a $GABA_A$ receptor could contain the long C-terminal tail, which may have caused the reduction of receptor surface levels with coexpression of α1β2(tail+) subunits, α1(tailΔ) and β2(tail+) subunits were coexpressed. However, in this condition, α1 and β2 subunit levels were synergistically reduced to 22% and 24% of control subunit levels, respectively (n = 5, Figure 12C2).

The data suggested that the α1 subunit C-terminal tail was important for receptor surface expression, and that this was potentially the basis for the reduced impact of α1 subunit loop deletion on surface expression compared to β2 and γ2S subunits. Introduction of the α1 subunit C-terminal tails into β2 subunits reduced surface levels of both the mutant β2 subunits and the partnering α1 subunits, whether or not the α1 subunits contained the long C-terminal tails. This suggested that that the positions of the α1 subunit tails in the receptor pentamer were important, allowing interaction with other subunit regions, presumably N-terminal and M4 domains, to support receptor surface expression.

A fourteen amino acid motif at the C-terminal end of the β2 subunit M3-M4 loop was required for receptor surface expression

To determine the molecular mechanism for the β2(loopΔ) subunit-induced reduction of receptor surface expression, cDNA constructs with smaller portions of the β2 M3-M4 loop deleted were made (Figure 13A). The β2 subunit M3-M4 loop contains several protein binding motifs involved in receptor trafficking and endocytosis including BIG2, GRIF-1 and AP2 binding motifs (Figure 3). Based on BIG2 and GRIF-1 binding motifs, the M3-M4 loop was divided into three regions and constructs with individual

motifs deleted were made: β2(BIG2Δ), β2(GRIF-1Δ) and β2(postGRIF-1Δ) subunits. Coexpression of β2(BIG2Δ) with α1 subunits led to a small but significant increase of α1 subunit surface levels (121% of control α1 subunits, $p < 0.01$, $n = 6$) but no significant change in β2 subunit surface levels relative to the control condition (Figure 13B). In contrast, coexpression of α1 and β2(GRIF-1Δ) subunits significantly reduced surface levels of both subunit types (both types of subunits were 80% of control α1 and β2 levels; $p < 0.05$ for α1 subunits and $p < 0.05$ for β2(GRIF-1Δ) subunits, $n = 6$) (Figure 13B). Finally, coexpression of α1 with β2(postGRIF-1Δ) subunits resulted in a large reduction of cell surface levels of both subunits to levels comparable to those with α1β2(loopΔ) subunit coexpression (3% and 2% of control α1 and β2 subunit levels, respectively) ($n = 7$; Figure 13B).

Based on these results, the region of interest was narrowed to the C-terminal portion of the β2 M3-M4 loop (Figure 13A). A β2 subunit construct containing only the region after the GRIF-1 sequence (β2(postGRIF-1+) subunit; a $\beta2_{327\text{-}419}$ subunit deletion) was then made to determine if the post GRIF-1 region was sufficient for appreciable receptor surface expression (Figure 13A). Although significantly lower than control subunit surface levels ($p < 0.001$, $n = 8$), α1 and β2(postGRIF-1+) subunit surface levels were still 64% and 54% of control α1 and β2 subunit levels, respectively (Figure 13B), and were significantly higher than those with α1β2(loopΔ) and α1β2(postGRIF1Δ) subunit coexpression ($p < 0.001$, $n = 8$; for both subunits and both transfection conditions; Figure 13B). The β2(postGRIF-1+) construct contained the AP2 binding motif, $\beta2_{426\text{-}437}$, that has been shown to down regulate receptor surface expression (Figure 3).

Using a similar strategy, the post GRIF-1 motif was further divided into three regions based on the AP2 binding motif and three constructs were made with individual regions deleted: β2(postGRIF1+preAP2Δ), β2(postGRIF1+AP2Δ), and β2(postGRIF1+postAP2Δ) (Figure 13A). Deletion of the six amino acids before the AP2 binding motif (β2(postGRIF1+preAP2Δ) further decreased surface levels compared with α1 and β2(postGRIF1+) subunit surface levels (29% and 24% of control α1 and β2 subunit levels, respectively, $p < 0.001$, $n = 8$) (Figure 8B2). Conversely, deletion of the 12 amino acid AP2 binding motif (β2(postGRIF1+AP2Δ)) led to similar surface levels as those with α1 and β2(postGRIF1+) subunit coexpression (Figure 13B). Finally, deletion of the 14 amino acids distal to the AP2 binding motif (β2(postGRIF1+postAP2Δ)) yielded surface expression levels that were not different from those observed following deletion of the majority of the loop (β2(loopΔ)) or deletion of the postGRIF-1 region (β2(postGRIF-1Δ)). To confirm that this region was essential for receptor surface expression, a construct that only lacked the post-AP2 region (β2(postAP2Δ)) was made. Coexpression of this construct with the α1 subunit reduced subunit surface levels comparably to those obtained by expressing α1 and β2(loopΔ) subunits (Figure 13B). In addition, to determine if this region was sufficient for α1 and β2 subunit surface expression, a construct that only contained this region to link the M3 and M4 domains (β2(postAP2+); Figure 13A) was made. Supporting the sufficiency of the post AP2 region, α1β2(postAP2+) and the α1β2(postGRIF1+) receptor surface levels were not significantly different (Figure 13B). Taken together, these results suggested that the stretch of 14 amino acids after the AP2 binding motif played a major role in supporting surface expression of α1β2 receptors (more than 50% of control receptors; Figure 13B).

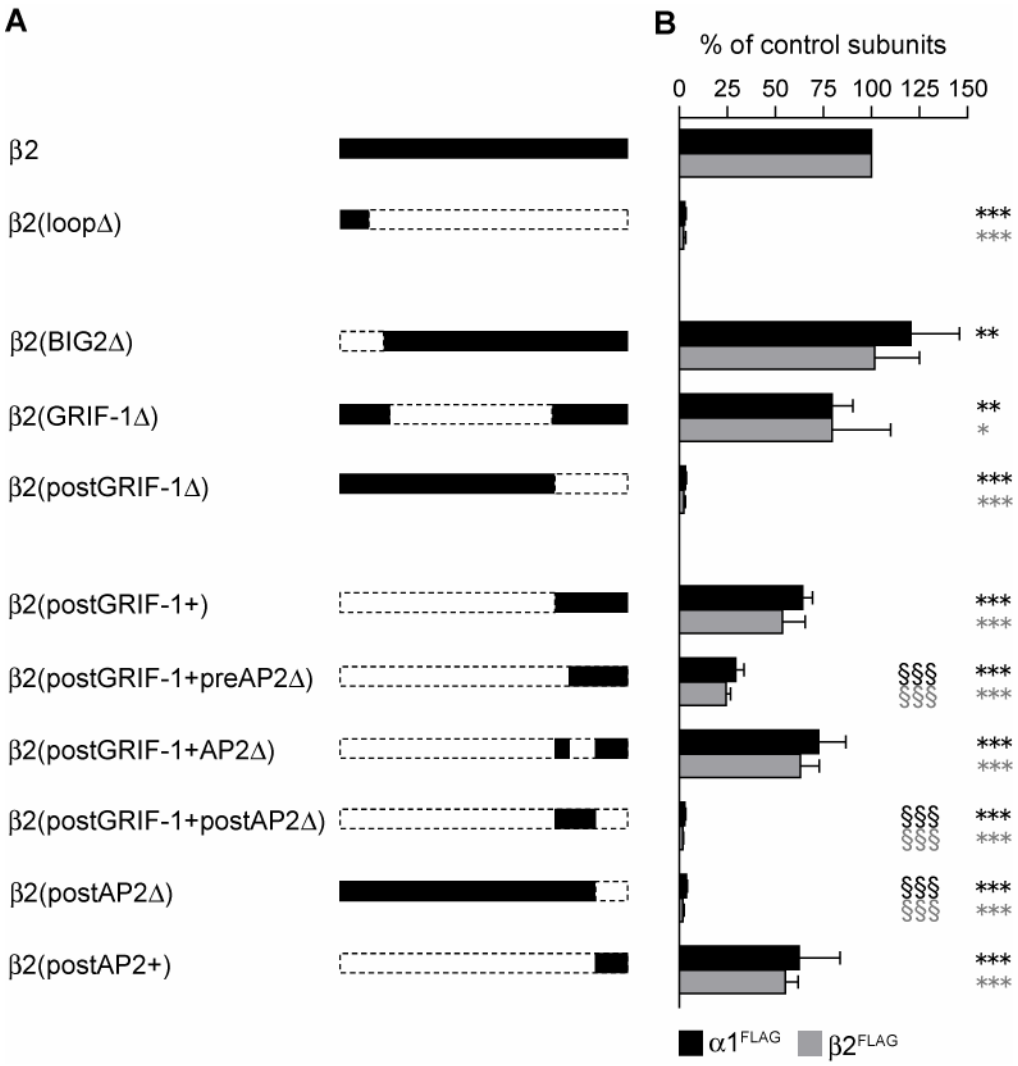

Figure 13. Segmental deletions of the β2 subunit M3-M4 loop decreased α1β2 receptor surface levels

A, Schematics of the β2 subunit M3-M4 loop segmental deletion constructs are shown. Retained regions of the M3-M4 loop are shown in black, while deleted regions are bordered by dotted lines. **B**, Relative surface expression levels of $\alpha1^{FLAG}$ (black bars) and $\beta2^{FLAG}$ (grey bars) subunits when each of the each of the β2 subunit deletion constructs was coexpressed with a wild type α1 subunit. *, **, and *** indicate $p < 0.05$, $p < 0.01$, and $p < 0.001$, respectively, relative to control α1β2 subunit coexpression. §§§ indicates $p < 0.001$ relative to α1β2(postGRIF-1+) subunit coexpression.

A nineteen amino acid motif at the C-terminal end of γ2S subunit M3-M4 loop, which overlaps with the $GABA_A$ receptor GABARAP binding motif, was important for α1β2γ2S receptor surface expression

We hypothesized that a motif in the γ2S subunit equivalent to the post-AP2 distal motif in the β2 subunit was responsible for the reduction of γ2 subunit surface expression with coexpression of α1, β2 and γ2(loopΔ) subunits. To test this hypothesis, the role of a nineteen amino acid motif located in a similar position, which almost completely overlapped with the GABARAP binding motif, on ternary receptor surface expression was explored.

Coexpression of α1 and β2 subunits with a γ2S subunit that lacked this nineteen amino acid motif (γ2S(GABARAPΔ)) resulted in a substantial reduction of γ2 subunit surface levels (14% of control; $p < 0.001$, $n = 3$; Figure 14). To further explore the importance of this sequence, a γ2 subunit construct containing only these nineteen amino acids linking its M3 and M4 domains (γ2(GABARAP+)) was made. Coexpression of α1 and β2 subunits with the γ2(GABARAP+) subunit resulted in γ2 subunit surface levels that were significantly higher than γ2S(GABARAPΔ) subunit surface levels with ternary subunit coexpression ($p < 0.001$, $n = 3$), and were 33% of control ($n = 3$). Although γ2S(GABARAPΔ) subunit surface levels with α1β2γ2S(GABARAPΔ) subunit coexpression were significantly higher than those with α1β2γ2(loopΔ) subunit coexpression ($p < 0.01$, $n = 3$), α1β2γ2S(GABARAPΔ) and α1β2γ2(GABARAP+) subunit coexpression data nonetheless indicated that this 19 amino acid motif was more important than the remainder of the M3-M4 loop (68 amino acids) for α1β2γ2S receptor surface expression and was consistent with data obtained with β2 subunit segmental

deletions, which indicated that distal portions of M3-M4 loops were much more important than the rest of the loops.

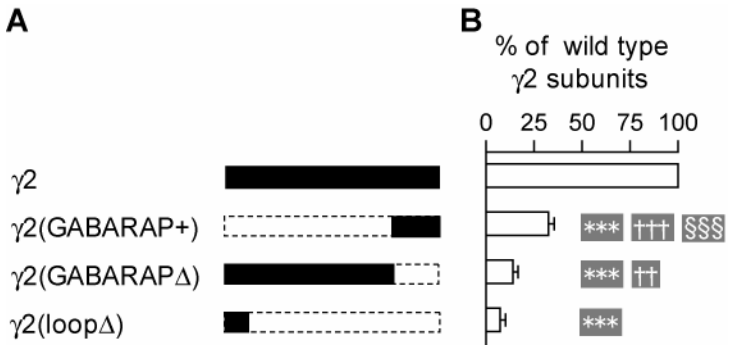

Figure 14. Segmental deletions of the γ2 subunit M3-M4 loop decreased α1β2γ2 receptor surface levels

A, Schematics of the γ2 subunit M3-M4 loop segmental deletion constructs are shown. Retained regions of the M3-M4 loop are shown in black, while deleted regions are bordered by dotted lines. **B**, Relative surface expression levels of $\gamma2^{FLAG}$ subunits when each of the each of the γ2 subunit deletion constructs was coexpressed with a wild type α1 and β2 subunit. *** indicates $p < 0.001$ relative to $\gamma2^{FLAG}$ surface level with α1β2γ2 subunit coexpression; †† and ††† indicate $p < 0.01$ and 0.001, respectively, relative to $\gamma2^{FLAG}$ surface level with α1β2γ2(loopΔ) subunit coexpression; §§§ indicates $p < 0.001$ relative to $\gamma2^{FLAG}$ surface level with α1β2γ2(GABARAPΔ) subunit coexpression.

Discussion

Deletion of the M3-M4 loop altered the cellular distribution of $GABA_A$ receptor subunits

By definition, total cellular subunit expression levels include subunits localized to both surface and intracellular compartments (~2:1 ratio, Botzolakis and Macdonald, unpublished). The significant reductions of surface, but not total, cellular levels of α1(loopΔ) and β2(loopΔ) subunits thus implied a relative increase of intracellular levels. Interestingly, immunoprecipitation studies revealed that α1(loopΔ) and β2(loopΔ) subunits oligomerized with partnering subunits, suggesting that subunit folding and subunit-subunit interactions were not abolished. In contrast, partnering wild type α1, β2 and γ2S subunit total cellular levels were reduced with both binary and ternary subunit coexpression, consistent with a decrease in surface, but not intracellular, subunit levels. Thus, the reduced surface levels and immature glycosylation of partnering wild type and loop-deleted α1 and β2 subunits suggested impaired forward trafficking and ER retention of both wild type and mutant subunits. In addition, the increased intracellular levels of loop-deleted subunits suggested that M3-M4 loops may be involved in subunit degradation, possibly via ERAD. It is possible that motifs in the missing portions of subunit M3-M4 loops were required for recognition by the ERAD machinery, thus decreasing the degradation efficiency of loop-deleted subunits.

In contrast to the unchanged α1(loopΔ) and β2(loopΔ) subunit total cellular protein levels with β2 and α1 subunit coexpression, a small but significant reduction of γ2(loopΔ) subunit total proteins with ternary subunit coexpression was observed. Similar to α1(loopΔ) and β2(loopΔ) subunits, γ2(loopΔ) subunits also significantly reduced total

cellular proteins of partnering α1 and β2 subunits despite the ability of α1β2 receptors to reach the cell surface with α1β2γ2(loopΔ) subunit coexpression. The reduction of partnering α1 and β2 subunit total expression levels may explain why surface levels of α1β2 receptors with α1β2γ2(loopΔ) subunit coexpression were lower than those with α1β2 subunit coexpression.

$GABA_A$ receptor subunit M3-M4 loops were involved in process(es) conferring permission to forward traffic beyond the ER

Regardless of the mechanism(s) stabilizing loop-deleted subunits, if loop deleted and wild type partnering subunits form pentamers, both types of subunits should have similar maturation, which could be determined by assessing glycosylation patterns. Therefore, if the reduction of total wild type partnering subunits was due to increased internalization from the cell surface and subsequent degradation in lysosomes, the accumulated mutant subunits should have had mature oligosaccharides that were resistant to endo H digestion. However, the majority of β2 and γ2 loop-deleted subunits were endo H sensitive, suggesting that the reduction of partnering subunits was not due to endocytosis from the surface, but instead, was due to degradation in the ER, likely ERAD. Coexpression of $\alpha 1_{\beta 2}$β2(loopΔ) subunits further supported the idea that loop-deletion of α1 or β2 subunits caused ER retention of both mutant and partnering subunits. The failure of $\alpha 1_{\beta 2}$ subunits to restore surface expression reduced by the β2(loopΔ) subunits weakened the hypothesis that $GABA_A$ receptor pentamers containing β2(loopΔ) subunits trafficked to the cell surface, and that reduced surface subunit levels were due to the requirement for the β2 subunit M3-M4 loop to stabilize "α1β2(loopΔ) receptors" on the cell surface.

In contrast to loop-deleted β2 and γ2 subunits, loop-deleted α1 subunits attained higher surface levels and endo H resistant fractions, suggesting less ER retention. Therefore, we cannot rule out the possibility that the reduction of partnering subunit total protein with α1(loopΔ)β2 subunit coexpression could have been due to destabilization of surface α1(loopΔ)β2 receptors that underwent fast endocytosis and sorting into lysosome for degradation and/or ER retention.

Potential underlying mechanisms for loop-deletion-induced $GABA_A$ receptor subunit ER retention

Based on the interchangeability of M3-M4 loops among different types of subunits and the presence of the extracellular long C-terminal tail that could be the cryptic signal used by α1(loopΔ) subunits for appreciable receptor surface expression, we propose that a shared signal is present at the distal ends of $GABA_A$ receptor subunit M3-M4 loops that is involved in trafficking of receptors beyond the ER. Long α subunit tails are also present in glycine receptors, which are also anionic Cys-loop receptors and are evolutionally derived from $GABA_A$ receptors (Ortells and Lunt, 1995). The long extracellular tails of glycine receptor α subunits may also regulate glycine receptor surface expression, but this remains to be elucidated.

Failure of oligomerization was excluded as the major cause of impaired β2(loopΔ) and γ2(loopΔ) subunit surface expression, since partnering subunits coexisted with loop-deleted subunits in coimmunoprecipitated complexes. Paradoxically, the surface expression profiles of $GABA_A$ receptors containing the loop-deleted mutant subunits were compatible with loop-deleted subunits causing impaired receptor assembly. Although the wild type and loop-deleted subunits appeared to be capable of

oligomerization, this does not ensure full assembly of receptor pentamers. In support of this argument, nACh receptor M3-M4 loops have been implicated in regulating nACh receptor assembly (Quiram et al., 1999;Roccamo and Barrantes, 2007).

Impaired γ2(loopΔ) subunit surface expression with appreciable α1β2 receptor surface expression with α1β2γ2(loopΔ) subunit coexpression may have a similar explanation. Prior to assembly, it is likely that subunit dimers, trimers, and tetramers are formed (Klausberger et al., 2001a). Our results imply failure of α1γ2(loopΔ) and β2γ2(loopΔ) subunit-containing oligomers to assemble with other oligomers or monomers and success of α1β2 subunit-containing oligomers to assemble into pentamers. Although γ2 subunits have been shown to be preferentially incorporated into $GABA_A$ receptor pentamers with α1 and β1 subunits (Angelotti and Macdonald, 1993), the failure of incorporation of γ2(loopΔ) subunit-containing oligomers during pentameric assembly could explain the observed surface expression of α1β2 receptors but not α1β2γ2(loopΔ) receptors with α1β2γ2(loopΔ) subunit coexpression.

We can not exclude, however, other possible explanations for the appearance α1β2 receptors on the cell surface despite γ2 subunit loop deletion. For example, distal motifs in the M3-M4 loops may be essential for sorting receptors into COPII complexes or masking ER retention signals in adjacent subunits. In either case, pentameric assembly might not be impaired, but forward trafficking of pentamers containing the mutant loop-deleted subunits might be impaired due to failed sorting into forward trafficking cargo or retrieval of fully assembled pentamers. The surface expression of α1β2 receptors with α1β2γ2(loopΔ) subunit coexpression might thus reflect α1β2 receptor simply being permitted to forward traffic while α1β2γ2(loopΔ) receptors are not.

Nevertheless, since assembly of pentamers is a prerequisite step for forward trafficking, we propose that the distal motifs in subunits M3-M4 loops are essential for permission to forward traffic beyond ER.

Jansen and colleagues have demonstrated that large portions of the M3-M4 loops of the 5-HT_{3A} subunits and ρ1 subunits, which can form homopentamers of 5-HT_3 and $GABA_C$ receptors, respectively, are not absolutely required for receptor assembly, surface expression and function. Thus, the biogenesis of Cys-loop receptors seems not to require any of the five M3-M4 loops in a receptor pentamer. However, their M3-M4 loop-deletion constructs keep a few amino acids at each ends of the M3-M4 loops (four amino acids, A-I-D-K, for the ρ1 subunit distal end; six amino acids, V-L-D-R-L-L, for the 5-HT_{3A} subunit distal end) and introduce a heptapeptide (S-Q-P-A-R-A-A), which is a prokaryotic equivalent of the eukaryotic M3-M4 loops (Jansen et al., 2008). Thus, the constructs may contain all essential elements of subunit M3-M4 loops for functional receptor surface expression. It is worth pointing out that their finding and the observations shown in this chapter are not in conflict. Furthermore, based on their finding, a smaller and more distal region of interest in the M3-M4 loops of $GABA_A$ receptor subunits is inferred and will be discussed in next chapter.

Interactions of C-terminal motifs with intracellular proteins for forward trafficking from the ER

In agreement with previous reports, our study revealed that deletion of GRIF-1 or GABARAP binding motifs reduced receptor surface levels, and deletion of AP2 binding motifs increased receptor surface levels (data not shown). In contrast to a previous report demonstrating that interactions between BIG2 and $GABA_A$ receptors facilitated receptor

export beyond the ER (Charych et al., 2004), deletion of BIG2 binding motifs increased receptor surface levels. It is possible that the BIG2 binding motif also interacted with other proteins that negatively regulated receptor surface expression.

Because of the location of the distal M3-M4 motifs, it is unlikely that these motifs are involved in inter-subunit interactions. Instead, the motifs are likely involved in recruiting intracellular proteins that regulate $GABA_A$ receptor assembly, forward trafficking, or masking of ER retention signals. Proteins interacting with distal motifs of subunit M3-M4 loops to regulate $GABA_A$ receptor forward trafficking remain to be identified. Since the distal motif responsible for appreciable surface expression of γ2 subunits almost completely overlaps the motif that binds the microtubule-associated protein, GABARAP (Wang et al., 1999;Wang and Olsen, 2000), it is possible that interactions between $GABA_A$ receptors and microtubules are involved in assembly of receptor pentamers and/or their forward trafficking. In support of this argument, ER exports are functionally coupled with microtubules (Watson et al., 2005). Although GABARAP only binds to γ1/2 subunits and not to α1-6, β1-3, δ, ε and ρ1 subunits (Nymann-Andersen et al., 2002), this does not exclude the possibility that the distal motifs in β2 subunit M3-M4 loops associate with other microtubule-associated proteins (MAPs). These predictions and the identities of MAPs associated with α1 and β2 subunits will need to be explored in future studies.

Alternatively, the distal motifs in the M3-M4 loops are involved in interactions with cellular chaperones, and deletions of these distal motifs cause misfolding of $GABA_A$ receptor subunits. If this is the case, decreasing temperature would facilitate subunit

folding and increase assembly efficiency and receptor surface levels. This postulate remains to be investigated.

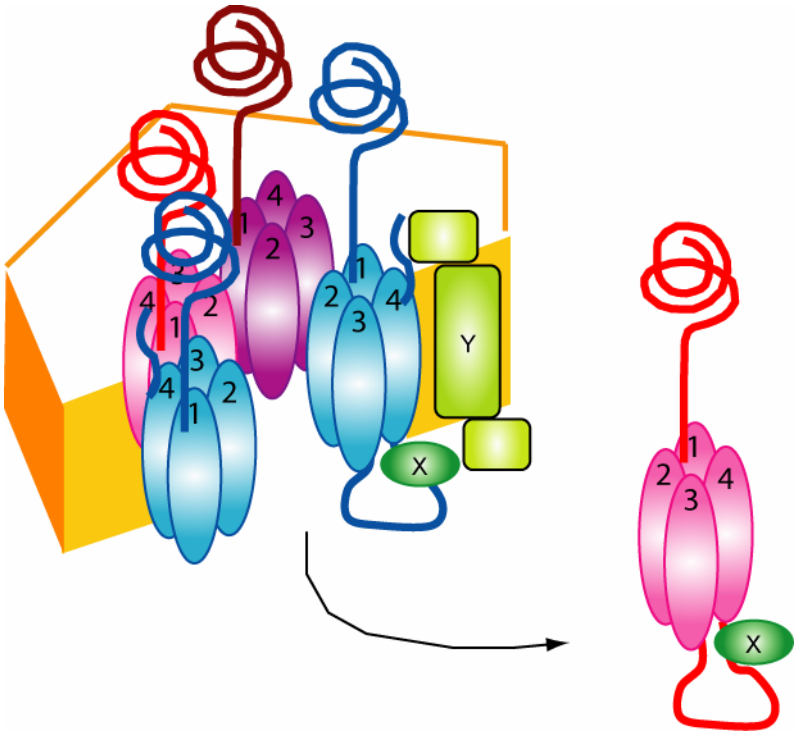

Figure 15. Proposed roles of the distal motifs in the M3-M4 loops of the $GABA_A$ receptor subunits

A schematic of an α1β2γ2 $GABA_A$ receptor is presented with the α1 subunits in blue, the β2 subunits in red, the γ2 subunit in purple and the lipid bilayer in yellow. The distal motifs of the subunit M3-M4 loops are involved in interacting with cellular proteins (X and Y) and are required for receptor assembly and/or forward trafficking. A transmembrane protein (Y) is predicted to interact with the unique extracellular tails of the α1 subunits as well and facilitate receptor assembly and/or forward trafficking. Microtubule associated proteins (X, which regulate receptor assembly and/or forward trafficking) and chaperones (X and/or Y, which regulate receptor subunit folding) are candidates for the interacting proteins.

CHAPTER III

A CONSERVED CYS-LOOP RECEPTOR ASPARTATE RESIDUE IN THE M3-M4 CYTOPLASMIC LOOP IS REQUIRED FOR $GABA_A$ RECEPTOR ASSEMBLY

Introduction

The Cys-loop superfamily of ligand-gated ion channels, which includes $GABA_A$ and $GABA_C$, nACh, glycine, and 5-HT_3 receptors, mediates fast synaptic transmission in the nervous system. Mutations that alter Cys-loop receptor surface density by affecting receptor biogenesis have been associated with IGEs (Frugier et al., 2007;Gallagher et al., 2004;Harkin et al., 2002;Kang and Macdonald, 2004), startle syndromes (Bakker et al., 2006), CMSs (Shen et al., 2005), and psychiatric disorders (Niesler et al., 2001a). Unfortunately, because the structural and cellular determinants of receptor biogenesis are poorly understood, development of effective treatment strategies remains a significant challenge.

A wealth of evidence suggests that Cys-loop receptors are assembled as heteropentamers from a large repertoire of neuronal subunits (Macdonald and Olsen, 1994;Le Novere and Changeux, 1999;Millar, 2003;Lynch, 2004). Subunits share a similar topology that includes an extracellular N-terminal domain, four transmembrane domains, three loops including a large cytoplasmic loop, and a variable length extracellular C-terminal tail (Macdonald and Olsen, 1994;Unwin, 2005). Receptor assembly is thought to occur in the ER following glycosylation and folding of *de novo* synthesized subunits (Smith et al., 1987;Green and Claudio, 1993;Connolly et al.,

1996;Gallagher et al., 2007). Assembly is closely monitored by ER quality control machinery, and consequently, subunits that fail to assemble properly are retained and degraded (Wang et al., 2002;Gallagher et al., 2005;Gallagher et al., 2007). While N-terminal motifs are known to be important for subunit assembly (Klausberger et al., 2001b;Hales et al., 2005), recent studies in nACh receptors suggest that C-terminal motifs may also play a role (Roccamo and Barrantes, 2007).

$GABA_A$ receptors are the most abundant Cys-loop receptor in the mammalian brain, and are responsible for the majority of fast inhibitory neurotransmission. Like other Cys-loop superfamily receptors, they are assembled from 16 subtypes of subunits (α1-6, β1-3, γ1-3, δ, ε, θ, and π) (Macdonald and Olsen, 1994). The β2 subunit, in particular, is an essential component of several widely distributed $GABA_A$ receptor isoforms (McKernan and Whiting, 1996) and is known to interact directly with several cellular regulatory proteins via its intracellular M3-M4 loop. For instance, it interacts with BIG2 and GRIF-1, which promote forward trafficking of $GABA_A$ receptors (Beck et al., 2002;Charych et al., 2004), and with AP2, which participates in clathrin-mediated receptor endocytosis (Kittler et al., 2000a).

To better understand how C-terminal motifs regulate Cys-loop receptor biogenesis, the role of the $GABA_A$ receptor cytoplasmic M3-M4 loop in receptor surface expression was evaluated in the previous chapter. Segmental deletions of the M3-M4 loops revealed that the C-terminal portions of the M3-M4 loops were important for receptors exiting from the ER. A multiple sequence alignment of Cys-loop receptor subunits reveals a highly conserved aspartate residue at the boundary of the M3-M4 loop and M4 domain. The study presented here demonstrates that the conserved residue in the

$GABA_A$ receptor α1, β2, or γ2 subunit is required for binary and/or ternary receptor surface expression. Results from endo H digestion, brefeldin A treatment, and analytic centrifugation revealed that mutation of this aspartate residue caused mutant and partnering subunits to be retained in the ER, the result of impaired higher-order oligomerization. The data thus provide evidence that C-terminal motifs are also important for receptor assembly.

Materials and methods

Preparation of cDNA constructs

The cDNAs encoding human α1, β2, and γ2S subunit polypeptides including their signal peptides were inserted into the pcDNA3.1(+) vector as described previously (Gallagher et al., 2005). The cDNA encoding the FLAG peptide, D-Y-K-D-D-D-D-K, was introduced between the 8th and 9th amino acid of the mature α1 subunit and the 4th and 5th amino acid of the mature β2 and γ2S subunits. Of note, murine β2 and γ2 subunits (which have identical sequences to their human counterparts) containing FLAG tags at the same position have previously been demonstrated to form receptors that are functionally indistinguishable from wild-type receptors (Connolly et al., 1996). Consistent with this finding, we demonstrated that insertion of the FLAG tag between the 8th and 9th amino acid of the human α1 subunit did not alter $GABA_A$ receptor current amplitude, GABA EC_{50}, or surface expression (Lo et al., 2008). Point mutations were performed with the QuikChange Site-Directed Mutagenesis Kit (Stratagene).

Table 4. Forward sequences of primer pairs for Site-Directed mutagenesis II

Mutation	Forward primer sequence (5' to 3')
Mutating the conserved aspartate residues in the α1, β2 and γ2 subunits	
α1(D420A)	GTC AGC AAA ATT **GCC*** CGA CTG TCA AG
β2(D450A)	GTG AAC GCC ATT **GCT** CGG TGG TCC CGC
β2(D450E)	GTG AAC GCC ATT **GAG** CGG TGG TCC CGC
γ2(D442A)	CGC ATT GCC AAA ATG **GCC** TCC TAT GCT CGG

* codons in bold were responsible for the designed point mutation.

Cell culture and transfection

HEK293T cells were purchased from ATCC (CRL-11268). Cells were incubated at 37°C in humidified 5% CO_2/95% air and grown in Dulbecco's Modified Eagle Medium (Invitrogen) supplemented with 10% fetal bovine serum, 100 i.u./mL penicillin, and 100 μg/mL streptomycin (Invitrogen). For binary subunit coexpression, cells were cotransfected with equal amounts (by mass) of α1 and β2 subunit cDNAs using the FuGene6 transfection reagent (Roche) (6 μL of reagent per 2 μg of cDNA per 60-mm diameter culture dish), and for ternary subunit coexpression, cells were transfected with equal amounts of α1, β2, and γ2S subunit cDNAs (9 μL of reagent per 3 μg of cDNA at a 1:1:1 cDNA ratio per 60-mm culture dish). The cDNA-FuGene6 mixture volumes were scaled up or down proportionally to the surface areas of different sized cell culture dishes. Forty-eight hours later, transfected cells were subjected to the following experiments.

Flow cytometry

To collect cells for flow cytometry analysis, monolayer cultures of HEK293T cells were dissociated by 37°C trypsin (Invitrogen) for 2 minutes. Trypsinization then

was stopped in 4°C PBS containing 2% fetal bovine serum and 0.05% sodium azide (FACS buffer). Although trypsin could cleave the extracellular N-terminal domain, thereby removing the FLAG epitope, the relative surface expression profile of FLAG-tagged subunits from cells dissociated by trypsin was similar to that of cells dissociated by protease-free cell detaching solution, (2 mM EDTA in PBS) (Gurba and Macdonald, unpublished).

Following washes with FACS buffer, cells were incubated with anti-FLAG IgG directly conjugated with R-Phycoerythrin (PE, 1:50 dilution, Martek) for 1 hour. Cells were then washed with FACS buffer again and fixed with 2% paraformaldehyde. Samples were run on a BectonDickson FACS Calibur equipped with 488 nm argon-ion and 635 nm red-diode lasers. For each staining condition, 50,000 cells were analyzed. Non-viable cells were excluded from analysis based on forward- and side-scatter profiles (chapter II), as determined by staining with 7-AAD (Invitrogen), which was excited using the 488 nm laser and detected with a 670 nm longpass filter (FL3). The PE fluorophore was excited using the 488 nm laser and detected with a 585/42 bandpass filter (FL2). Data were acquired using CellQuest (BD Biosciences) and analyzed offline using FlowJo 7.1 (Treestar, Inc.). For each sample, the fluorescence index (FI) was calculated by determining the percentage of positively-transfected cells (i.e., cells with a fluorescence intensity greater than 99% of mock-transfected cells) and multiplying this value by the mean fluorescence intensity of those cells. The FI of each experimental condition was then normalized to that of the control condition (i.e., $\alpha 1^{FLAG}\beta 2$ or $\alpha 1\beta 2^{FLAG}$) for comparison. Unless otherwise specified, a one-way ANOVA with Tukey's post test was

used to determine if there were significant differences in surface levels among transfection conditions. Data were expressed as mean ± SD.

Multiple sequence alignment

45 polypeptide sequences of human Cys-loop superfamily receptor subunits were aligned using Multalin software (bioinfo.genopole-toulouse.prd.fr/multalin/multalin.html) (Corpet, 1988). Penalties (subtractions of alignment scores) were applied to insertion and extension of internal gaps, and also to terminal gaps. This was required for proper alignment of C-terminal domains.

Immunoblotting

Membrane proteins in transfected cells were extracted in modified RIPA containing 10-50 mM Tris-HCl (pH 7.4), 150 mM NaCl, 1.0 mM EDTA, 1-2% NP-40, 0.25-0.5% sodium deoxycholate, and protease inhibitor cocktail (complete mini, Roche). Cell lysates were cleaned by centrifugation at 10,000X g for 30 minutes. The supernatants were subjected to further experiments or directly to SDS-PAGE. Proteins in gels were transferred to PVDF membranes (Millipore).

Monoclonal anti-$GABA_A$ receptor α1 subunit antibodies (final concentration 5 μg/mL, clone: BD24, Chemicon) and monoclonal anti-$GABA_A$ receptor β2/3 antibodies (4 μg/mL, clone: 62-3G1, Upstate) were used to detect wild type or modified human α1 and β2 subunits, respectively. Anti-sodium potassium ATPase antibodies (0.2 μg/mL, clone: ab7671, Abcam) were used to check loading variability. Following incubation with primary antibodies, secondary goat anti-mouse IgG heavy and light chain antibodies

conjugated with horseradish peroxidase were used in 1:10,000X dilution (Immunoresearch laboratories) for the visualization of specific bands in enhanced chemiluminescent detection system (Amersham Biosciences).

The signals were collected in a digital ChemImager (Alpha Innotech). The IDV, pixel intensity X mm^2, were then calculated using the FluorChem 5500 software. To compare the expression levels between the same subtype subunits with different mutations, we normalized adjusted IDVs (normalized to loading control Na^+/K^+ ATPase IDVs) to those of control conditions (coexpression of wild type α1 and β2 subunits).

Biotinylation of cell surface proteins

Cell surface proteins were biotinylated with membrane impermeable reagent sulfo-NHS-SS-biotin (1 mg/mL, Pierce) in phosphate buffered saline containing 1.0 mM $MgCl_2$ and 0.1 mM $CaCl_2$ (PBS+MC) at 4°C for 30 minutes. After incubation, biotin was quenched with 0.1 M glycine in PBS+MC. Following washes with PBS+MC, cells were lysed in RIPA buffer with protease inhibitors. After centrifugation to pellet cellular debris, the biotin-labeled plasma membrane proteins were pulled down by streptavidin beads (Pierce) from the supernatant. Pulled down proteins were eluted with sample buffer (Pierce) and were subjected to SDS-PAGE and western blots.

Glycosidase digestion

Whole cell lysates obtained from 10 mM-Tris RIPA buffer (10 mM Tris-HCl, 150 mM NaCl, 1.0 mM EDTA, 1% NP-40, 0.25% sodium deoxycholate) extraction were subjected to endo H and PNGaseF digestion (New England BioLab) following the

manufacturer's recommended protocol. The digestion reactions were carried out at 37°C for 3 hours and terminated by addition of sample buffer.

Brefeldin A treatment

The forward trafficking of fully assembled $GABA_A$ receptors is a slow process. Although pentamer formation peaks six hours after *de novo* synthesis, appreciable surface expression is not detected until eight hours after subunit synthesis (Gorrie et al., 1997). Thus, to block fully assembled receptor pentamers from trafficking beyond the ER and being expressed on the cell surface, HEK293T cells were treated with 0.5 μg/mL brefeldin A (Sigma) six hours after transfection, and 24 hours after transfection, cells were harvested. The surface and total cellular protein levels were then measured using flow cytometry and immunoblots, respectively.

Analytic centrifugation

The use of sucrose density gradient fractionation to analyze the size of $GABA_A$ receptor subunit protein-complexes has been described (Taylor et al., 1999;Taylor et al., 2000). Membrane proteins were extracted using high-detergent RIPA buffer, which consisted of 25 mM Tris-HCl (pH 7.4), 150 mM NaCl, 1 mM EDTA, 2% NP-40, and 0.5% sodium deoxycholate. Supernatants were loaded on a 5-20% sucrose density gradient in high-detergent RIPA buffer with protease inhibitors. To calibrate each gradient, BSA was added as a control marker (sedimentation coefficient of 4.3 S). Endogenous aldolase was used as a second marker (sedimentation coefficient of 7.4 S). To separate protein complexes of different sizes, gradients were centrifuged in a

Beckman SW41 rotor at 33,500 rpm for 20 hours at 4°C. Each gradient was then manually fractionated at 500 μL intervals. The distributions of $GABA_A$ receptor subunits and protein markers within the sucrose density gradients were analyzed by Western blot.

Immunoprecipitation

Protein complexes containing FLAG-tagged $GABA_A$ receptor subunits were immunoprecipitated using EZview Red Anti-FLAG M2 beads (Sigma) at 4°C overnight. After three washes with extracting RIPA buffer, protein complexes were eluted with 100 μg/mL FLAG peptide (Sigma). The presence of $GABA_A$ receptor subunits was determined by Western blot.

Results

A conserved aspartate residue was required for α1β2 receptor surface expression

By comparing the α1 and β2 subunit M3-M4 loop sequences, only three amino acids, I-D-R, were found to be shared between α1 and β2 subunits in the β2 subunit postAP2 region (Figure 16). Furthermore, multiple sequence alignments showed that the aspartate in the I-D-R motif was conserved in the entire Cys-loop receptor superfamily (Figure 16). We thus hypothesized that the loss of this residue was responsible for the β2(loopΔ) induced loss of receptor surface expression. To test this hypothesis, the conserved aspartate was mutated to alanine in the α1 and β2 subunits, and the surface levels of α1(D420A)β2 and α1β2(D450A) receptors were measured using flow cytometry. Relative to the control condition, the α1(D420A) mutation caused more than a 90%

reduction in surface levels of both α1(D420A) and β2 subunits, while the β2(D450A) mutation resulted in more than a 95% surface reduction of both subunits (n = 4) (Figure 17A, B), demonstrating that the conserved aspartate residue was required for receptor surface expression.

Figure 16. Alignment of human Cys-loop receptor subunits revealed a conserved aspartate residue at the junction of the M3-M4 loop and the M4 domain

Partial sequences surrounding the junction of the M3-M4 cytoplasmic loop and the M4 transmembrane domain are shown for a subset of Cys-loop receptor subunits. The I-D-R and comparable motifs were highlighted in grey, and the conserved aspartate residues were bolded. Note that all forty-five known human Cys-loop receptor subunits contain this residue.

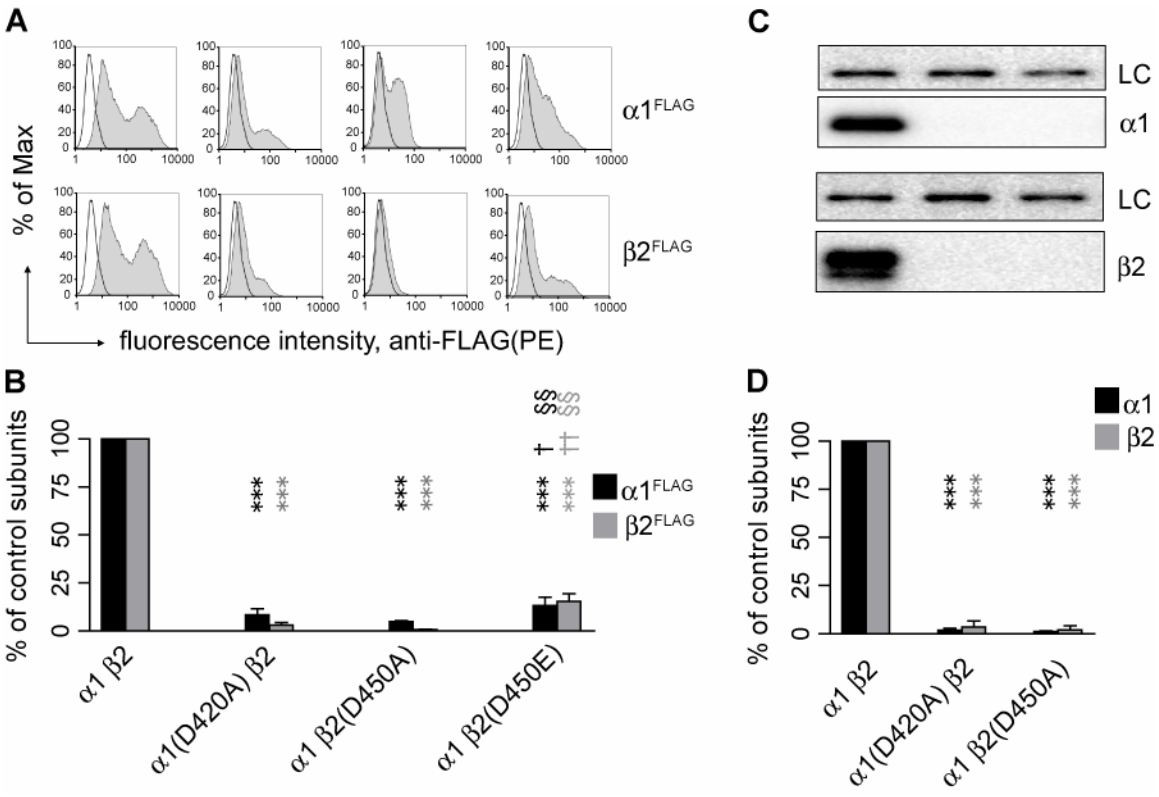

Figure 17. Mutation of the conserved M3-M4 aspartate residue in either α1 or β2 subunits markedly reduced α1β2 receptor surface levels

A, Representative fluorescence histograms of cells with control α1β2 (first column), α1(D420A)β2 (second column), α1β2(D450A) (third column), or α1β2(D450E) (fourth column) subunit coexpression were generated. Upper panels indicated surface $\alpha1^{FLAG}$ subunit levels while lower panels indicated surface $\beta2^{FLAG}$ subunit levels. **B**, Surface $\alpha1^{FLAG}$ (black bars) and $\beta2^{FLAG}$ (grey bars) subunit levels were quantified in each condition as a percentage of control subunit coexpression. **C**, Biotinylation was used to measure surface expression levels of α1 or β2 subunits. HEK 293T cells surface proteins were labeled with sulfo-NHS-SS-biotin, and then were pulled down using streptavidin beads. α1 and β2 subunits and loading control (LC, Na^+/K^+ ATPase) were detected using monoclonal antibodies, clones BD24, 62-3G1 and ab7671, respectively. **D**, To control the variations from the streptavidin pull-down, integrated density volumes (IDV, pixel intensity X mm^2) of various α1 and β2 subunits were normalized to those of Na^+/K^+ ATPase (LC). To compare surface expression levels of various α1 and β2 subunits with expression of α1β2, α1(D420A)β2 and α1β2(D450A) subunits, adjusted IDVs for various α1 and β2 subunits were further normalized to those of wild type α1 or β2 subunits. *** indicates $p < 0.001$ relative to control α1β2 subunit coexpression. † and †† indicate $p < 0.05$ and $p < 0.01$, respectively, relative to α1(D420A)β2 subunit coexpression. §§ indicates $p < 0.01$ relative to α1β2(D450A) subunit coexpression.

To determine if the loss of negative charge conferred by the aspartate residue was an important factor in the loss of surface expression, the conserved β2 subunit aspartate (D450) was mutated to glutamate, which is structurally conserved and has the same charge as aspartate. Expression of the β2(D450E) subunit, however, yielded α1β2 receptor surface levels that were still less than 10% of control levels. Although the reduction was significantly less than that produced by the D to A mutations ($p < 0.05$ for α1 subunits and $p < 0.01$ for β2 subunits as compared between α1(D420A)β2 and α1β2(D450E) expression; $p < 0.01$ for comparison between α1β2(D450A) and α1β2(D450E) expression for both subtypes of subunits; $n = 4$) (Figure 17A, B), the results nonetheless suggested that the loss of charge of the aspartate residue was not responsible for the reduction of receptor surface expression.

Surface biotinylation assays were also conducted to compare with results from flow cytometry analysis (Figure 17C). The α1(D420A) mutation led to more than a 95% reduction in α1(D420A)β2 receptor surface levels, while the β2(D450A) mutation led to more than a 98% reduction of surface levels (Figure 17D) as indicated by normalized IDVs. Thus, both techniques were in agreement and revealed that surface expression was abolished by the D450A mutant subunits. The slight difference in the extent of the reduction may originate from different affinities of the anti-FLAG, anti-α1 and anti-β2 antibodies.

The α1(D420A) or β2(D450A) subunit mutations reduced total protein levels and promoted ER retention of mutant and partnering subunits

There are several possible explanations for the low surface levels of α1(D420A) and β2(D450A) subunits. These include accelerated degradation, inefficient assembly,

impaired forward trafficking, and decreased cell surface stability. For multimeric subunit protein complexes such as the $GABA_A$ receptor, the ER is the frontline of quality control where misfolded and/or improperly assembled subunits are retained. Indeed, several mutations associated with IGEs have been shown to cause ER retention of $GABA_A$ receptor subunits (Harkin et al., 2002;Kang and Macdonald, 2004;Gallagher et al., 2005;Kang et al., 2006). We thus first determined if the loss of α1(D420A)β2 and α1β2(D450A) receptor surface expression was associated with ER retention. To explore this possibility, we took advantage of the fact that $GABA_A$ receptor subunits are glycosylated proteins and that oligosaccharide processing in the Golgi compartment confers resistance to endo H glycosidase digestion (Helenius and Aebi, 2004). As a result, $GABA_A$ receptor subunits that are ER retained should display endo H sensitivity, and endo H digestion should reduce the ER-retained subunit molecular mass to that produced by PNGaseF digestion (which removes all N-linked carbohydrates).

Endo H resistance was determined for α1 and β2 subunits expressed alone and also with α1β2, α1(D420A)β2, and α1β2(D450A) subunit coexpression (Figure 18). In agreement with reports that single subunits were retained in the ER (Connolly et al., 1996), expression of α1 or β2 subunits alone resulted in no visible bands with molecular masses higher than 46 kDa (for α1) or 48 kDa (for β2) after endo H digestion. Furthermore, the patterns for single subunit endo H digestions showed no difference from those for PNGaseF digestions (Figure 18A, B). Quantification of the endo H resistant fractions indicated that less than 3% of total proteins were endo H resistant (Figure 18C). In contrast, approximately 80% of α1 or β2 subunit total proteins were endo H resistant

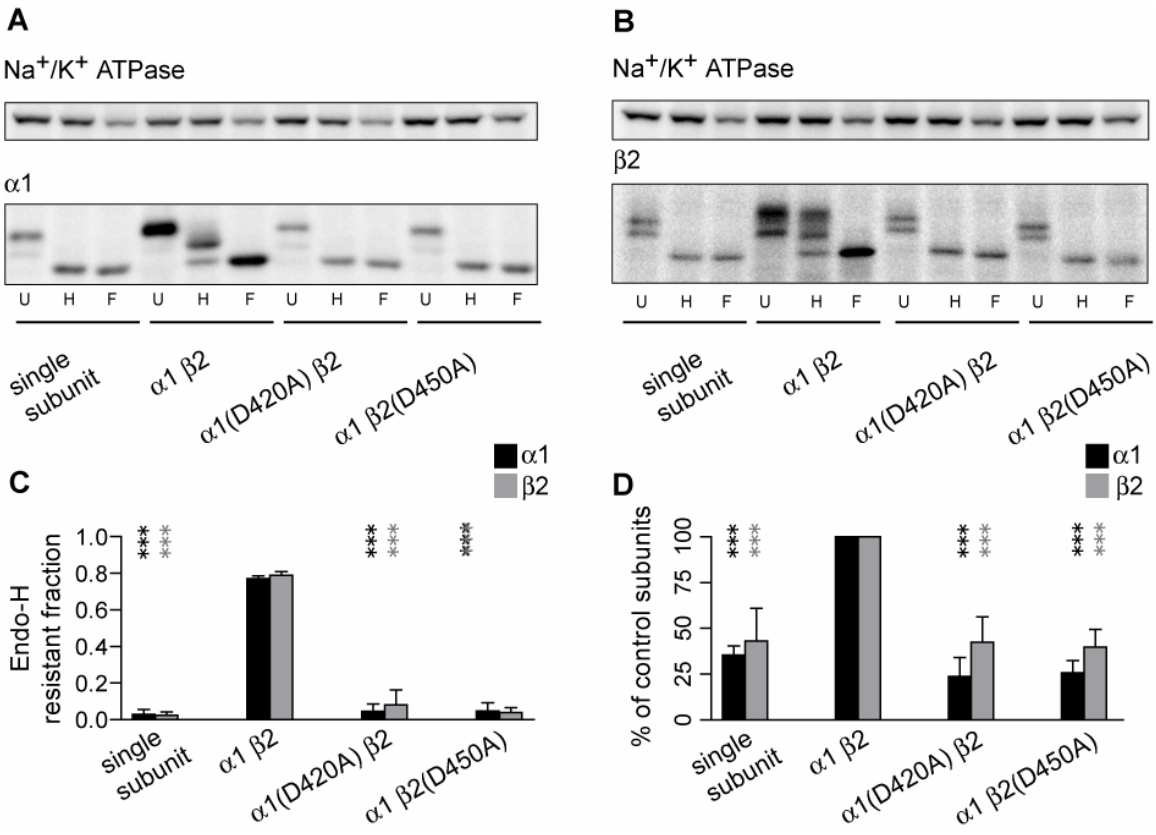

Figure 18. Mutation of the conserved aspartate residue resulted in reduced subunit total protein levels and ER retention of both mutant and partnering subunits

A, 10 mM Tris-RIPA buffer extracted proteins from expression of the α1 subunit alone ("single subunit") or coexpression of α1β2, α1(D420A)β2, and α1β2(D450A) subunits were undigested (U) or digested with endo H (H) or PNGaseF (F). An equal amount of total protein was loaded in each well. The undigested α1 subunits had mobility mainly at 50 kDa with a less apparent band that migrated at 48 kDa. After Endo H digestion, α1 subunits with mobility equal to that of subunits digested with PNGaseF (46 kDa) were considered endo H sensitive, while those with a higher molecular masses were considered endo H resistant. **B**, The criteria used in A were used to distinguish endo H sensitive and resistant populations of β2 subunits. Therefore, subunits that migrated at 54 and 51 kDa were considered to be endo H resistant, while those that migrated at 47 kDa were considered to be endo H sensitive. **C**, The fractions of endo H resistant populations of total α1 (black bars) or β2 (grey bars) subunits in the four expression conditions were quantified by dividing the IDVs of the Endo H resistant bands by the summed IDVs of the Endo H resistant and sensitive bands. **D**, Total subunit levels in each of the four expression conditions were compared. IDVs of α1 or β2 subunits were normalized to those obtained with control subunit coexpression. *** indicated $p < 0.001$ relative to control subunit coexpression.

with control α1β2 subunit coexpression, as represented by the presence of bands with molecular masses higher than 46 kDa (for α1) and 48 kDa (for β2) following endo H digestion (Figure 18A, B, C). The D to A mutations resulted in receptor subunit ER retention, and no more than 8% of α1 or β2 subunit total proteins were endo H resistant with α1(D420A)β2 and α1β2(D450A) subunit coexpression (Figure 18A, B, C).

Interestingly, while the α1(D420A) and β2(D450A) subunit endo H resistant fractions were significantly different from those of the control condition, they were not significantly different from those with single subunit expression. Similarly, while both α1 and β2 subunit total protein levels were reduced with α1(D420A)β2 and α1β2(D450A) subunit coexpression, total subunit levels were not significantly different from those with single subunit expression (Figure 18D). Thus, the results revealed that the majority of subunits with α1(D420A)β2 and α1β2(D450A) subunit coexpression were not distributed in compartments beyond the ER, and moreover, demonstrated that mutant subunits were processed similarly to individually transfected wild-type subunits.

The loss of receptor surface expression caused by the D to A mutation was not due to impaired forward trafficking or accelerated endocytosis from the cell surface

The observation that mutant subunits were retained in the ER suggested that the loss of receptor surface expression was mediated either by impaired receptor assembly or, alternatively, by impaired forward trafficking of normally assembled receptors. However, the possibility also remained that receptors were normally assembled and forward trafficked, but that surface levels appeared reduced because of markedly accelerated endocytosis. To distinguish between altered trafficking (either due to a decreased rate of forward trafficking or an increased rate of endocytosis) and impaired assembly, forward

trafficking of receptors was blocked by brefeldin A, a compound that inhibits receptor trafficking beyond the ER by collapsing the Golgi apparatus (Fujiwara et al., 1988). Indeed, if the loss of surface expression was caused by accelerated endocytosis, then in the absence of an appreciable surface pool, total expression levels should be the same for those subunits with control and mutant subunit coexpression. Similarly, if mutant subunits had impaired forward trafficking, then there should be no difference in total expression levels between wild-type and mutant receptors when neither is capable of leaving the ER. In contrast, if assembly of mutant subunits was compromised, then the reduction in total expression would still be expected, even when forward trafficking is blocked.

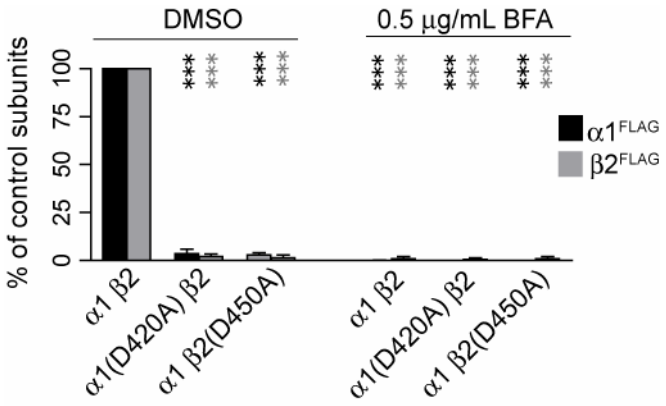

Figure 19. Application of 0.5 µg/mL brefeldin A could successfully block receptor surface expression

Surface $\alpha1^{FLAG}$ (black bars) and $\beta2^{FLAG}$ (grey bars) subunit levels were quantified in each condition as a percentage of control α1β2 subunit coexpression after applying either DMSO (left) or 0.5 µg/mL brefeldin A (BFA; right) six hours after transfection. *** indicates $p < 0.001$ relative to control subunit coexpression with DMSO treatment.

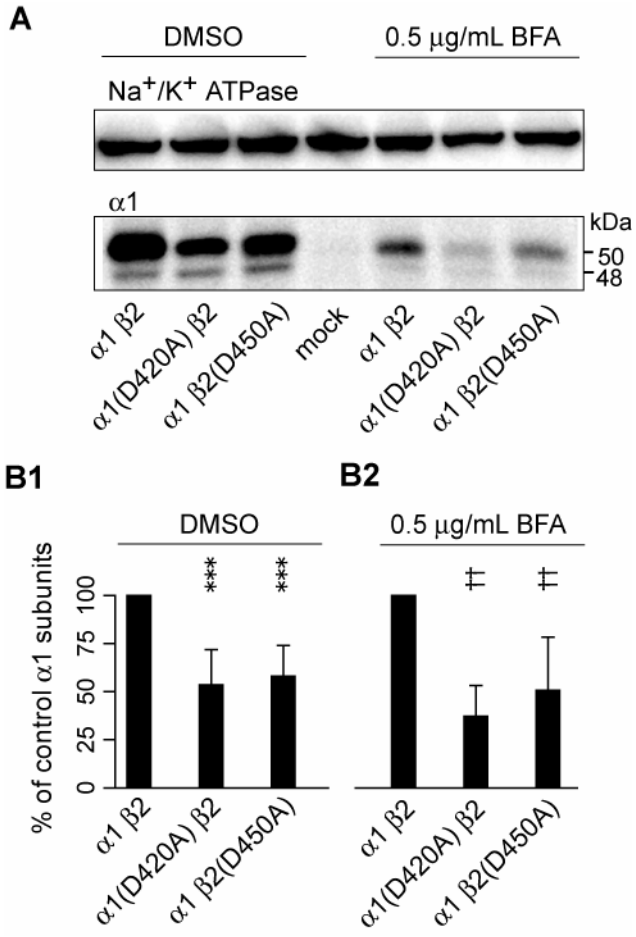

Figure 20. Control subunit total protein levels remained higher than those with α1(D420A)β2 or α1β2(D450A) subunit coexpression when retained in the ER

A, Immunoblots measuring Na^+/K^+ ATPase (upper panel, loading control) and α1 subunit (lower panel) total protein levels with α1β2, α1(D420A)β2, or α1β2(D450A) subunit coexpression after applying either DMSO (left) or 0.5 μg/mL brefeldin A (BFA; right) six hours after transfection. B1, Normalized total α1 protein levels with DMSO treatment. B2, Normalized total α1 protein levels with BFA treatment. *** indicates $p < 0.001$ relative to control subunit coexpression with DMSO treatment. †† indicates $p < 0.01$ relative comparison to control subunit coexpression with BFA treatment.

Measuring receptor subunit surface levels using flow cytometry revealed that 0.5 μg/mL brefeldin A successfully blocked cellular forward trafficking, as surface levels of control subunits were similar to those observed with α1(D420A)β2 or α1β2(D450A) subunit coexpression (n = 4; Figure 19). While treatment with brefeldin A decreased total expression levels for all conditions, presumably due to its cellular toxicity, total protein levels were still substantially higher with control α1β2 subunit coexpression than with α1(D420A)β2 or α1β2(D450A) subunit coexpression ($p < 0.01$ for both conditions; n = 5) (Figure 20A, B2). Thus, the accumulation of mutant subunits in the ER and reduction in total subunit levels could not be attributed to impaired forward trafficking or accelerated endocytosis of mutant receptors. Instead, the results suggested that mutation of the conserved aspartate residue affected early steps in receptor biogenesis.

With single subunit expression, mutant α1(D420A) and β2(D450A) subunits had the same total protein levels as wild type subunits but different glycosylation patterns

We demonstrated previously that the $GABA_A$ receptor α1(A322D) mutation caused subunit misfolding that resulted in rapid ERAD of mutant subunits prior to oligomerization (Gallagher et al., 2007). To determine if the total protein reductions observed with α1(D420A)β2 and α1β2(D450A) subunit expression were caused also by reductions in individual subunit availability, we compared expression of individual wild type α1 and β2 subunits to that of individual α1(D450A) and β2(D450A) subunits. Interestingly, we found that total protein levels of α1 or β2 single subunits were not significantly reduced by the D to A mutations (Figure 21A, B), suggesting that the mutation did not cause gross subunit misfolding (which would have been expected to trigger subunit degradation) (Gallagher et al., 2007). Both mutant subunits, however, had

altered glycosylation patterns, indicating that their cellular processing was abnormal. The β2(D450A) mutation shifted the molecular masses of the two major bands from 54 and 51 kDa to 52 and 50 kDa (Figure 21A), and while the α1(D420A) mutation did not produce mobility shifts, it increased the population migrating at 48 kDa at the expense of the population migrating at 50 kDa (Figure 21A).

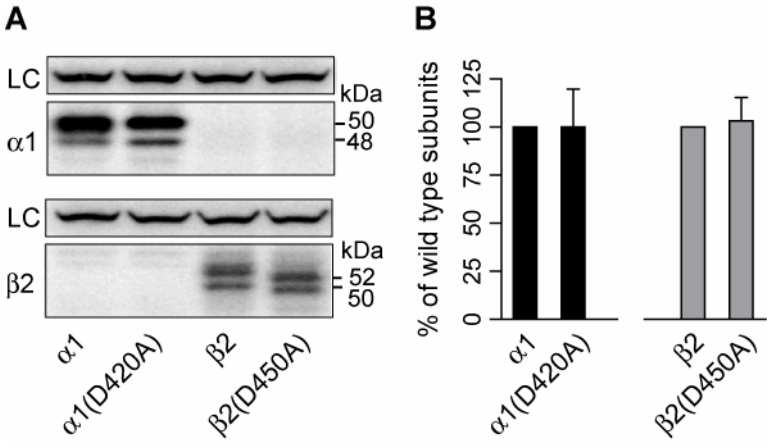

Figure 21. Single subunit total protein levels were determined using Western blot analysis

A, Total proteins were extracted from cells expressing single α1, α1(D420A), β2, or β2(D450A) subunits using RIPA buffer and immunoblotted with monoclonal anti-α1 (upper panels) and anti-β2 (lower panels) antibodies. Na^+/K^+ ATPase was used as loading control (LC). **B**, Total protein levels with single subunit expression were quantified. Black bars represented α1 subunit levels, while grey bars represented β2 subunit levels. To control for loading variability, the specific IDVs of α1 or β2 subunits were normalized to those of Na^+/K^+ ATPase. To compare wild type and mutant subunits, the adjusted IDVs of mutant subunits were further normalized to those of wild type subunits.

The α1(D420A) and β2(D450A) mutations impaired α1β2 receptor pentamer formation

The results in the previous sections suggested that mutation of the conserved aspartate residue in α1 or β2 subunits likely affected receptor biogenesis prior to pentameric forward trafficking and did not likely affect the availability of subunits for assembly. Thus, reduction of mutant and partnering subunit surface and total proteins to levels similar to those with single subunit expression could be the result of impaired assembly. To evaluate this possibility, analytic centrifugation was conducted to investigate the mass and shape of protein complexes with single subunit expression and with α1β2, α1(D420A)β2, and α1β2(D450A) subunit coexpression.

Analyses using 5-20% sucrose density gradients revealed that the sedimentation coefficient of the α1 subunit transfected alone was 7.4S, which was slightly higher than the previously reported 5S coefficient (Gorrie et al., 1997;Taylor et al., 1999). The sedimentation coefficient of α1β2 receptor complexes was 10.5S, which was also higher than the previously reported 9S coefficient (Gorrie et al., 1997;Taylor et al., 1999). The sub-population of α1β2 receptors that migrated as protein complexes smaller than 10.5 pentamers were assumed to be incompletely assembled subunit monomers or oligomers (Figure 22A, B). In contrast, the major receptor population formed with α1(D420A)β2 and α1β2(D450A) subunit had a sedimentation coefficient of 7.4S, with a profile that appeared to overlap with that of single subunit expression. However, a sub-population was evident with a sedimentation coefficient higher than 9S, suggesting that some pentamer formation could not be excluded entirely (Figure 22A2, B2). Nonetheless, even if this was the case, the results demonstrated that pentameric assembly was

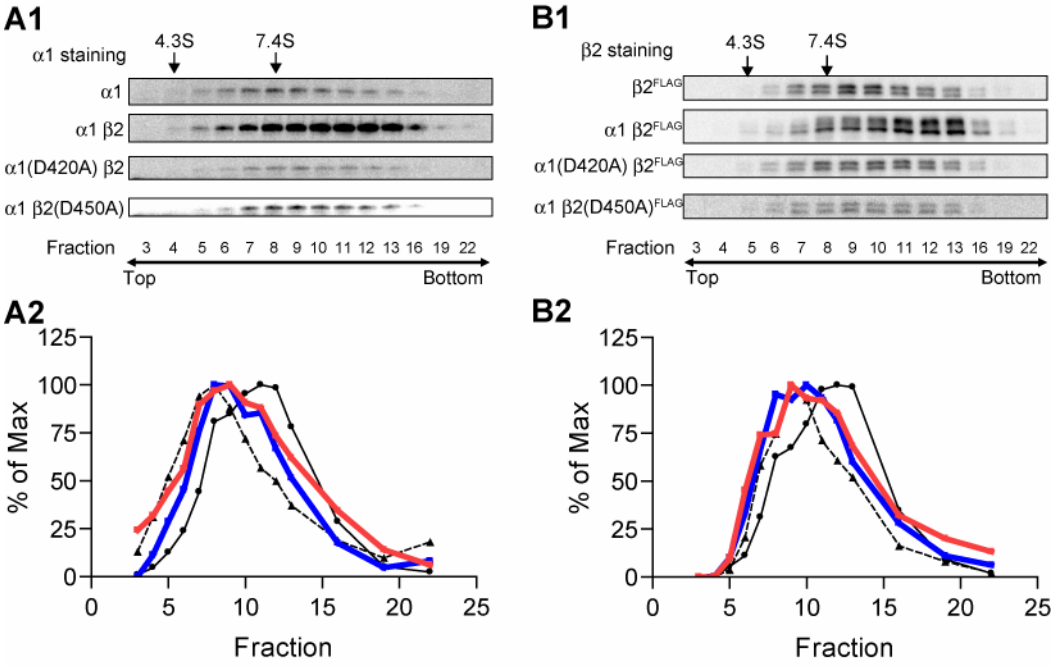

Figure 22. $GABA_A$ receptor protein complexes were analyzed using sucrose density gradients

Whole cell lysates were extracted using high-detergent RIPA buffer and subjected to 5-20% linear sucrose density gradients. Following centrifugation to separate protein complexes of different sizes, gradients were fractionated into 23 fractions from the top to bottom. 14 fractions were selected to analyze the sedimentation coefficients using Western blot and compared to proteins with known sedimentation coefficients (BSA, 4.3S; aldolase, 7.4S). The chosen fractions were indicated beneath the Western blots. **A1**, Representative Western blots of α1 subunit staining in single subunit (α1), α1β2, α1(D420A)β2, and α1β2(D450A) expression conditions were presented. **A2**, The distribution of α1 subunits in protein complexes with α1(D420A)β2 (thick blue line) and α1β2(D450A) (thick red line) subunit coexpression was plotted. The distributions of α1 subunits in protein complexes with single subunit expression (dotted line with ▲) or α1β2 subunit coexpression (hair-line with ●) were included for comparison. **B1 and B2**, As in Panels A1, A2, and A3, except that staining was for $\beta2^{FLAG}$ subunits using anti-β2 antibodies following immunoprecipitation with anti-FLAG M2 beads (to eliminate non-specific staining; see Figure 20).

substantially impaired by mutation of the conserved aspartate residue. It should be noted that the observed shifts to sedimentation coefficients higher than those predicted may have been caused by the strong association of interacting proteins with receptor complexes.

The α1(D420A) and β2(D450A) subunits oligomerized with partnering subunits

The sub-populations migrating with sedimentation coefficients higher than those of single subunit expression seen with α1(D420A)β2 and α1β2(D450A) subunit coexpression suggested that subunit oligomerization was still possible in the absence of the conserved aspartate residue. To determine if partnering subunits could, in fact, still associate with D to A mutated subunits, immunoprecipitation experiments were performed. With coexpression of D to A mutant and wild type partnering subunits, anti-FLAG M2 beads specifically immunoprecipitated FLAG-tagged β2 subunits whether they contained the D to A mutation or not (lower panel of Figure 23), but did not precipitate non-FLAG-tagged β2 subunits (data not shown, and Figure 9). Furthermore, the immunoprecipitated protein complexes contained associated partnering subunits whether or not they contained the D to A mutation (upper panel, Figure 23). Thus, the subunit surface level and total cellular protein reductions with α1(D420A)β2 and α1β2(D450A) subunit coexpression was not due to lack of subunit oligomerization.

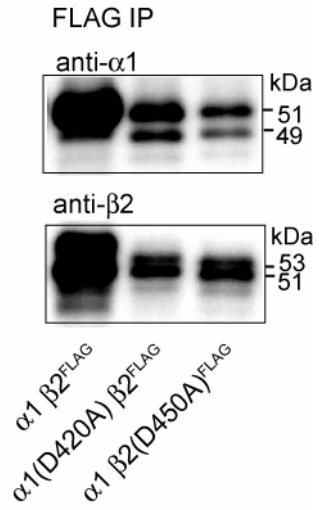

Figure 23. FLAG-tagged and partnering $GABA_A$ receptor subunits were coimmunoprecipitated

Representative immunoblots of proteins immunoprecipitated from cells with $\alpha1\beta2^{FLAG}$, $\alpha1(D420A)\beta2^{FLAG}$, and $\alpha1\beta2(D450A)^{FLAG}$ subunit coexpression using anti-FLAG M2 beads. Immunoprecipitated proteins were detected using monoclonal anti-α1 (upper panel) or anti-β2 antibodies (lower panel). Note the 1 kDa shift in molecular mass due to insertion of the FLAG epitope in the β2 subunit (compared to immunoblots of untagged subunits shown previous figures).

The conserved aspartate residue was required for α1β2γ2S receptor surface expression

Having established the importance of the conserved aspartate residue for binary α1β2 receptor expression, which is the simplest subunit combination supporting functional receptor surface expression, we next determined if the conserved residue was also required for surface expression of ternary α1β2γ2S receptors. Relative to control subunits, the D to A mutation in the α1 or β2 subunit caused significant surface level reductions of mutant and partnering subunits with ternary subunit coexpression ($p < 0.001$ for all subtypes of subunits and for both expression categories, n = 4-7) (Figure 24B). Subunit surface levels with α1(D420A)β2γ2S subunit coexpression were 27%, 36%, and 32% of control α1, β2, and γ2S subunit surface levels, respectively. With

α1β2(D450A)γ2S subunit coexpression, subunit surface levels were 11%, 8%, and 26% of control α1, β2, and γ2S subunit surface levels, respectively. Relative to α1(D420A)β2γ2S subunit coexpression, surface levels of α1 and β2 subtype subunits with α1β2(D450A)γ2S subunit coexpression were significantly lower ($p < 0.05$ for both subtype, $n = 4$), while γ2S subtype levels were not. Comparing the effects of the D to A mutation on ternary and binary receptor surface expression revealed that the presence of γ2S subunits could partially restore surface expression levels of α1 and β2 subunits when either of them contained the D to A mutation (to more than double the levels observed with binary subunit coexpression) (Figure 17B). However, the γ2S subunit is known to be able to reach the cell surface when expressed alone (Connolly et al., 1999b). It is therefore possible that these partnering subunits in incompletely-assembled intermediates associated with γ2S subunits and escaped from the ER.

Interestingly, while the γ2(D442A) subunit coexpressed with α1 and β2 subunits had very low surface expression (2% of control γ2S subunits, $p < 0.001$, $n = 4$), surface levels of partnering α1 subunits were not significantly affected (87% of control α1 subunits, $n = 3$), and surface levels of partnering β2 subunits were even increased (143% of control β2 subunits, $p < 0.001$, $n = 4$). These data indicated that the conserved residue of the γ2S subunit was essential for α1β2γ2S receptor surface expression, but not for α1β2 receptor surface expression. An explanation for this finding was that while γ2(D442A) subunits could not be incorporated into pentameric receptors, α1 and β2 subunits remained free to assemble and forward traffic.

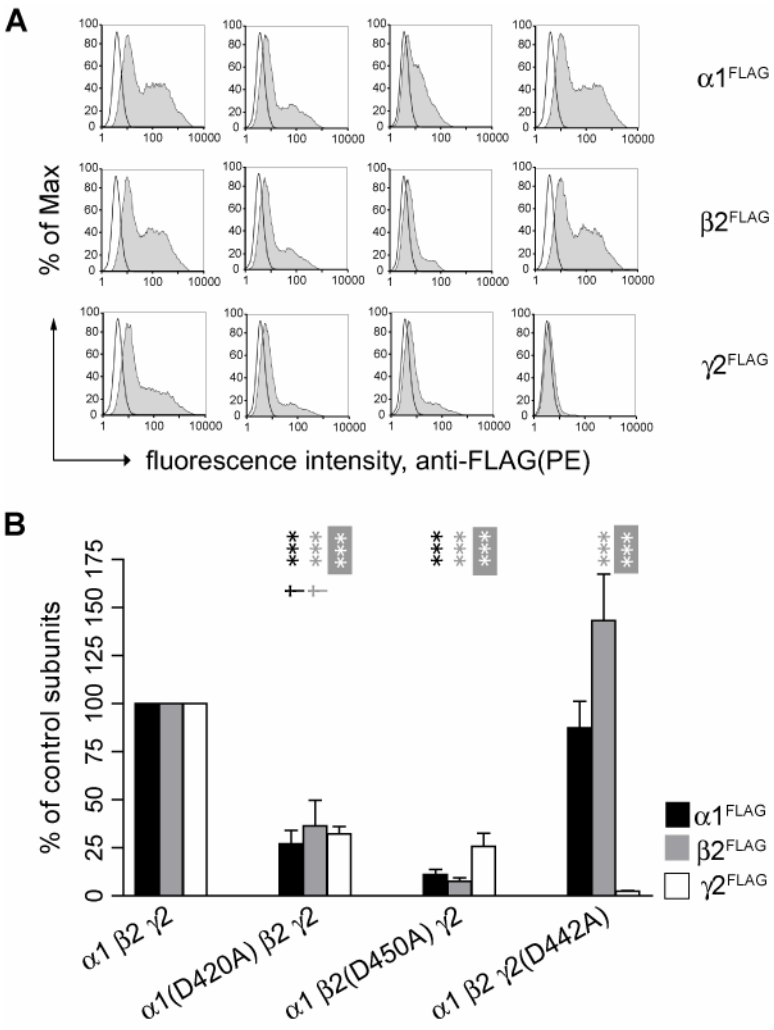

Figure 24. Mutation of the conserved aspartate residue to alanine in α1, β2, or γ2S subunits markedly reduced α1β2γ2S receptor surface levels

A, Representative fluorescence histograms of cells with control α1β2γ2S (first column), α1(D420A)β2γ2S (second column), α1β2(D450A)γ2S (third column), or α1β2γ2S(D442A) (fourth column) subunit coexpression were generated. Upper panels indicated surface $\alpha1^{FLAG}$ subunit levels, middle panels indicated surface $\beta2^{FLAG}$ subunit levels, and lower panels indicated surface $\gamma2S^{FLAG}$ levels. **B**, Surface $\alpha1^{FLAG}$ (black bars), $\beta2^{FLAG}$ (grey bars), and $\gamma2S^{FLAG}$ (white bars) subunit levels were quantified in each condition as a percentage of control subunit coexpression. *** indicates $p < 0.001$ relative to control α1β2γ2S subunit coexpression. † indicates $p < 0.05$ relative to α1β2(D450A)γ2S subunit coexpression.

Discussion

Mutation of a highly-conserved aspartate residue decreased $GABA_A$ receptor surface expression by impairing an early step in receptor biogenesis

Using a combination of flow cytometry, M3-M4 loop swaps, segmental deletions, and multiple sequence alignments, we identified an aspartate residue that was highly conserved among members of the Cys-loop receptor superfamily and required for $GABA_A$ receptor surface expression. Analysis of subunit maturation using glycosidase digestion and Western blotting revealed that mutation of this conserved residue resulted in ER retention of both mutant and partnering subunits, thereby decreasing their surface levels. This decrease in subunit surface levels was not due to impaired forward trafficking or accelerated endocytosis, as the relative total subunit levels were similar for control, α1(D420A)β2, and α1β2(D450A) subunit coexpression in the presence of brefeldin A, which prevented forward trafficking. Indeed, absolute total subunit levels with α1(D420A)β2 and α1β2(D450A) subunit coexpression were still lower than the control condition in the presence of brefeldin A, suggesting that subunits were trapped in the ER because of impaired receptor assembly.

Mutation of the conserved aspartate residue compromised pentameric receptor assembly without causing severe subunit misfolding

In combination, the glycosylation and brefeldin A experiments suggested that mutation of the conserved aspartate residue impaired an early step in receptor biogenesis, either by decreasing subunit availability for oligomerization, impairing subunit oligomerization, or preventing complete pentameric assembly. Our results, however,

argued against decreased subunit availability. We have previously demonstrated that an alanine to aspartate mutation in the $GABA_A$ receptor α1 subunit associated with juvenile myoclonic epilepsy, α1(A322D), caused protein misfolding and an increased rate of ERAD. Consequently, total cellular expression of α1(A322D) subunits was significantly reduced when expressed individually (Gallagher et al., 2005;Gallagher et al., 2007). Thus, if the α1(D420A) and β2(D450A) subunits were severely misfolded, we would have expected a similar outcome. However, with single subunit expression, mutating the conserved aspartate residues did not alter total subunit levels, suggesting that the rates of *de novo* synthesis and degradation of the α1(D420A) and β2(D450A) subunits were unchanged. This suggested that the observed reduction of partnering subunit total protein levels was secondary to reduced pentamer formation, as neither α1 nor β2 subunits are trafficking-competent when expressed alone (Connolly et al., 1996).

Using analytic centrifugation, we provided direct evidence that the conserved aspartate residue was required for receptor assembly. In agreement with previous reports that demonstrated that intact N-terminal domains were capable of mediating inter-subunit interactions (also demonstrated here using immunoprecipitation), protein complexes showing higher sedimentation coefficient than 7.4S with α1(D420A)β2 and α1β2(D450A) subunit coexpression were observed, indicating the presence of oligomerized subunit assembly intermediates. While we cannot rule out the possibility that some pentamers were formed, the lack of an appreciable 10.5 S sedimentation fraction suggests the pentameric population was relatively small. Thus, we concluded that mutating the conserved aspartate residue permitted some degree of subunit oligomerization, but prevented complete assembly of pentameric receptors.

The role of C-terminal motifs in the assembly of other Cys-loop family members

While this is the first report implicating a region other than the N-terminal domain in $GABA_A$ receptor assembly, the M3-M4 loop and M4 domain are known to be important for assembly of nACh receptors (Quiram et al., 1999). A three-amino acid deletion in the nicotinic acetylcholine receptor β subunit M3-M4 loop, β426ΔEQE, associated with CMS has been demonstrated to impair the interaction between β and δ subunits (Quiram et al., 1999). Moreover, mutation of histidine 408 in the α subunit, which is adjacent to the conserved aspartate residue, impaired receptor assembly and reduced the 9S pentamer population (Roccamo and Barrantes, 2007). The significance of the conserved aspartate residue was further emphasized by the finding that the nACh receptor εN436Δ subunit mutation associated with CMS, which is adjacent to the conserved aspartate residue in the ε subunit, reduced $\alpha_2\beta\delta\varepsilon$ receptor surface expression, as did deletion of the conserved aspartate residue, εD435Δ (Shen et al., 2005). While it remains unclear if this loss of surface expression also reflected impaired assembly, these examples nonetheless support the idea that C-terminal motifs are important determinants of Cys-loop receptor biogenesis.

The conserved aspartate residue may be exposed to the intracellular milieu

Increasing experimental evidence suggests that the conserved aspartate residue is not buried within subunit interfaces, and may actually be exposed to the intracellular milieu. For example, the H408 residue in nACh receptor α subunits, which is adjacent to the conserved D407 residue, was found to be labeled by the photoactivatable compound, 3-[^{3}H]azioctanol (Pratt et al., 2000). Thus, the region in nACh receptor α subunits

containing the M-D-H motif, which is analogous to the I-D-R motif in $GABA_A$ receptor α1 and β2 subunits, was not protected by intersubunit interactions. Support for this hypothesis comes from homology alignments to muscle nACh receptors, where the conserved aspartate residue appears exposed, even in the context of fully-assembled pentamers (Unwin, 2005). Furthermore, mass spectrometry of a motif containing the conserved aspartate residue in glycine receptors has been demonstrated to be exposed to the intracellular milieu (Leite et al., 2000). Although a crystal structure of the $GABA_A$ receptor has yet to be generated, given the degree of homology between $GABA_A$ receptors and the remainder of the Cys-loop family, these findings suggest that the conserved aspartate residue is exposed on the surface of pentamer complex (regardless of its location in the M3-M4 loop or M4 domain).

The conserved aspartate residue may be involved in interactions with other proteins

Based on the resolved structure of the nACh receptor, it has been suggested that the conserved aspartate residue is located at the beginning of a helix comprising the end to the M3-M4 loop and the M4 (Unwin, 2005). Because charged residues are hydrophilic, the conserved aspartate reside is favored to be in the cytoplasmic milieu (White and von Heijne, 2005). Substitution of the conserved aspartate with alanine could cause transmembrane helix tilt to move the hydrophobic alanine into the lipid. This allosteric change could theoretically affect subunit assembly. However, the D to E mutations in the β2 subunits disfavored this hypothesis as the conservative substitution, which is less likely to cause allosteric change, also caused significant reduction of surface receptor levels.

Mutation of the conserved aspartate not only caused ER retention of α1 and β2 subunits but also affected their glycosylation patterns. Although altered glycosylation did not preclude receptor surface expression (Buller et al., 1994) (data not shown), the results nonetheless demonstrated that C-terminal motifs could affect post-translational modification of N-terminal domains. This suggested the existence of mechanisms that coordinate intracellular and extracellular protein processing. Assuming that the conserved aspartate residue is not buried within subunit interfaces, one possibility is that it interacts with transmembrane and/or cytoplasmic proteins, which in turn, mediate communication between subunit domains located in extracellular, membrane, and/or intracellular environments. The observation that the conservative substitution of the aspartate residue with a glutamate residue could only partially restore receptor surface expression suggested that the residue could be located in a tightly structured environment where both charge and side-chain length play an important role for interaction. Furthermore, the aspartate residue could be important for maintaining critical secondary structure for protein interaction, although this secondary structure did not impair subunit oligomerization or cause protein degradation before oligomerization.

While the identity of the interacting cellular machinery and its distribution among different types of cells remains to be established, ER chaperones such as calnexin (a type I-integral membrane protein) (Ou et al., 1995) have been shown to regulate receptor subunit folding, assembly, and half-life, and are thus potential components of the yet-to-be-identified protein complex (Gelman et al., 1995;Wanamaker and Green, 2007). It is worth noting that Cys-loop superfamily receptors are present not only in neurons, but also in myocytes, epithelial cells, and lymphocytes (Maus et al., 1998;Skok et al., 2003). A

naturally occurring mutation in nACh receptor subunit M3-M4 loops associated with CMS has been shown to affect receptor assembly within muscle cells (Quiram et al., 1999). Furthermore, charged residues including the conserved aspartate in subunit M3-M4 loops have been demonstrated to affect receptor assembly in epithelium-like cells (Roccamo and Barrantes, 2007). Thus, the conserved aspartate residue may interact with ubiquitous cellular machinery.

Conclusions

With the simplest binary combination that allowed for functional $GABA_A$ receptor surface expression, our results demonstrated that the conserved aspartate residue at the boundary of the M3-M4 loop and the M4 transmembrane domain was required for Cys-loop receptor assembly. Consistent with this finding, D to A mutation in α1 and β2 subunits substantially decreased surface levels of ternary α1β2γ2S $GABA_A$ receptors, the most abundant isoform expressed in the mammalian brain (McKernan and Whiting, 1996). Interestingly, while D to A mutation of the γ2S subunit also reduced the ternary receptor population, it did not prevent formation of binary α1β2 receptors. This reflected the fact that α1 and β2 subunits could still assemble in the absence of γ2S subunits. Notably, α1 and β2 subunit surface levels were not reduced at all by the mutant γ2S subunit, supporting the hypothesis that the mutant γ2S subunit was unable to oligomerize with α1 and β2 subunits, or if it did oligomerize, the interaction was not sufficient for the γ2S subunit to have a dominant negative effect on assembly of α1β2 receptors.

CHAPTER IV

GLYCOSYLATION OF $GABA_A$ RECEPTOR β2 SUBUNITS

Introduction

N-linked glycosylation is important for biogenesis of glycosylated membrane proteins (Helenius and Aebi, 2004). Specifically, it plays an important role in protein folding, stability and trafficking. Co-translational conjugation of a *N*-glycan precursor, which is composed of two *N*-acetylglucosamine, nine mannose and three glucose residues, to the nascent polypeptide (Figure 25), is directed by the consensus sequence, N-X-S/T (where X can be any amino acid except proline). This post-translational covalent modification increases hydrophilicity of nascent polypeptides and prevents aggregation of folding intermediates (Ruddock and Molinari, 2006).

Several ER resident proteins have been demonstrated to facilitate protein folding. The removal of the outermost two glucose residues from an *N*-glycan by glucosidase I and II, respectively, leads to direct binding of calnexin and calreticulin to the nascent polypeptide (Hammond et al., 1994). The ER chaperones then introduce the nascent polypeptide to other proteins involved in protein folding such as ERp57, a homologue of protein disulfide isomerase (PDI), which has been shown to facilitate formation of structural disulfide bonds (Frickel et al., 2002). Conversely, removal of the third (innermost) glucose residue by glucosidase II leads to release of the glycoprotein from calnexin and calreticulin. Because the calnexin/calreticulin complex is part of the ER quality control machinery, polypeptides that dissociate from the ER chaperone complex

are directed to one of two pathways. If the glycoprotein folds and assembles properly (for multimeric proteins), it will exit from the ER and be trafficked to its final destination. However, if the glycoprotein is not in its native conformation, a UDP-glucose: glycoprotein glucosyltransferase (UGGT) can add back a single glucose to the outermost mannose residue on branch A (Parodi, 2000) (Figure 25), which results in re-association of the glycoprotein with the calnexin/calreticulin protein complex. It is worth noting that though a glycoprotein may contain multiple folding domains, the UGGT will only re-glycosylate *N*-glycans in the misfolded region.

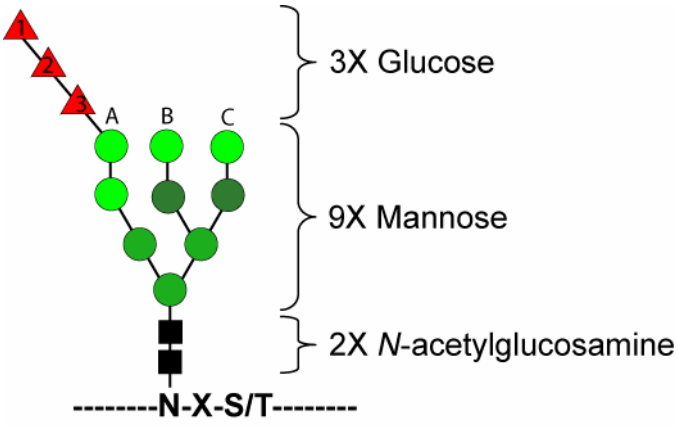

Figure 25. The schematic presentation of a precursor of all N-glycans added to a protein

Unprocessed oligosaccharides are composed of two *N*-acetylglucosamine residues (black squares), nine mannose residues (green circles), and three glucose residues (red triangles), which are numbered based on their extremity. The three branches in the glycan are labeled as A, B, C. Figure adapted from Ruddock and Molinari, 2006.

It has been proposed that cycles of deglucosylation/reglucosylation of *N*-glycans and disassociation/reassociation with calnexin/calreticulin are limited by a "mannose-timer" (Helenius, 1994). The model postulates that, once mannose trimming occurs, the proteins responsible for translocating glycoproteins from the ER to the cytosol for ERAD compete with calnexin for glycoprotein binding. In support of this model, inhibition of demannosylation protects misfolded glycoproteins from ERAD (Liu et al., 1999;Su et al., 1993), while overexpression of mannosidase accelerates onset of ERAD (Wu et al., 2003).

Blocking glycosylation of $GABA_A$ receptors using tunicamycin has been demonstrated to abolish receptor biogenesis at a stage later than receptor subunit oligomerization (Connolly et al., 1996). Furthermore, two glycosylation sites in the rat $GABA_A$ receptor α1 subunit have been shown to be important for receptor subunit folding as mutation of either of the two glycosylation sites decreased surface and total receptor expression at 37°C (Buller et al., 1994). Based on the consensus sequence, N-X-S/T, the human β2 subunit is predicted to have three glycosylation sites. Whether or not the predicted glycosylation sites are functional remains to be elucidated since predicted glycosylation sites are not always glycosylated (Apweiler et al., 1999;Kowarik et al., 2006). Furthermore, as demonstrated in chapter III, mutation of the absolutely conserved aspartate residue affected glycosylation of the β2 subunit N-terminal domain. To understand better how glycosylation regulates $GABA_A$ receptor biogenesis, particularly if the receptor surface level reduction caused by the β2 subunit mutation, D450A, is due to the disturbed glycosylation, the potential glycosylation sites in the β2 subunit were examined.

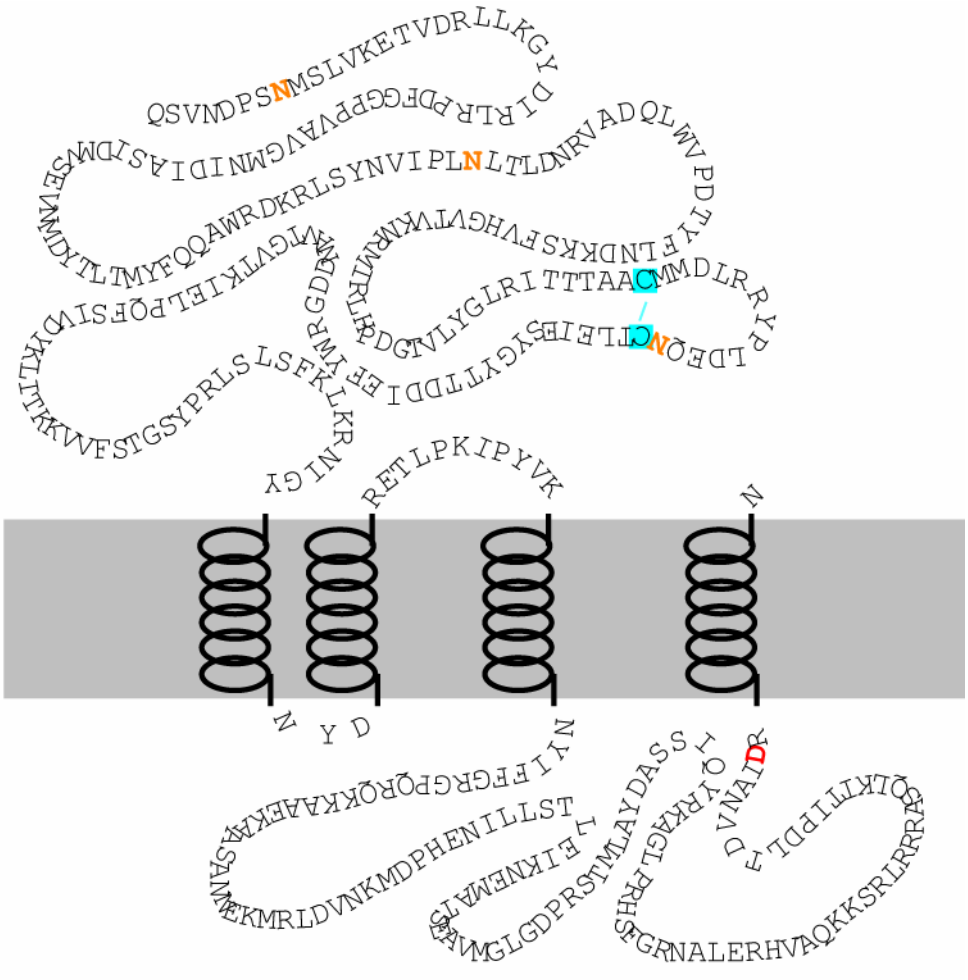

Figure 26. A schematic presentation of the human β2 subunit

The primary sequences of the N-terminal domain and the four loops were incorporated. The three glycosylation sites were marked in orange. Note that the third putative glycosylation site, N173 (including the signal peptide), is adjacent to the second residue of the two Cys-loop cysteines (highlighted in blue), which form the disulfide bond of the signature Cys-loop. The conserved aspartate residue at the boundary of the M3-M4 loop and the M4 domain was marked in red.

Materials and methods

DNA constructs

The cDNAs for native and FLAG-tagged human α1 and β2 subunits were prepared as described in previous chapters. Briefly, one FLAG epitope was introduced between the 8th and 9th position and the 4th and 5th position of the α1 and β2 subunit, respectively. FLAG-tagged subunits were functionally indistinguishable from native subunits in their electrophysiological properties and effects on partnering-subunit surface levels (Lo et al., 2008). Three potential glycosylation sites, N32, N104 and N173, were individually mutated to glutamine (N to Q mutations) using QuikChange Site-Directed Mutagenesis Kit (Stratagene). Furthermore, double- and triple-point mutations were performed on backbones containing single- and double-point mutations, respectively. The forward sequences of the primer pairs used to mutate the putative glycosylation sites are listed below.

Table 5. Forward sequences of primer pairs for Site-Directed mutagenesis III

Mutation	Forward primer sequence (5' to 3')
Mutating the conserved aspartate residues in the α1, β2 and γ2 subunits	
β2(N32Q)	C AAT GAC CCT AGT **CAA** ATG TCG CTG G
β2(N104Q)	GTA ATC CCT TTA **CAA** TTG ACT TTG GAC
β2(N173Q)	CCA CTG GAT GAA CAA **CAA** TGC ACG TTG GAG

***** codons in bold were responsible for the designed point mutation.

Cell culture and transfection

HEK293T cells were incubated at 37°C in humidified 5% CO_2/95% air and grown in Dulbecco's Modified Eagle Medium (Invitrogen) supplemented with 10% fetal bovine serum, 100 i.u./mL penicillin, and 100 μg/mL streptomycin (Invitrogen). For single subunit expression, binary subunit and ternary subunit coexpression, cells were transfected with 1 μg, 2 μg and 3 μg (containing individual subtypes of subunits in an equal amount) of cDNA using 3 μL, 6 μL and 9 μL of FuGene6 transfection reagent per 60 mm diameter culture dish, respectively. The cDNA-FuGene6 volumes were scaled up or down proportionally to the surface area of cell culture dishes. Cells were subjected to the following experiments 48 hours after transfection.

Western blots

Cell membranes were lysed using RIPA buffer composed of 50 mM Tris-HCl (pH 7.4), 150 mM NaCl, 1 mM EDTA, 1% NP40, 0.25% sodium deoxycholate and protease inhibitor cocktail (Sigma). Cell lysates were cleaned by centrifugation at 10,000X g for 30 minutes. The supernatants were subjected to SDS-PAGE, and proteins in gels were transferred to PVDF membranes (Millipore).

Monoclonal anti-$GABA_A$ receptor α1 subunit antibodies (final concentration 5 μg/mL, clone: BD24, Chemicon) and monoclonal anti-$GABA_A$ receptor β2/3 antibodies (4 μg/mL, clone: 62-3G1, Upstate) were used to detect wild type or modified human α1 and β2 subunits, respectively. Anti-sodium potassium ATPase antibodies (0.2 μg/mL, clone: ab7671, Abcam) were used to control for loading variability. Following incubation with primary antibodies, secondary goat anti-mouse IgG heavy and light chain

antibodies conjugated with horseradish peroxidase were used in 1:10,000X dilution (Immunoresearch laboratories) for the visualization of specific bands in enhanced chemiluminescent detection system (Amersham Biosciences).

The signals were collected in a digital ChemImager (Alpha Innotech). The IDV of each band, pixel intensity X mm^2, was then calculated using the FluorChem 5500 software. To compare the expression levels between the same subtype subunits with different mutations, adjusted IDVs (normalized to loading control Na^+/K^+ ATPase IDVs) were normalized to those of control conditions.

Glycosidase digestion

Whole cell lysates obtained from RIPA buffer extraction were subjected to endo H and PNGaseF digestion (New England BioLab) following the manufacturer's recommended protocol. The digestion reactions were carried out at 37°C for 3 hours and terminated by addition of sample buffer.

Flow cytometry

Cells were detached from culture dishes using trypsin, washed with FACS buffer, and incubated with anti-FLAG antibodies directly conjugated with PE (50X diluted in FACS buffer) for 1 hour on ice. Stained cells were fixed with 2% paraformaldehyde. The surface fluorescence intensity of each cell was measured using a FacsCalibur (Becton, Dickinson and Company). Data were acquired using Cell Quest (BD Biosciences) and analyzed offline using FlowJo (Treestar, Inc.).

To exclude non-specific staining presented in dead cells, viable cells were selected based on 7-AAD exclusion. The distributions of cellular PE fluorescence were plotted as frequency histograms. Based on the fluorescence histogram of mock transfection, a fluorescence gate was set such that only the brightest 1% of cells were included. For each experimental condition, two numbers, the % of viable cells with fluorescence higher than the gate and the mean fluorescence of these cells, were determined. Subunit surface levels for whole cell population were than compared using fluorescence index, the product of multiplying the two numbers. Because fluorescence unit is arbitrary, the subunit surface level of each experimental condition was expressed as % of those of control-wild-type subunit coexpression. One-way ANOVA with Tukey's post test was used to evaluate the significance of relative level differences.

Results

All three predicted glycosylation sites of the $GABA_A$ receptor β2 subunit contained N-glycans, which contributed differently to molecular mass shifts

Endo H and PNGaseF glycosidase digestions revealed that there were glycosylation modifications on $GABA_A$ receptor subunits, since removing the covalently conjugated *N*-glycans decreased subunit molecular masses (Figure 8 and Figure 18). Furthermore, as demonstrated in chapter III, the conserved aspartate residue located in the cytoplasmic compartment affected glycosylation on the extracellular N-terminal domain of the β2 subunit and caused a shift in molecular mass (Figure 21). To determine whether or not the three putative β2 subunit glycosylation sites (N32, N104 and N173) are functional and how their glycans interact with the conserved aspartate residue located

in the cytoplasmic side and with partnering subunits, three β2 subunit constructs with a N to Q mutation on one of the three glycosylation sites were made. Molecular mass analyses using SDS-PAGE revealed that the three glycosylation sites were functional as mutations of individual putative glycosylation sites of β2 subunit resulted in a decreased molecular mass. Interestingly, β2(N32Q), β2(N104Q) and β2(N173Q) subunits did not migrate at the same molecular mass. Furthermore, the mutation of the conserved β2 subunit residue, D450A, caused a molecular mass shift similar to that of mutation of the third glycosylation site (Figure 27A, B).

To understand better how individual *N*-glycans on each glycosylation site contributed to the shifts in β2 subunit molecular masses, double-Q and triple-Q β2 subunit mutations (mutating two or three asparagines to glutamines) were made such that only one or no glycosylation site, respectively, remained. The triple-Q β2 subunit, β2(N32Q/N104Q/N173Q) moved in SDS-PAGE as a single band at a molecular mass of 47 kDa, while the major bands of the three double-Q mutant subunits, which retained only the N32, N104 or N173 site, migrated at higher molecular masses of 49, 50 and 48 kDa, respectively. Furthermore, 34% of β2(N104Q/N173Q) subunits migrated at a lower molecular mass equal to that of the triple-Q mutants, suggesting that appreciable β2(N104Q/N173Q) subunits were de-glycosylated or non-glycosylated (possibly due to weak recognition of the consensus sequence). Consistent with this conclusion, apparent-additional populations that migrated at smaller molecular masses only occurred with those subunits that did not contain a mutation of the first glycosylation site, i.e. wild-type β2, β2(D450A), β2(N104Q), β2(N173Q) and β2(N104Q/N173Q) (Figure 27A, B).

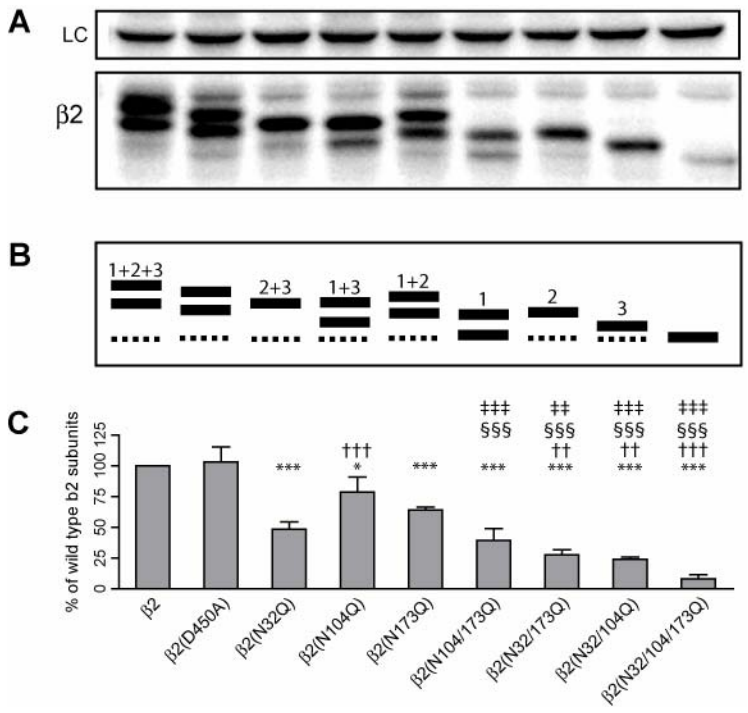

Figure 27. The β2 subunits with various combinations of glycosylation-site mutations were expressed alone

A, Relative to the wild-type β2 subunit, the shifts of molecular masses and changes of subunit total-protein levels of single-, double- and triple-N to Q mutants with single subunit expression were evaluated using Western blots. Upper panel presented the anti-Na^+/K^+ ATPase staining for the purpose of loading control (LC); lower panel presented the anti-β2 subunit staining. The third to fifth lanes stained for single-Q mutants, in an order such that N32, N104 and N173, respectively, mutated; the sixth to eighth lanes stained for double-Q mutants, in an order such that N32, N104 and N173, respectively, remained; the last lane stained for triple-Q mutant where no putative glycosylation site were remained. Also note that the D450A mutation of β2 subunits was also presented in lane two. **B**, A schematic presentation was added to facilitate analysis of the β2 subunit staining. The bottom bands (47kDa) were the forms of the polypeptide with no glycosylation and were labeled as dash-line in most of lane since they were less apparent. 1, 2 and 3 represent the contribution from N-glycans at N32, N104 and N173 glycosylation sites, respectively. **C**, Quantification of single subunit expression of β2 subunit glycosylation-site mutants is presented. The band intensity of each lane, after being corrected for loading variation, was expressed as % of the intensity of the wild-type β2 subunit presented in lane one. Data were presented as mean ± standard deviation. * and *** indicate $p < 0.05$ and 0.001, respectively, relative to wild-type β2 subunit expression; †† and ††† indicate $p < 0.01$ and 0.001, respectively, relative to β2(N32Q) subunit expression; §§§ indicates $p < 0.001$ relative to β2(N104Q) subunit expression; ‡‡ and ‡‡‡ indicate $p < 0.01$ and 0.001, respectively, relative to β2(N173Q) subunit expression.

Glycosylation of β2 subunits was important for single subunit expression

The importance of glycosylation on individual sites for β2 subunit folding before heteromeric oligomerization was also evaluated by measuring subunit total-protein levels. It has been demonstrated that the misfolded $GABA_A$ receptor α1(A322D) subunit, is rapidly degraded by ERAD before heteromeric oligomerization (Gallagher et al., 2007). Thus, subunits with glycosylation-site mutations may also be misfolded or have impaired oligomerization and result in decreased total protein levels. Supporting the importance of glycosylation for subunit folding and oligomerization, single-, double-, and triple-Q mutations significantly reduced subunit total-protein levels, relative to wild-type β2 subunits expressed alone. Furthermore, the glycosylation mutations had additive effects, and total-protein levels of β2(N32Q/N104Q), β2(N32Q/N173Q) and β2(N32Q/N104Q/N173Q) subunits were significantly decreased relative to those of β2(N32Q) subunits ($p < 0.01$ for double-Q and $p < 0.001$ for triple-Q mutants) (Figure 27C).

Mutation of the β2(N104) glycosylation site caused greater reductions in surface $GABA_A$ receptor expression than mutations in the two other glycosylation sites

To further evaluate how individual glycosylation sites regulate $GABA_A$ receptor biogenesis, β2 subunits with glycosylation-sites mutated were coexpressed with wild-type α1 subunits and surface levels of both subunits were measured using flow cytometry. To facilitate measurement, one FLAG epitope was introduced into the α1 and the β2 subunit (see Methods). Subunits were coexpressed in a way such that only one subtype was tagged. For instance, to evaluate the effect of the N32Q mutation, two transfection

conditions were carried out, i.e. $\alpha1^{FLAG}\beta2(N32Q)$ and $\alpha1\beta2(N32Q)^{FLAG}$ subunit coexpression.

Expression profiles of single-Q mutated subunits revealed that the N104Q mutation significantly decreased surface receptor levels ($p < 0.001$, $n = 5$), while N32Q and N173Q mutations did not alter surface levels. With α1β2(N104Q) subunit coexpression, only 50% and 39% of control α1 and β2 subtype-surface levels, respectively, remained (Figure 28). Interestingly, the double-Q mutant expression profile demonstrated that the presence of the single N104 glycosylation site (β2(N32Q/N173Q)) only was sufficient to support full levels of subunit surface expression. On the other hand, removing more glycosylation sites from the β2(N104Q) subunit caused further reduction of receptor surface levels. Consequently, there was no significant difference between surface receptor levels with α1β2(N32Q/N104Q), α1β2(N104Q/N173Q) and α1β2(N32Q/N104Q/N173Q) subunit coexpression ($n = 4$). 10%, 22% and 3% of control α1 and 14%, 14% and 4% of control β2 subunit with α1β2(N32Q/N104Q), α1β2(N104Q/N173Q) and α1β2(N32Q/N104Q/N173Q) subunit coexpression, respectively, remained.

Taken together, the data were consistent with the conclusion that glycosylation at the β2 subunit N104 site was responsible for attaining maximal level of surface α1β2 receptors. Importantly, despite the finding that the glycosylation pattern change caused by the β2 subunit mutation, N173Q, was similar to that caused by the β2 subunit mutation, D450A, loss of glycosylation at residue N173 was not the cause of the profound decrease of surface receptors when the conserved aspartate residue, β2(D450), was mutated to alanine (Figure 28).

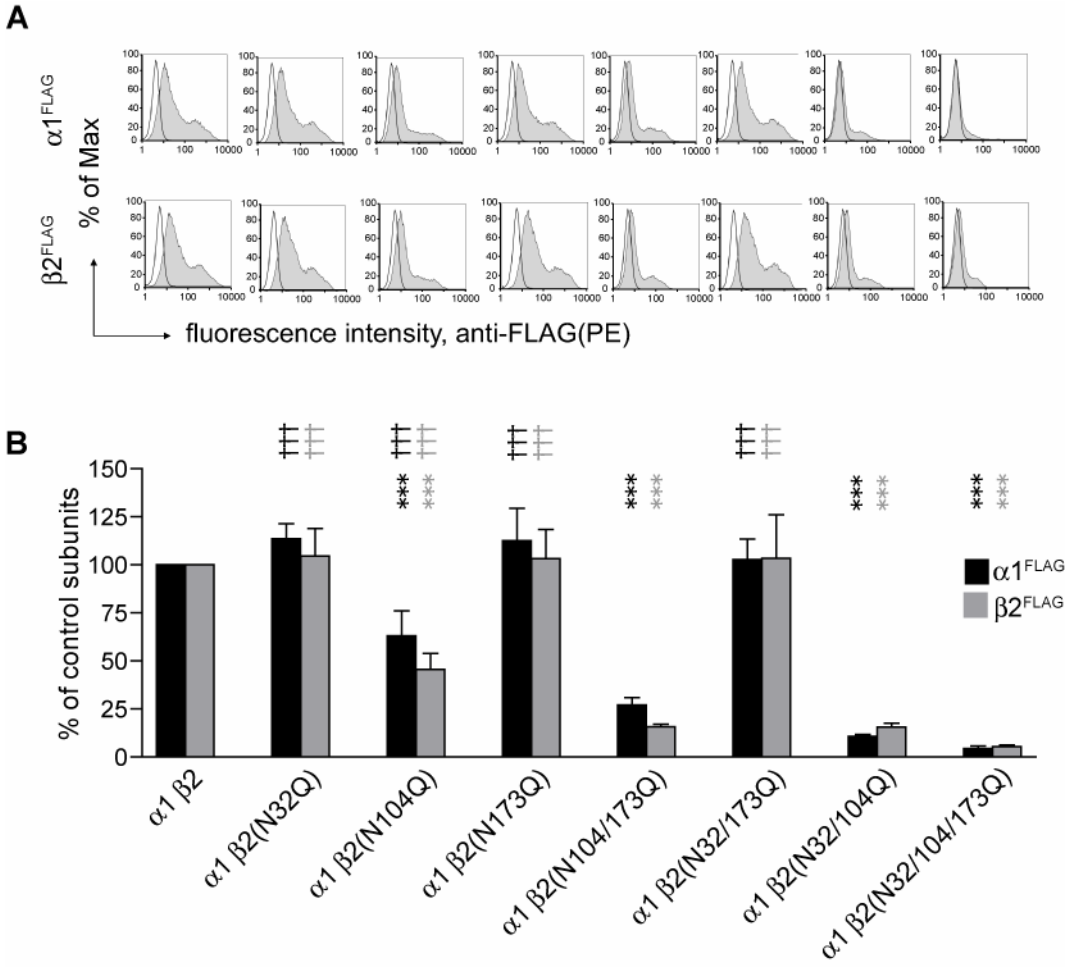

Figure 28. With binary subunit coexpression, subunit surface levels of α1 and β2 subunits were changed in response to different combinations of β2 subunit glycosylation site mutations

Effects of glycosylation-site mutations on α1 and β2 subunit-surface levels in the context of α1 and β2 subunit coexpression were evaluated. **A**, The histogram with each binary coexpression was overlapped with that of mock expression. Upper panels showed histograms of surface $\alpha1^{FLAG}$ subunit staining with various coexpression conditions, while the lower panels showed those of $\beta2^{FLAG}$ subunits. **B**, Fluorescence indexes of surface $\alpha1^{FLAG}$ (black bars) and $\beta2^{FLAG}$ (grey bars) subunit levels were obtained in each condition and expressed as a percentage of control $\alpha1^{FLAG}$ or $\beta2^{FLAG}$ subunits, the wild-type FLAG-tagged α1 and β2 subunit coexpressed with non-FLAG-tagged wild-type β2 and α1 subunits, respectively. Data were presented as mean ± standard deviation. *** indicates $p < 0.001$ relative to control α1β2 subunit coexpression; ††† indicates $p < 0.001$ relative to α1β2(N32Q/N104Q/N173Q) subunit coexpression.

With binary subunit coexpression, subunit surface levels were not the only factors determining subunit total protein levels

It is worth pointing out that individual glycosylation sites had different levels of significance for single subunit expression and binary receptor surface levels. The N32Q or N173Q mutations reduced total subunit levels with single subunit expression; while the N104Q mutation was more crucial for binary receptor surface expression. Decreasing the availability of subunits due to their misfolding could profoundly affect pentameric-$GABA_A$ receptor assembly (Gallagher et al., 2005;Gallagher et al., 2007). On the other hand, relative to single subunit expression, binary subunit coexpression could prolong both subunit half-lives and result in a two to three fold increase of subunit total protein levels (Figure 18). It is possible that coexpression of partnering α1 subunits differentially increases the total protein levels of individual β2 subunits with distinct combinations of glycosylation site mutations. To examine this possibility, total protein levels of both subtypes of subunits with various combinations of wild-type α1 and glycosylation site-mutated β2 subunits coexpression were evaluated by Western blotting.

The total protein profile of partnering α1 subunits was similar to the binary receptor surface expression profile. In the single Q mutation subset, mutating the N104 residue caused significant reduction of total α1 subunit proteins (60% of control α1 subunits remained, $p < 0.05$, $n = 4$). In the double Q mutation subset, the N32Q/N173Q mutation led to no significant change, while the N104Q/N173Q or N32Q/N104Q mutation caused more than 50% reductions of α1 subunit total proteins ($p < 0.01$ and 0.001 with α1β2(N104Q/N173Q) and α1β2(N32Q/N104Q) subunit coexpression, respectively, $n = 4$).

Interestingly, coexpression of α1 subunits differentially increased surface protein expression of β2 subunits containing various combinations of glycosylation site mutations. With α1β2(N32Q) subunit coexpression, the β2(N32Q) subunit total protein level was significantly reduced (60% of control subunits, $p < 0.001$, $n = 3$). This was a surprising result because mutation of the N32 glycosylation site did not decrease surface receptor and partnering α1 subunit total protein levels. The inconsistency may originate from subunit misfolding caused by the mutation. Alternatively, this finding also suggested that fewer than control subunit total protein levels could support full level of surface receptor expression. Consistent with this, 33% of control subunit level of β2(N32Q/N173Q) subunits maintained full receptor surface levels. It has been demonstrated before that the β2 subunit total protein level with α1β2 subunit coexpression is 2.6 times of that with single subunit expression (Figure 18). After correcting for this factor, α1 subunit coexpression increased total protein levels of β2 subunits with or without glycosylation site mutations. However, only those mutated β2 subunits showing no significant reductions at surface expression levels were increased more by the partnering subunits.

In summary, changes of subunit total protein levels did not always correlate with changes in receptor surface levels. Conversely, total protein expression of glycosylation site mutated β2-subunit directly correlated receptor surface levels and may possibly be determined by the rate of protein degradation induced by subunit misfolding.

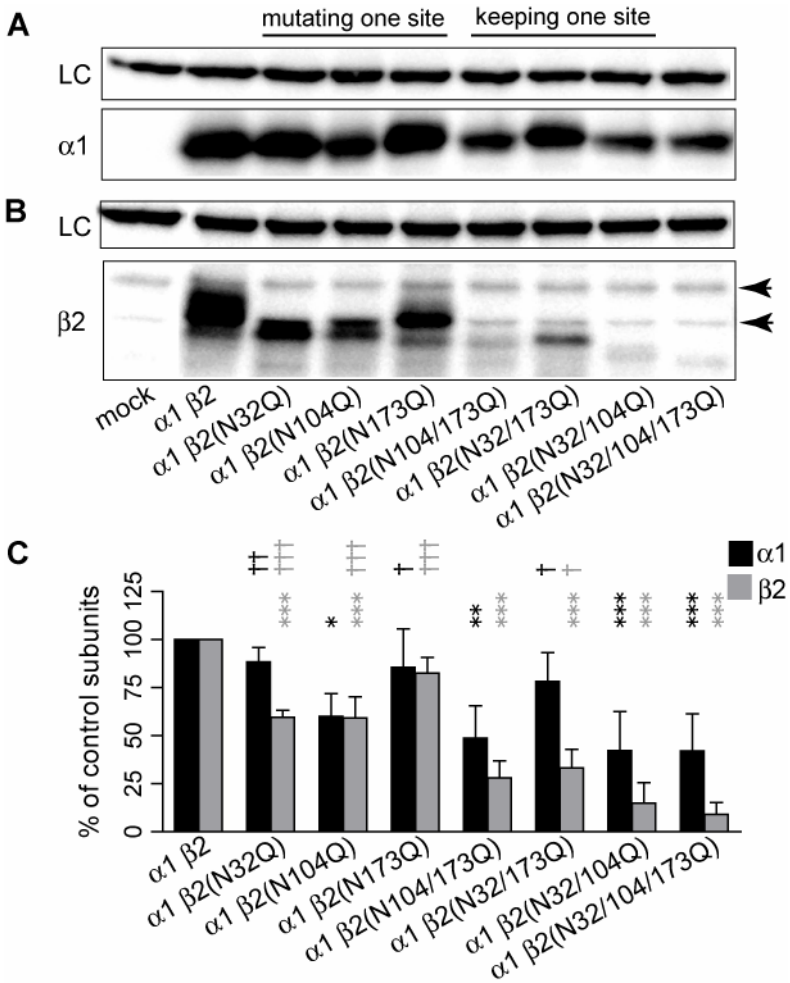

Figure 29. With α1β2 subunit coexpression, α1 and β2 subunit surface levels were not the only factors determining subunit total protein levels

Effects of glycosylation-site mutations on α1 and β2 subunit total-protein levels in the context of α1β2 subunits coexpression were evaluated. **A**, Total proteins were extracted from cells with mock, control α1β2, α1β2(N32Q), α1β2(N104Q), α1β2(N173Q), α1β2(N104Q/N173Q), α1β2(N32Q/N173Q), α1β2(N32Q/N104Q) and α1β2(N32Q/N104Q/N173Q) subunit coexpression and probed with anti-α1 antibodies. Na^+/K^+ ATPase was used as loading control (LC). **B**, Duplicate of A but probed with anti-β2 antibodies. **C**, The band intensity of each lane, after being corrected for loading variation, was expressed as % of the intensity of the control subunits. Black bars represented α1 subunit levels, while grey bars represented β2 subunit levels. Data were presented as mean ± standard deviation. *, ** and *** indicate $p < 0.05$, 0.01 and 0.001, respectively, relative to control α1β2 subunit coexpression; †, †† and ††† indicate $p < 0.05$, 0.01 and 0.001, respectively, relative to α1β2(N32Q/N104Q/N173Q) subunit coexpression. Note that non-specific bands (arrowheads) were detected in β2 subunit staining by this batch of antibodies.

Total protein level changes of α1 and β2 subunits with α1β2γ2 subunit coexpression were similar to those with α1β2 subunit coexpression but were less dependent on the β2(N104) residue

The α1β2γ2 receptor is the most abundant receptor isoform in the central nervous system (McKernan and Whiting, 1996;Sieghart and Sperk, 2002). In addition, it has been demonstrated that incorporation of γ2 subunits into $GABA_A$ receptor pentamers changes receptor single channel conductance and macroscopic current kinetics (Angelotti and Macdonald, 1993;Haas and Macdonald, 1999). To determine if incorporation of γ2 subunits into receptor pentamers affects the dependence on β2 subunit glycosylation sites for subunit total protein levels, relative amount of α1 and β2 subunits with or without glycosylation site mutations were measured with ternary subunit coexpression.

With α1β2γ2 subunit coexpression, changes of α1 subunit total protein levels were similar to that found with binary subunit coexpression except that β2(N104Q) did not significantly reduce α1 subunit expression (n = 3). Likewise, the β2 subunit total protein profile was comparable to that with binary subunit coexpression except that the β2(N104Q) subunit total protein level was not significantly reduced (n = 3) (Figure 30). This observation suggested that the total protein levels of α1 and β2 subunits with ternary subunit coexpression were less affected by the mutation of the N104 glycosylation site.

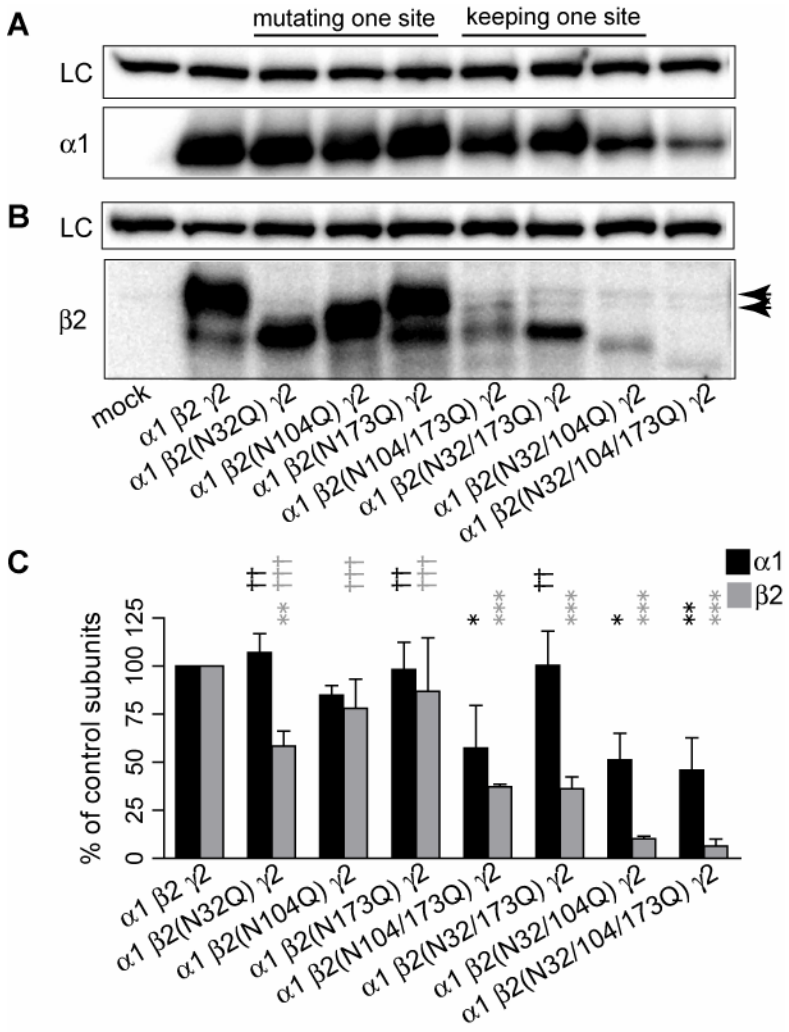

Figure 30. With ternary α1β2γ2 subunit coexpression, α1 and β2 subunit total protein levels were differentially affected by mutations of β2 subunit glycosylation sites

A, Total proteins were extracted from cells with mock, control α1β2γ2, α1β2(N32Q)γ2, α1β2(N104Q)γ2, α1β2(N173Q)γ2, α1β2(N104Q/N173Q)γ2, α1β2(N32Q/N173Q)γ2, α1β2(N32Q/N104Q)γ2 and α1β2(N32Q/N104Q/N173Q)γ2 subunit coexpression and probed with anti-α1 antibodies. Na^+/K^+ ATPase was used as loading control (LC). **B**, Duplicate of A but probed with anti-β2 antibodies. **C**, The band intensity of each lane was expressed as % of the intensity of the control subunits. Black bars represented α1 subunit levels; grey bars represented β2 subunit levels. Data were presented as mean ± standard deviation. *, ** and *** indicate $p < 0.05$, 0.01 and 0.001, respectively, relative to control α1β2γ2 subunit coexpression; †† and ††† indicate $p < 0.01$ and 0.001, respectively, relative to α1β2(N32Q/N104Q/N173Q)γ2 subunit coexpression. Note that non-specific bands (arrowheads) were detected in β2 subunit staining.

The endo H digestion patterns of β2 subunits with α1β2 subunit coexpression were different from those with α1β2γ2 subunit coexpression.

It has been demonstrated that folding, oligomerization and assembly of oligomeric proteins can affect *N*-glycan processing at certain positions by hindering their presentation to the Golgi resident enzyme, mannosidase II, which confers *N*-glycans with endo H resistance (Cals et al., 1996;Kornfeld and Kornfeld, 1985). Thus, *N*-glycans conjugated at those sites were removed by endo H glycosidase even though they were conjugated to matured glycoproteins. To determine if *N*-glycans conjugated to subunits in α1β2 receptors are differentially processed compared to those in α1β2γ2 receptors in the Golgi apparatus, endo H digestion patterns of *N*-glycans of α1 and β2 subunits were analyzed. It was predicted that if *N*-glycan processing at a specific site is hindered by partnering γ2 subunits, the *N*-glycan at that site will be removed by endo H glycosidase, which then will appreciably decrease molecular mass of the subunit having the *N*-glycan removed because *N*-glycans have appreciable molecular masses (more than 1 kDa because the core of all forms of *N*-glycans, which contains two *N*-acetylglucosamine and three mannose residues, weights about 1 kDa).

With binary α1β2 or ternary α1β2γ2 subunit coexpression, "mature" α1 subunits, possessed both endo H sensitive and insensitive *N*-glycans even though these "mature" peptides had presumably been exposed to the Golgi resident glycosidase. This is consistent with the prediction that *N*-glycan processing at one of the two glycosylation sites was hindered by subunit folding and assembly. Consequently, endo H digestion decreased the molecular mass of the mature α1 subunit by 2 kDa, while PNGase F digestion reduced its mass by 4 kDa (Figure 31A). Likewise, with α1β2γ2 subunit

coexpression, mature β2 subunits migrated at 51 kDa and contained both endo H resistant and sensitive *N*-glycans (Figure 31B).

Interestingly, with α1β2, but not α1β2γ2 subunit coexpression, we observed two endo H resistant β2 subunit bands with molecular mass 54 and 51 kDa. This result is consistent with two forms of mature β2 subunits. One mature form contained both endo H resistant and sensitive *N*-glycans as what with α1β2γ2 subunit coexpression; the other contained solely endo H resistant *N*-glycans, which were accessible by Golgi resident mannosidase II (Figure 31B, asterisk).

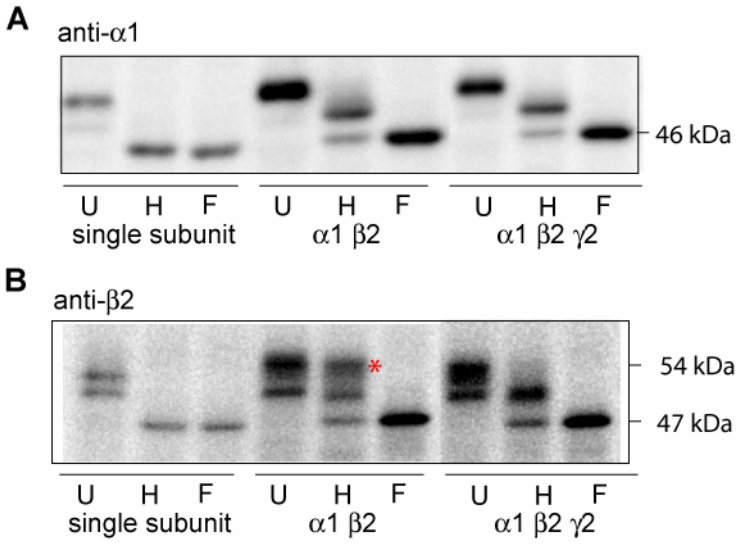

Figure 31. A 54 kDa endo H resistant band was detected in lysates from cells with α1β2, but not α1β2γ2 subunit coexpression

A, RIPA buffer extracted proteins from cells with single subunits (first set), α1β2 (second set) and α1β2γ2 (third set) subunit coexpression were undigested (U), or digested with endo H (H) or PNGaseF (F). Proteins were probed with anti-α1 antibodies. These α1 subunits, after endo H digestion, showing similar molecular masses (46 kDa) to those after PNGaseF digestion were considered endo H sensitive. **B**, Duplicate of A but probed with anti-β2 antibodies. * indicates the β2 subunit population, which had all three conjugated *N*-glycans resistant to endo H digestion.

The N-glycans at the β2(N32) and β2(N104), but not the β2(N173), glycosylation sites were involved in the presence of endo H resistant β2 subunits migrating at 54 kDa

The molecular mass difference between the 54 kDa endo H resistant band and the lower 51 kDa molecular mass endo H resistant bands was similar to those caused by N32Q or N104Q mutation. We hypothesized that *N*-glycans at the N32 or N104 site of mature β2 subunits with 54 kDa masses were endo H resistant while those of mature β2 subunits with 51 kDa masses were endo H sensitive. Thus, following the removal of the *N*-glycans, the endo H resistant β2 subunits with α1β2 subunit coexpression would migrate as single band migrating at the same molecular mass as those with α1β2γ2 subunit coexpression. To determine which N-glycans (at N32 or N104) are involved in the presence of the endo H resistant band with 54 kDa, single-Q mutant β2 subunits with binary subunit coexpression were compared with those with ternary subunit coexpression.

With α1β2 subunit coexpression, the β2(N32Q) and β2(N104Q) subunits migrated as a single endo H resistant band of the same molecular mass as that of undigested and fully glycosylated subunits (51 kDa). In contrast, the β2(N173Q) subunit migrated as two endo H resistant bands with the lower molecular mass endo H resistant band containing a endo H sensitive *N*-glycan at one of the two remaining glycosylation sites. Molecular masses of endo H resistant β2(N32Q) subunits with ternary subunit coexpression were similar to those with binary subunit coexpression, although preliminary data (n = 2) suggested that the β2(N32Q) subunit population with the remaining two *N*-glycans being endo H resistant in α1β2γ2 pentamers was smaller (Figure 32A). Likewise, the endo H digestion patterns of β2(N104Q) subunits with binary or ternary subunit coexpression were similar although the endo H resistant population with ternary subunit coexpression was bigger (Figure 32B). Importantly, the

β2 subunit endo H digestion patterns with α1β2(N173Q) or α1β2(N173Q)γ2 subunit coexpression were different from each other (Figure 32C).

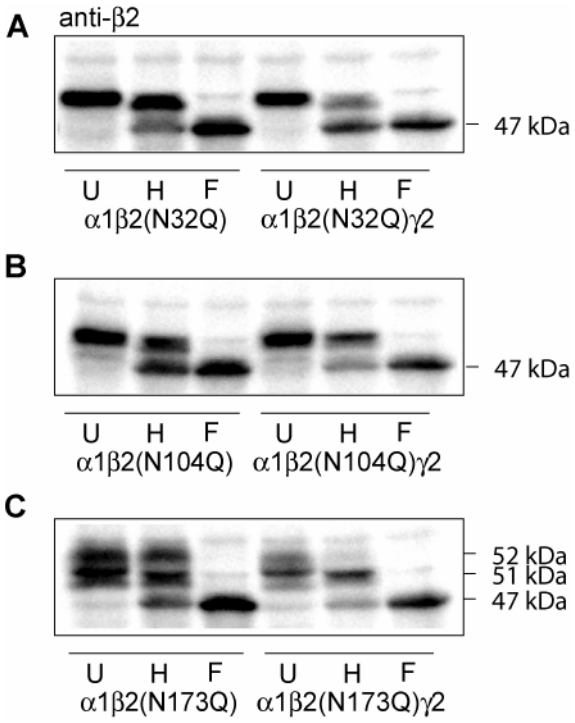

Figure 32. Processing of the N-glycans at the β2(N173) site was not involved in the presence of two endo H resistant bands of β2 subunits with α1β2 subunit coexpression

RIPA buffer extracted proteins from cells with binary α1β2 subunits (lanes 1-3, first set), and ternary α1β2γ2 (lanes 4-6, second set) subunit coexpression were undigested (U), or digested with endo H (H) or PNGaseF (F). The β2 subunits in theses expression conditions contained single Q mutation at N32 (A, upper panel), N104 (B, middle panel), or N173 (C, bottom panel). Proteins were probed anti-β2 antibodies. Note that there were two non-specific bands migrating at 54 and 51 kDa, which were different from previous blots (due to different batches of antibodies, which were used in figure 29).

Taken together, the data suggest that processing of *N*-glycans at the N32 and N104, but not the N173, sites were involved in conferring the distinct endo H digestion patterns of β2 subunits from α1β2 and α1β2γ2 pentamers.

Discussion

The N-glycans conjugated to individual β2 subunit glycosylation sites had different masses

By analyzing the molecular masses of the β2 subunits containing no, single Q, double Q, or triple Q mutation of the three N-linked glycosylation sites, it was revealed that the *N*-glycans conjugated to individual β2 subunit glycosylation site had different masses. The decrease in molecular mass by removing individual glycosylation sites (single Q mutation) correlated well with the increase in molecular mass by keeping individual glycosylation sites (double Q mutation). For instance, relative to the wild-type β2 subunit, mutation of the N173 site resulted in a smaller decrease in molecular mass than mutation of N32 or N104 sites, consistent with a smaller contribution by the N-glycan at the N173 site (evaluated by subtracting the molecular mass of the triple Q subunit from that of the β2(N32Q/N104Q) subunit) than those at other two glycosylation sites. This consistency weakened the possibility that the molecular mass differences were caused by modifications at other regions secondary to the N to Q mutations. Of note, due to rounding off error, the observed molecular mass of the fully glycosylated β2 subunit (54 kDa) was slightly higher than the calculated molecular mass (53 kDa) (obtained by adding the molecular mass contributions from individual *N*-glycans).

It is worth pointing out that the two apparent populations of β2(N104Q/N173Q) subunits migrating at 47 and 49 kDa suggested that only a fraction (66%) of the β2 subunits are glycosylated at N32. Incomplete N32 glycosylation could have resulted from weak recognition of the glycosylation site, i.e., the glycosylation site might not be fully glycosylated. Alternatively, incomplete glycosylation could have resulted from removal of the whole *N*-glycan from this site during the folding and maturation processes, i.e. the glycosylation site might be de-glycosylated.

The β2(N104) site is on the minus side of subunit-subunit interface

Based on homology modeling, the β2(N104) site of $GABA_A$ receptors is comparable to the α(K77) site (numbering from mature peptide) of nACh receptors from *T. marmorata* (Ernst et al., 2005;Akabas, 2004). Since α(K77) site of the nACh receptor is close to the minus side of α subunit interface R79 (Unwin, 2005), it is predicted that the N104 site is located on the minus side of $GABA_A$ receptor β2 subunit inter-subunit interface and that glycosylation at this site is important for α1-β2, β2-β2, and γ2-β2 subunit interactions (Figure 33).

Consistent with the predicted role of the N104 glycosylation, with binary subunit coexpression, N104 is necessary and sufficient for full level of receptor surface expression. Because about 40% of control α1β2 receptor level remained following the β2(N104Q) mutation, the interactions between β2(N104Q) and partnering subunits were not likely to be totally abolished. In agreement with this prediction, α1, β2 and γ2L subunits co-immunoprecipitated from extracted of cells treated with tunicamycin

suggesting that glycosylation was not absolutely required for subunit oligomerization (Connolly et al., 1996).

Preliminary data examining effects of β2 subunit glycosylation site mutations on α1β2γ2 receptor surface levels showed similar trend as those of α1β2 receptors (data not shown). The surface level profile was also similar to the α1 subunit total protein levels. By referring to the α1 subunit total protein level profile, it is suggested that the N104 site is less necessary for ternary receptor biogenesis because mutations of the site did not significantly reduce α1 subunit total protein levels. The difference may result from the postulated replacement of a β2 subunit by a γ2 subunit in an α1β2γ2 pentamer, and thus, the impairment on α1β2γ2 receptor biogenesis is less severe (Figure 33).

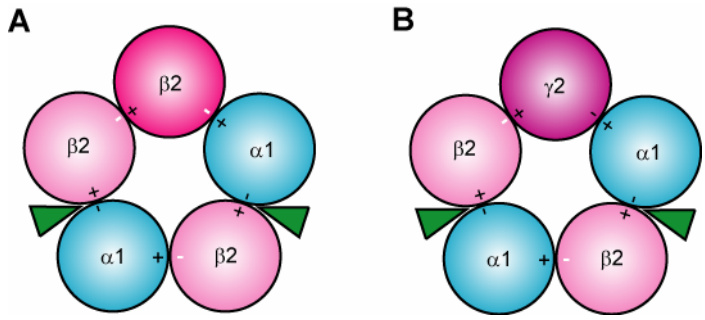

Figure 33. The N104 site in the β2 subunit was located on the minus side of inter-subunit interface and was predicted to play a role in α1-β2, β2-β2, or γ2-β2 subunit interaction

A, The predicted stoichiometry of the α1β2 receptor is presented. A $GABA_A$ receptor is believed to contain at least two α and two β subunits. The fifth position could be taken by a β subunit (as shown here) or α subunit. **B**, The predicted stoichiometry of the α1β2γ2 receptor is presented. The γ2 subunit is predicted to replace the β2 subunit (or α1 subunit) in the fifth position.

The distinct endo H digestion patterns of β2 subunits in α1β2 and α1β2γ2 receptors may result from conformational differences

Following endo H digestion, a population of β2 subunits that migrated at 54 kDa and contained all conjugated *N*-glycans being processed was specifically detected in lysates from cells transfected with α1 and β2 subunits but not from cells with α1β2γ2 subunit coexpression. The appearance of the special population could be contributed by the β2 subunits taking the fifth position, which could be incorporated into the receptor pentamer differently from the other two β2 subunits. Alternatively, the disappearance of this specific population could have resulted from the conformational changes induced by γ2 subunit incorporation, and steric hindrance preventing β2 subunit *N*-glycan processing by mannosidase II in the Golgi apparatus. If the population containing all of the three conjugated *N*-glycans being endo H resistant is contributed solely by the β2 subunits taking the fifth position, it is predicted that this population is 50% of (for $\alpha1_2\beta2_3$ stoichiometry) or smaller than (for mixed receptor isoforms, $\alpha1_2\beta2_3$ and $\alpha1_3\beta2_2$) the other endo H resistant population with lower molecular mass. Since the two endo H resistant populations were similar in size (Figure 31), it is likely that the exclusive presence of the 54 kDa endo H resistant β2 subunits in α1β2 receptors but not α1β2γ2 receptors resulted from the conformational differences between the two receptor isoforms.

With ternary subunit coexpression, the molecular masses of endo H resistant β2 subunits containing single-Q mutation at either N32 or N104 sites were the same as those undigested subunit that were fully glycosylated suggesting that the incorporation of γ2 subunits only decreases molecular masses of endo H resistant β2 subunits when both N32 and N104 sites were retained. Consistent with postulation, molecular masses of endo H resistant β2 subunits with the N173Q mutation were decreased by the incorporation of γ2

subunits. By comparing the molecular masses of the endo H resistant population of β2 subunits with α1β2γ2 subunit coexpression to the molecular masses of β2(N32Q/N104Q) subunits, it is less likely that the presence of γ2 subunits hindered glycan processing at both N32 and N104 sites, since it would result in removal of *N*-glycans at both sites and produce β2 subunits that would migrate at the same molecular mass as the β2(N32Q/N104Q) subunits. Thus, incorporation of γ2 subunits into a pentamer further hinders *N*-glycan processing at the N32 or N104 site but not at both.

Since pentameric assembly can hinder processing of *N*-glycans at specific sites, it is possible that some "mature" subunits, which have been trafficked beyond Golgi apparatus, contain no endo H resistant *N*-glycans and were not migrated at higher molecular mass than those digested with PNGaseF. With ternary subunit coexpression, a large population of β2 subunits containing the N32Q mutations migrated at molecular mass equal to those digested with PNGaseF. Given that the N32Q mutation did not reduce receptor surface levels, it is less likely that the β2 subunits with N32Q mutation were ER retained. It is possible that processing of N-glycans conjugated to the N104 and N173 sites of β2(N32Q) subunits were hindered by the presence of γ2 subunits and were removed by endo H glycosidase even though the β2(N32Q) subunits have been trafficked beyond the Golgi apparatus.

α1β2(D450A) and α1β2(N173Q) subunit coexpression

The molecular mass shifts caused by the β2 subunit D450A mutation, which resulted in profound subunit surface-level reductions to less than 10% of control subunits, were mimicked by the β2 subunit mutation, N173Q. However, α1β2(N173Q) receptor surface levels were not decreased significantly, suggesting that lacking glycosylation at the N173 site was not the cause of the reduced surface expression but resulted secondarily from the β2 subunit mutation, D450A. As shown in figure 25, the N173 site is right before one of the two cysteines that form the signature Cys-loop, and thus a change in Cys-loop disulfide bond formation might prevent glycosylation at N173. The integral membrane chaperone calnexin can interact with N-glycans of glycoproteins and regulate disulfide bond formation of the protein through its association with the ERp57, a homologue of protein disulfide isomerase (PDI) (Frickel et al., 2002).

It is possible that calnexin also interacts with the D450 residue and coordinates communication between the subunit N-terminal domain and the cytoplasmic loop, two regions separated by the lipid bilayer. The D to A mutation then might impair the interaction between calnexin and the subunit cytoplasmic loop (David et al., 1993), and affect formation of the signature disulfide bond in the N-terminal domain. Finally, due to this misfolding of the N-terminal domain microenvironment, glycosylation at the N173 site is blocked. It remains to be established whether or not the D to A mutation impairs Cys-loop disulfide bond formation, and whether or not the cytoplasmic loop interacts with calnexin (Figure 34).

The conserved aspartate residue is located at the boundary of the M3-M4 loop and M4 domain. Based on the homology modeling, it is at the N-terminal end of the M4

helix. Although mutations at the helix end are less likely to affect the insertion of helix (Gallagher et al., 2007;Hessa et al., 2005), we cannot rule out the possibility that the D to A mutations affect secondary structure of the M4 helix and cause the misfolding of the microenvironment containing the N173 site.

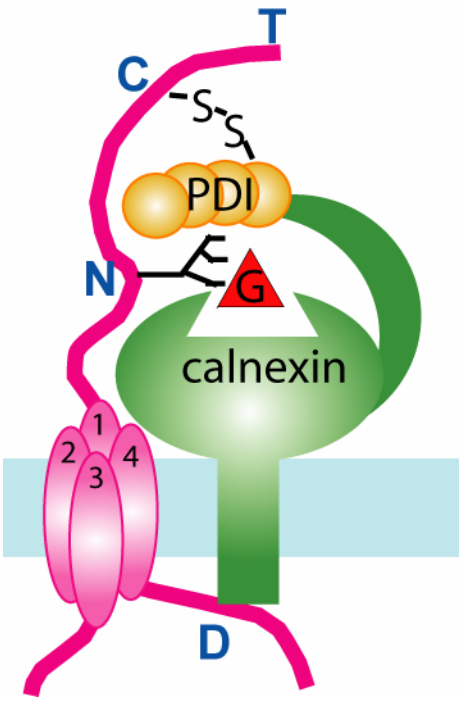

Figure 34. The conserved aspartate residue in the M3-M4 cytoplasmic loop might affect interaction between the β2 subunit microenvironment and the calnexin

The proposed interaction between the microenvironment of $GABA_A$ receptor β2 subunit and the calnexin is presented. It is postulated that the calnexin interacts with the *N*-glycan conjugated to N173 (in the consensus sequence N-C-T, where the C is the second cysteine involved in forming the signature Cys-loop) as well as a homologue of PDI, ERp57. The mutation of the conserved aspartate residue in the β2 subunit may impair interaction between the β2 subunit and calnexin. Consequently, signature Cys-loop formation of β2 subunit is affected, and glycosylation at N173 is blocked due to the mild misfolding of the local region.

Conclusions and future directions

This is the first demonstration showing that the three putative β2 subunit glycosylation sites are functional with their conjugated *N*-glycans having different molecular masses. The suggested differential *N*-glycan processing, such as de-glucosylation and de-mannosylation, requires further analysis of the structures of *N*-glycans conjugated the three β2 subunit glycosylation site. The finding that the β2 subunit site, N32, is not completely glycosylated further suggests the complex nature of glycosylation. It remains to be elucidated if other $GABA_A$ receptor subunits have their *N*-glycans processed differently and have incomplete *N*-glycan conjugation like N32.

Based on homology modeling, the N104 site is located on the β2 subunit minus side for subunit-subunit interaction. The significant decreases of α1 and β2(N104Q) subunit surface and total protein levels with α1β2(N104Q) subunit coexpression thus could have resulted from impairment of subunit oligomerization and receptor assembly. Consistently, it has been demonstrated in the muscle-type nACh receptor that some glycosylation sites are essential for receptor assembly (Wanamaker and Green, 2005). An immunoprecipitation assay could determine if the oligomerization of subunits is impaired or not.

Because the β2 subunit glycosylation site, N173, is in close proximity to one of the Cys-loop cysteines, the redox status of the Cys-loop cysteines may regulate glycosylation at this site. It is possible that the β2 subunit mutation, D450A, disturbs Cys-loop disulfide bond formation, which then affects glycosylation on residue N173. The redox status of Cys-loop cysteines could be evaluated by native gel electrophoresis.

Furthermore, the endo H digestion patterns suggest that incorporation of a γ2 subunit into the fifth position changes receptor conformation. Endo H resistance is conferred by a Golgi apparatus resident enzyme, and occurs only after assembly of pentameric receptors. Therefore, with coexpression of α1 and β2 subunits, existence of a β2 subunit population with three endo H resistant *N*-glycans would be an indication of the assembly of α1β2 receptors. It remains to be established if other subunits, such as δ, ε, θ and π, which are predicted to take the fifth position, could induce similar conformational changes and result in the disappearance of the 54 kDa endo H resistant β2 subunits. If this phenomenon is specific to α1β2 receptors, it may be applicable for the identification of α1β2 receptors *in vivo*.

CHAPTER V

CONCLUSIONS AND FUTURE DIRECTIONS

Studies presented in this dissertation provide information on $GABA_A$ receptor biogenesis

Genetic-linkage studies have associated several Cys-loop receptor mutations or polymorphisms with epilepsy syndromes, startle syndromes, congenital myasthenic syndromes and affective disorders, and many of these mutations have been shown to disturb the delicate balance between receptor biogenesis and turn over. The resultant alterations of receptor surface density are usually accompanied by dysfunction of Cys-loop receptors. In these cases, modulation of Cys-loop biogenic steps is a therapeutic option, which requires a good understanding of biogenic steps, particularly on how receptor subunits interact with one another and with regulatory cellular proteins.

For the studies reported in this dissertation, mutagenesis, which actively mutates regions of interests, was employed to identify structural determinants of receptor biogenesis because these sites are where interactions between subunits and regulatory cellular machineries occur. As an initial approach to structural domains involved in biogenesis, the relative requirement of individual α1, β2 and γ2 subunit M3-M4 loops was evaluated. Since a disturbance in any step of subunit or receptor biogenesis will alter receptor surface expression, subunit surface levels were measured using flow cytometry to determine whether or not specific structural domains are necessary for receptor surface expression. Consistent with receptor subunit heterogeneity, the three α1, β2 and γ2 subtype M3-M4 loops were differentially required for receptor surface expression. A

sequential deletion of subunit M3-M4 loops led to the identification of a structural residue located at the boundary of the M3-M4 loop and M4 domain that was indispensable for receptor surface expression. Furthermore, a combination of glycosidase digestion, BFA treatment, analytical centrifugation and immunoprecipitation established that this residue is required for late stages of receptor assembly.

The finding that a single C-terminal residue in the M3-M4 loop is required for receptor assembly explains the observation that γ2 subunit M3-M4 loop deletion drastically reduced γ2 subunit surface expression, but only mildly reduced α1β2 receptor surface expression. It has been demonstrated that the presence of the γ2 subunits resulted in preferential assembly of the ternary α1β1γ2 receptors (Angelotti and Macdonald, 1993). Therefore, the conserved residue may play a role in preferred α1β1γ2 receptor biogenesis. Given the observation that the residue was not absolutely required for the early steps of subunit oligomerization, the mechanism favoring ternary over binary receptor biogenesis may occur at later steps of pentameric assembly.

Furthermore, the requirement of the conserved aspartate residue or C-terminal portions of the M3-M4 loop suggest a pathogenic mechanism for the γ2 subunit mutation, Q351X, that is associated with associated an IGE. Since the Q351X mutation results in deletion of the conserved residue, the γ2(Q351X) subunit may be poorly incorporated into a receptor pentamer, and thus, would be retained in the ER. Consequently, the surface receptor isoform expression profile is changed. The Q351X mutation might mirror the effect of losing functional αβγ2 receptors in γ2 subunit knock-out mice, i.e. homozygously, causing neonatal lethal, and heterozygously/haploinsufficiently, causing increased anxiety (Chandra et al., 2005;Essrich et al., 1998). Furthermore, the ER

retained mutant γ2(Q351X) subunits could have additional effects and cause apoptosis of neuronal cells (Kang et al., unpublished).

Intriguingly, while α1(D420A) subunits caused a substantial reduction of receptor surface levels to an extent not significantly different from that caused by β2(D450A) subunits, α1(loopΔ) subunits caused significantly less receptor surface level reduction than that caused by β2(loopΔ) or β2(D450A) subunits. The relatively long extracellular tails of α subunits may account for the difference. It is possible that after removing large portions of the subunit M3-M4 loops, a second α1 subunit structural motif of receptor assembly is activated that allows some extent of receptor assembly. An α subunit motif at the boundary of the M4 domain and extracellular tail is either N-R-E-S/P (for α1-3 and 5) or S-K-D-T (for α4 and 6), which is similar to the I-D-R motif in a reverse way, is a potential candidate for the second assembly determinant. Supporting this postulate, deletion of the α1 subunit extracellular tail further reduced the surface level of α1(loopΔ)β2 receptors to an extent not different from α1β2(loopΔ) subunit coexpression. Several lines of evidence suggest that the extracellular tails of Cys-loop receptor subunits are important for pentamer assembly. The α subunit charged residues flanking both ends of its M4 domain have been demonstrated to be important for nACh receptor assembly and surface expression (Roccamo and Barrantes, 2007). Additionally, mutations of the nACh receptor ε subunit that resulted in the removal of a cysteine near the tip of the extracellular tail have also been shown to affect receptor surface expression (Ealing et al., 2002).

This is the first report showing that $GABA_A$ receptor assembly is regulated by a structural determinant that is not in the N-terminal domain and is on the opposite side of

the lipid bilayer. While the lipid-bilayer provides a two-dimensional plane for receptor folding, oligomerization, assembly, and finally (through membrane fusion) functional presentation on the cell surface, it imposes a physical barrier hindering communication of proteins binding to $GABA_A$ receptor subunit extracellular/ER luminal or cytoplasmic portions. Transmembrane proteins such as calnexin are predicted to coordinate the events occurring in the two compartments. Supporting the postulate that the cytoplasmic conserved aspartate residue interacts with some transmembrane protein, the cytoplasmic D to A mutation altered the glycosylation patterns of α1(D420A) and β2(D450A) subunits in the extracellular/ER luminal compartment.

The N-linked glycosylation site at the β2(N173) position is conserved in nACh and 5-HT_3 receptors (with the exceptions of the nACh receptor α9 and α10 subunits) and has been demonstrated to be essential for receptor assembly (Green and Wanamaker, 1997). Furthermore, mutation of this position in the $GABA_A$ receptor δ subunit, E177A, has been associated with IGEs and decreased $GABA_A$ receptor surface expression (Feng et al., 2006;Macdonald et al., 2004). The charged E177 residue in the δ subunit and the *N*-glycan-attached glycosylation site in the nACh and 5-HT_3 receptors may play similar roles in pentamer assembly, and the flexibility of glycosylation modification may confer another level of assembly regulation. Although glycosylation of $GABA_A$ and glycine receptors occurs less frequently at this position, all three $GABA_A$ receptor β subunits contain a glycosylation site here. Intriguingly, preventing glycosylation at the N173 site by N to Q mutation did not cause reduction of receptor surface level. Thus, the lack of glycosylation at N173 caused by the D to A mutation is more likely a result of the disturbed biogenesis step(s) and not a cause of the assembly failure. Cys-loop motifs

have asymmetric contributions to muscle-type nACh receptor subunit oligomerization (Fu and Sine, 1996), which may account for the different effects of the β2 subunit, N173Q, and δ subunit, E177A, mutations on $GABA_A$ receptor surface expression.

Based on homology modeling, the N104 glycosylation site is located on the β2 subunit minus side for subunit-subunit interaction. It is predicted that the N104Q mutation impaired, but did not abolish, subunit oligomerization, since glycosylation is not absolutely required for subunit oligomerization (Connolly et al., 1996). Supporting the hypothesis, the β2 subunit, N104Q, mutation incompletely decreased subunit surface and total protein levels of both mutated and wild-type partnering subunits with binary subunit coexpression. Based on the established stoichiometry of α1β2 and α1β2γ2 receptors and assuming that the γ2 subunit replaces a β2 subunit to form an α1β2γ2 receptor pentamer, the β2 subunit, N104Q, mutation would caused less severe reduction of subunit surface and total protein levels. Changes of α1 and β2 subunit total protein levels with ternary subunit coexpression in response to the N104Q mutation supported this prediction. Whether it is also true for receptor surface levels remains to be investigated.

Studies presented in this dissertation provide information on biogenesis of Cys-loop receptors

The aspartate residue described in chapter III is conserved across all 45 subunits of human Cys-loop receptors, and it may be conserved across all species, given that Cys-loop receptor subunit orthologs (genes from different species) share higher sequence similarity than paralogs (genes of the same species). While the structural determinant of $GABA_A$ receptor assembly identified in this study is the first residue that has been reported to be outside the N-terminal domain, several mutations in the subunit C-terminal

portions have been shown to affect receptor subunit oligomerization (Ealing et al., 2002;Quiram et al., 1999) or surface function (Rea et al., 2002;Shen et al., 2005).

Particularly, the nACh receptor ε subunit mutation, N436Δ, which is a mutation that deletes the asparagine residue in an L-D-N motif (an equivalent of the I-D-R motif of $GABA_A$ receptor α1 and β2 subunits) has been associated with CMS and shown to decrease receptor current amplitudes (Shen et al., 2005). The glycine receptor α1 subunit mutation, R428H, which mutates the arginine residue in the I-D-K-I-S-R motif to a histidine (where the I-D-K is the equivalent of the I-D-R motif of $GABA_A$ receptor α1 or β2 subunit), has been associated with startle disease and demonstrated to reduce receptor surface levels (Rea et al., 2002). While the mutations reveal the importance of the region near the M3-M4 loop and M4 domain junction for receptor function, the underlying mechanisms are less well understood. Given the postulate that Cys-loop receptors share early biogenic steps due to the similar topology and combinatory nature, the finding of this study might be applicable to other Cys-loop receptors. Therefore, it might be true for all Cys-loop receptors that the region at the boundary of the cytoplasmic loop and M4 domain contains structural determinants for receptor assembly, and mutations occurring in this region will disturb early steps of receptor biogenesis.

Future directions

The requirement of the cytoplasmic loop aspartate residue for receptor assembly and the necessity for glycosylation of the N-terminal residue (e.g. N173) suggest that events associated with the $GABA_A$ receptor subunit extracellular domain (e.g. glycosylation) and those associated with the intracellular loop manage to communicate

across the physical barrier presented by the lipid bilayer. Therefore, the protein machinery interacting with the conserved aspartate residue and regulating receptor assembly should contain at least a transmembrane protein coordinating the events occurring in the two compartments on opposite sides of the membrane.

A potential candidate for this task is the ER resident transmembrane protein, calnexin, which has been shown to associate with $GABA_A$ receptors (Connolly et al., 1996). Calnexin contains a large N-terminal domain that is located in the ER lumen, a transmembrane domain, and a 90 amino acid long cytoplasmic tail (David et al., 1993). The structure of its N-terminal domain has been resolved at 2.9Å and is composed of a lectin domain responsible for monovalent glycan binding and an extended arm involved in interaction with PDI (Schrag et al., 2001). Hypothetically, the effect of the β2 subunit mutation, D450A, could cause the disorientation of the calnexin and PDI-containing protein complex. Given that calnexin also coordinates disulfide-bond formation through its interaction with PDI and that the β2 subunit residue, N173, and the conserved Cys-loop cysteine are adjacent to each other, the D to A mutations might have direct effects on subunit disulfide bond formation, which in turn, cause de-glycosylation/non-glycosylation of N173. This putative effect preventing disulfide bond formation might not be severe enough to activate ERAD or to prevent subunit oligomerization, but might be the actual cause of the assembly failure at later steps.

Since calnexin is a lectin-like protein that can interact with $GABA_A$ receptor subunits through multiple glycosylation sites, the lack of glycosylation at the N173 site caused by the β2 subunit mutation, D450A, is not likely to abolish interactions between calnexin and β2(D450A) subunits. Thus, to verify the hypothesis postulated above, it is

necessary to establish the interactions between the C-terminal portions (downstream of the transmembrane domain) of calnexin and the cytoplasmic portions (containing the conserved aspartate residue) of $GABA_A$ receptor subunits. The interactions are not necessarily direct; therefore, an assay showing that a GST-fusion protein containing the cytoplasmic tail of calnexin pulls down a protein complex containing $GABA_A$ receptors, or vice versa, will establish the interaction. It is also necessary to determine if the D to A mutations prevent disulfide bond formation, and if preventing disulfide bond formation causes assembly failure. The later can be tested using reducing reagents such as glutathione on cells; while the former can be determined by separating $GABA_A$ receptor subunits using SDS-PAGE without reducing reagents. It is predicted that if the disulfide bond formation is affected by the D to A mutation, the mutant subunits will have different mobility from wild-type subunits.

The preliminary regional deletion results of this study suggested a role of α1 subunit extracellular tail in receptor biogenesis. The involvement of the reverse consensus R-E-P motif located on the opposite side of the lipid bilayer to regulate receptor biogenesis remains to be determined. If it is proven to be true, the associated proteins may have the capability to flip between different compartments.

The conserved aspartate residue is predicted to be important for assembly of all Cys-loop receptors based on its absolute conservation. Given the great heterogeneity of Cys-loop receptors, this prediction, particularly, whether the ε(N436Δ) mutation of nACh receptor and the α1(R428H) mutation of glycine receptor impair pentameric receptor assemble remain to be examined. Likewise, although it is postulated that the early biogenic steps of Cys-loop receptors are conserved in different cell types, such as

epithelial cells and neurons (based on the wide distribution of Cys-loop receptors), whether the conserved aspartate residue is as important as what have been shown in present studies in HEK cells remains to be examined.

By measuring the surface levels of α1 and β2(N104Q) subunits with binary subunit coexpression, it suggested that the biogenesis of α1β2(N104Q) receptors was disturbed by the glycosylation site mutation. Since the N104 glycosylation site is on the β2 subunit minus side for subunit-subunit interaction, it may decrease the efficiency for β2 subunits to oligomerize with partnering subunits. An immunoprecipitation assay may provide evidence of this prediction. Furthermore, analytic centrifugation analyzing oligomerized/assembled protein complexes containing $GABA_A$ receptor subunits would help to determine if the β2(N104Q) mutation caused receptor assembly impairment.

REFERENCES

Akabas MH (2004) $GABA_A$ receptor structure-function studies: a reexamination in light of new acetylcholine receptor structures. Int Rev Neurobiol 62: 1-43.

Alder NN, Johnson AE (2004) Cotranslational membrane protein biogenesis at the endoplasmic reticulum. J Biol Chem 279: 22787-22790.

Alldred MJ, Mulder-Rosi J, Lingenfelter SE, Chen G, Luscher B (2005) Distinct gamma2 subunit domains mediate clustering and synaptic function of postsynaptic $GABA_A$ receptors and gephyrin. J Neurosci 25: 594-603.

Angelotti TP, Macdonald RL (1993) Assembly of $GABA_A$ receptor subunits: alpha 1 beta 1 and alpha 1 beta 1 gamma 2S subunits produce unique ion channels with dissimilar single-channel properties. J Neurosci 13: 1429-1440.

Apweiler R, Hermjakob H, Sharon N (1999) On the frequency of protein glycosylation, as deduced from analysis of the SWISS-PROT database. Biochim Biophys Acta 1473: 4-8.

Aridor M, Traub LM (2002) Cargo selection in vesicular transport: the making and breaking of a coat. Traffic 3: 537-546.

Audenaert D, Schwartz E, Claeys KG, Claes L, Deprez L, Suls A, Van Dyck T, Lagae L, Van Broeckhoven C, Macdonald RL, De Jonghe P (2006) A novel GABRG2 mutation associated with febrile seizures. Neurology 67: 687-690.

Bakker MJ, van Dijk JG, van den Maagdenberg AM, Tijssen MA (2006) Startle syndromes. Lancet Neurol 5: 513-524.

Baulac S, Huberfeld G, Gourfinkel-An I, Mitropoulou G, Beranger A, Prud'homme JF, Baulac M, Brice A, Bruzzone R, LeGuern E (2001) First genetic evidence of GABA(A) receptor dysfunction in epilepsy: a mutation in the gamma2-subunit gene. Nat Genet 28: 46-48.

Beck M, Brickley K, Wilkinson HL, Sharma S, Smith M, Chazot PL, Pollard S, Stephenson FA (2002) Identification, molecular cloning, and characterization of a novel $GABA_A$ receptor-associated protein, GRIF-1. J Biol Chem 277: 30079-30090.

Bedford FK, Kittler JT, Muller E, Thomas P, Uren JM, Merlo D, Wisden W, Triller A, Smart TG, Moss SJ (2001) GABA(A) receptor cell surface number and subunit stability are regulated by the ubiquitin-like protein Plic-1. Nat Neurosci 4: 908-916.

Biggio G, Follesa P, Sanna E, Purdy RH, Concas A (2001) $GABA_A$ -receptor plasticity during long-term exposure to and withdrawal from progesterone. Int Rev Neurobiol 46: 207-241.

Blount P, Merlie JP (1988) Native folding of an acetylcholine receptor alpha subunit expressed in the absence of other receptor subunits. J Biol Chem 263: 1072-1080.

Blount P, Merlie JP (1990) Mutational analysis of muscle nicotinic acetylcholine receptor subunit assembly. J Cell Biol 111: 2613-2622.

Bollan K, Robertson LA, Tang H, Connolly CN (2003) Multiple assembly signals in gamma-aminobutyric acid (type A) receptor subunits combine to drive receptor construction and composition. Biochem Soc Trans 31: 875-879.

Boue-Grabot E, Roudbaraki M, Bascles L, Tramu G, Bloch B, Garret M (1998) Expression of GABA receptor rho subunits in rat brain. J Neurochem 70: 899-907.

Boyd GW, Low P, Dunlop JI, Robertson LA, Vardy A, Lambert JJ, Peters JA, Connolly CN (2002) Assembly and cell surface expression of homomeric and heteromeric 5-HT3 receptors: the role of oligomerization and chaperone proteins. Mol Cell Neurosci 21: 38-50.

Bradley CA, Taghibiglou C, Collingridge GL, Wang YT (2008) mechanisms involved in the reduction of $GABA_A$ receptor alpha 1 subunit expression caused by the epilepsy mutation A322D in the trafficking competent receptor. J Biol Chem.

Brandon NJ, Jovanovic JN, Smart TG, Moss SJ (2002) Receptor for activated C kinase-1 facilitates protein kinase C-dependent phosphorylation and functional modulation of GABA(A) receptors with the activation of G-protein-coupled receptors. J Neurosci 22: 6353-6361.

Brandon NJ, Uren JM, Kittler JT, Wang H, Olsen R, Parker PJ, Moss SJ (1999) Subunit-specific association of protein kinase C and the receptor for activated C kinase with GABA type A receptors. J Neurosci 19: 9228-9234.

Brejc K, van Dijk WJ, Klaassen RV, Schuurmans M, van Der OJ, Smit AB, Sixma TK (2001) Crystal structure of an ACh-binding protein reveals the ligand-binding domain of nicotinic receptors. Nature 411: 269-276.

Bruneau E, Sutter D, Hume RI, Akaaboune M (2005) Identification of nicotinic acetylcholine receptor recycling and its role in maintaining receptor density at the neuromuscular junction in vivo. J Neurosci 25: 9949-9959.

Buller AL, Hastings GA, Kirkness EF, Fraser CM (1994) Site-directed mutagenesis of N-linked glycosylation sites on the gamma-aminobutyric acid type A receptor alpha 1 subunit. Mol Pharmacol 46: 858-865.

Cals MM, Guenzi S, Carelli S, Simmen T, Sparvoli A, Sitia R (1996) IgM polymerization inhibits the Golgi-mediated processing of the mu-chain carboxy-terminal glycans. Mol Immunol 33: 15-24.

Castaldo P, Stefanoni P, Miceli F, Coppola G, Del Giudice EM, Bellini G, Pascotto A, Trudell JR, Harrison NL, Annunziato L, Taglialatela M (2004) A novel hyperekplexia-causing mutation in the pre-transmembrane segment 1 of the human glycine receptor alpha1 subunit reduces membrane expression and impairs gating by agonists. J Biol Chem 279: 25598-25604.

Chandra D, Korpi ER, Miralles CP, De Blas AL, Homanics GE (2005) $GABA_A$ receptor gamma 2 subunit knockdown mice have enhanced anxiety-like behavior but unaltered hypnotic response to benzodiazepines. BMC Neurosci 6: 30.

Charych EI, Yu W, Miralles CP, Serwanski DR, Li X, Rubio M, De Blas AL (2004) The brefeldin A-inhibited GDP/GTP exchange factor 2, a protein involved in vesicular trafficking, interacts with the beta subunits of the GABA receptors. J Neurochem 90: 173-189.

Chebib M (2004) $GABA_C$ receptor ion channels. Clin Exp Pharmacol Physiol 31: 800-804.

Christianson JC, Green WN (2004) Regulation of nicotinic receptor expression by the ubiquitin-proteasome system. EMBO J 23: 4156-4165.

Collinson N, Kuenzi FM, Jarolimek W, Maubach KA, Cothliff R, Sur C, Smith A, Otu FM, Howell O, Atack JR, McKernan RM, Seabrook GR, Dawson GR, Whiting PJ, Rosahl TW (2002) Enhanced learning and memory and altered GABAergic synaptic transmission in mice lacking the alpha 5 subunit of the $GABA_A$ receptor. J Neurosci 22: 5572-5580.

Connolly CN, Kittler JT, Thomas P, Uren JM, Brandon NJ, Smart TG, Moss SJ (1999a) Cell surface stability of gamma-aminobutyric acid type A receptors. Dependence on protein kinase C activity and subunit composition. J Biol Chem 274: 36565-36572.

Connolly CN, Krishek BJ, McDonald BJ, Smart TG, Moss SJ (1996) Assembly and cell surface expression of heteromeric and homomeric gamma-aminobutyric acid type A receptors. J Biol Chem 271: 89-96.

Connolly CN, Uren JM, Thomas P, Gorrie GH, Gibson A, Smart TG, Moss SJ (1999b) Subcellular localization and endocytosis of homomeric gamma2 subunit splice variants of gamma-aminobutyric acid type A receptors. Mol Cell Neurosci 13: 259-271.

Corpet F (1988) Multiple sequence alignment with hierarchical clustering. Nucleic Acids Res 16: 10881-10890.

Cossette P, Liu L, Brisebois K, Dong H, Lortie A, Vanasse M, Saint-Hilaire JM, Carmant L, Verner A, Lu WY, Wang YT, Rouleau GA (2002) Mutation of GABRA1 in an autosomal dominant form of juvenile myoclonic epilepsy. Nat Genet 31: 184-189.

Darlison MG, Pahal I, Thode C (2005) Consequences of the evolution of the GABA(A) receptor gene family. Cell Mol Neurobiol 25: 607-624.

David V, Hochstenbach F, Rajagopalan S, Brenner MB (1993) Interaction with newly synthesized and retained proteins in the endoplasmic reticulum suggests a chaperone function for human integral membrane protein IP90 (calnexin). J Biol Chem 268: 9585-9592.

Delpire E, Mount DB (2002) Human and murine phenotypes associated with defects in cation-chloride cotransport. Annu Rev Physiol 64: 803-843.

Ealing J, Webster R, Brownlow S, Abdelgany A, Oosterhuis H, Muntoni F, Vaux DJ, Vincent A, Beeson D (2002) Mutations in congenital myasthenic syndromes reveal an epsilon subunit C-terminal cysteine, C470, crucial for maturation and surface expression of adult AChR. Hum Mol Genet 11: 3087-3096.

Ehya N, Sarto I, Wabnegger L, Sieghart W (2003) Identification of an amino acid sequence within GABA(A) receptor beta3 subunits that is important for receptor assembly. J Neurochem 84: 127-135.

Ernst M, Bruckner S, Boresch S, Sieghart W (2005) Comparative models of $GABA_A$ receptor extracellular and transmembrane domains: important insights in pharmacology and function. Mol Pharmacol 68: 1291-1300.

Essrich C, Lorez M, Benson JA, Fritschy JM, Luscher B (1998) Postsynaptic clustering of major $GABA_A$ receptor subtypes requires the gamma 2 subunit and gephyrin. Nat Neurosci 1: 563-571.

Fang C, Deng L, Keller CA, Fukata M, Fukata Y, Chen G, Luscher B (2006) GODZ-mediated palmitoylation of GABA(A) receptors is required for normal assembly and function of GABAergic inhibitory synapses. J Neurosci 26: 12758-12768.

Feng HJ, Kang JQ, Song L, Dibbens L, Mulley J, Macdonald RL (2006) Delta subunit susceptibility variants E177A and R220H associated with complex epilepsy alter channel gating and surface expression of alpha4beta2delta $GABA_A$ receptors. J Neurosci 26: 1499-1506.

Follesa P, Biggio F, Talani G, Murru L, Serra M, Sanna E, Biggio G (2006) Neurosteroids, $GABA_A$ receptors, and ethanol dependence. Psychopharmacology (Berl) 186: 267-280.

Frickel EM, Riek R, Jelesarov I, Helenius A, Wuthrich K, Ellgaard L (2002) TROSY-NMR reveals interaction between ERp57 and the tip of the calreticulin P-domain. Proc Natl Acad Sci U S A 99: 1954-1959.

Frugier G, Coussen F, Giraud MF, Odessa MF, Emerit MB, Boue-Grabot E, Garret M (2007) A {gamma}2(R43Q) Mutation, Linked to Epilepsy in Humans, Alters $GABA_A$ Receptor Assembly and Modifies Subunit Composition on the Cell Surface. J Biol Chem 282: 3819-3828.

Fu DX, Sine SM (1996) Asymmetric contribution of the conserved disulfide loop to subunit oligomerization and assembly of the nicotinic acetylcholine receptor. J Biol Chem 271: 31479-31484.

Fujiwara T, Oda K, Yokota S, Takatsuki A, Ikehara Y (1988) Brefeldin A causes disassembly of the Golgi complex and accumulation of secretory proteins in the endoplasmic reticulum. J Biol Chem 263: 18545-18552.

Fumagalli G, Engel AG, Lindstrom J (1982) Ultrastructural aspects of acetylcholine receptor turnover at the normal end-plate and in autoimmune myasthenia gravis. J Neuropathol Exp Neurol 41: 567-579.

Gallagher MJ, Ding L, Maheshwari A, Macdonald RL (2007) The $GABA_A$ receptor {alpha}1 subunit epilepsy mutation A322D inhibits transmembrane helix formation and causes proteasomal degradation. Proc Natl Acad Sci U S A 104: 12999-13004.

Gallagher MJ, Shen W, Song L, Macdonald RL (2005) Endoplasmic reticulum retention and associated degradation of a $GABA_A$ receptor epilepsy mutation that inserts an aspartate in the M3 transmembrane segment of the alpha1 subunit. J Biol Chem 280: 37995-38004.

Gallagher MJ, Song L, Arain F, Macdonald RL (2004) The juvenile myoclonic epilepsy GABA(A) receptor alpha1 subunit mutation A322D produces asymmetrical, subunit position-dependent reduction of heterozygous receptor currents and alpha1 subunit protein expression. J Neurosci 24: 5570-5578.

Gelman MS, Chang W, Thomas DY, Bergeron JJ, Prives JM (1995) Role of the endoplasmic reticulum chaperone calnexin in subunit folding and assembly of nicotinic acetylcholine receptors. J Biol Chem 270: 15085-15092.

Gorrie GH, Vallis Y, Stephenson A, Whitfield J, Browning B, Smart TG, Moss SJ (1997) Assembly of $GABA_A$ receptors composed of alpha1 and beta2 subunits in both cultured neurons and fibroblasts. J Neurosci 17: 6587-6596.

Green WN, Claudio T (1993) Acetylcholine receptor assembly: subunit folding and oligomerization occur sequentially. Cell 74: 57-69.

Green WN, Wanamaker CP (1997) The role of the cystine loop in acetylcholine receptor assembly. J Biol Chem 272: 20945-20953.

Greengard P (2001) The neurobiology of slow synaptic transmission. Science 294: 1024-1030.

Haas KF, Macdonald RL (1999) $GABA_A$ receptor subunit gamma2 and delta subtypes confer unique kinetic properties on recombinant $GABA_A$ receptor currents in mouse fibroblasts. J Physiol 514 (Pt 1): 27-45.

Hales TG, Deeb TZ, Tang H, Bollan KA, King DP, Johnson SJ, Connolly CN (2006) An asymmetric contribution to gamma-aminobutyric type A receptor function of a conserved lysine within TM2-3 of alpha1, beta2, and gamma2 subunits. J Biol Chem 281: 17034-17043.

Hales TG, Tang H, Bollan KA, Johnson SJ, King DP, McDonald NA, Cheng A, Connolly CN (2005) The epilepsy mutation, gamma2(R43Q) disrupts a highly conserved inter-subunit contact site, perturbing the biogenesis of $GABA_A$ receptors. Mol Cell Neurosci 29: 120-127.

Hammond C, Braakman I, Helenius A (1994) Role of N-linked oligosaccharide recognition, glucose trimming, and calnexin in glycoprotein folding and quality control. Proc Natl Acad Sci U S A 91: 913-917.

Harkin LA, Bowser DN, Dibbens LM, Singh R, Phillips F, Wallace RH, Richards MC, Williams DA, Mulley JC, Berkovic SF, Scheffer IE, Petrou S (2002) Truncation of the GABA(A)-receptor gamma2 subunit in a family with generalized epilepsy with febrile seizures plus. Am J Hum Genet 70: 530-536.

Helenius A (1994) How N-linked oligosaccharides affect glycoprotein folding in the endoplasmic reticulum. Mol Biol Cell 5: 253-265.

Helenius A, Aebi M (2004) Roles of N-linked glycans in the endoplasmic reticulum. Annu Rev Biochem 73: 1019-1049.

Hessa T, Kim H, Bihlmaier K, Lundin C, Boekel J, Andersson H, Nilsson I, White SH, von Heijne G (2005) Recognition of transmembrane helices by the endoplasmic reticulum translocon. Nature 433: 377-381.

Humeny A, Bonk T, Becker K, Jafari-Boroujerdi M, Stephani U, Reuter K, Becker CM (2002) A novel recessive hyperekplexia allele GLRA1 (S231R): genotyping by MALDI-TOF mass spectrometry and functional characterisation as a determinant of cellular glycine receptor trafficking. Eur J Hum Genet 10: 188-196.

Iversen LL (1984) The Ferrier Lecture, 1983. Amino acids and peptides: fast and slow chemical signals in the nervous system? Proc R Soc Lond B Biol Sci 221: 245-260.

Jacob TC, Bogdanov YD, Magnus C, Saliba RS, Kittler JT, Haydon PG, Moss SJ (2005) Gephyrin regulates the cell surface dynamics of synaptic $GABA_A$ receptors. J Neurosci 25: 10469-10478.

Jansen M, Bali M, Akabas MH (2008) Modular design of Cys-loop ligand-gated ion channels: functional 5-HT3 and GABA rho1 receptors lacking the large cytoplasmic M3M4 loop. J Gen Physiol 131: 137-146.

Jin P, Walther D, Zhang J, Rowe-Teeter C, Fu GK (2004) Serine 171, a conserved residue in the gamma-aminobutyric acid type A ($GABA_A$) receptor gamma2 subunit, mediates subunit interaction and cell surface localization. J Biol Chem 279: 14179-14183.

Kalamida D, Poulas K, Avramopoulou V, Fostieri E, Lagoumintzis G, Lazaridis K, Sideri A, Zouridakis M, Tzartos SJ (2007) Muscle and neuronal nicotinic acetylcholine receptors. Structure, function and pathogenicity. FEBS J 274: 3799-3845.

Kanematsu T, Yasunaga A, Mizoguchi Y, Kuratani A, Kittler JT, Jovanovic JN, Takenaka K, Nakayama KI, Fukami K, Takenawa T, Moss SJ, Nabekura J, Hirata M (2006) Modulation of GABA(A) receptor phosphorylation and membrane trafficking by phospholipase C-related inactive protein/protein phosphatase 1 and 2A signaling complex underlying brain-derived neurotrophic factor-dependent regulation of GABAergic inhibition. J Biol Chem 281: 22180-22189.

Kang JQ, Macdonald RL (2004) The $GABA_A$ receptor gamma2 subunit R43Q mutation linked to childhood absence epilepsy and febrile seizures causes retention of alpha1beta2gamma2S receptors in the endoplasmic reticulum. J Neurosci 24: 8672-8677.

Kang JQ, Shen W, Macdonald RL (2006) Why does fever trigger febrile seizures? $GABA_A$ receptor gamma2 subunit mutations associated with idiopathic generalized epilepsies have temperature-dependent trafficking deficiencies. J Neurosci 26: 2590-2597.

Keller CA, Yuan X, Panzanelli P, Martin ML, Alldred M, Sassoe-Pognetto M, Luscher B (2004) The gamma2 subunit of GABA(A) receptors is a substrate for palmitoylation by GODZ. J Neurosci 24: 5881-5891.

Keller SH, Lindstrom J, Ellisman M, Taylor P (2001) Adjacent basic amino acid residues recognized by the COP I complex and ubiquitination govern endoplasmic reticulum to cell surface trafficking of the nicotinic acetylcholine receptor alpha-Subunit. J Biol Chem 276: 18384-18391.

Keller SH, Taylor P (1999) Determinants responsible for assembly of the nicotinic acetylcholine receptor. J Gen Physiol 113: 171-176.

Kirsch J (2006) Glycinergic transmission. Cell Tissue Res 326: 535-540.

Kittler JT, Chen G, Honing S, Bogdanov Y, McAinsh K, Arancibia-Carcamo IL, Jovanovic JN, Pangalos MN, Haucke V, Yan Z, Moss SJ (2005) Phospho-dependent binding of the clathrin AP2 adaptor complex to $GABA_A$ receptors

regulates the efficacy of inhibitory synaptic transmission. Proc Natl Acad Sci U S A 102: 14871-14876.

Kittler JT, Delmas P, Jovanovic JN, Brown DA, Smart TG, Moss SJ (2000a) Constitutive endocytosis of $GABA_A$ receptors by an association with the adaptin AP2 complex modulates inhibitory synaptic currents in hippocampal neurons. J Neurosci 20: 7972-7977.

Kittler JT, Moss SJ (2003) Modulation of $GABA_A$ receptor activity by phosphorylation and receptor trafficking: implications for the efficacy of synaptic inhibition. Curr Opin Neurobiol 13: 341-347.

Kittler JT, Wang J, Connolly CN, Vicini S, Smart TG, Moss SJ (2000b) Analysis of $GABA_A$ receptor assembly in mammalian cell lines and hippocampal neurons using gamma 2 subunit green fluorescent protein chimeras. Mol Cell Neurosci 16: 440-452.

Klausberger T, Ehya N, Fuchs K, Fuchs T, Ebert V, Sarto I, Sieghart W (2001a) Detection and binding properties of GABA(A) receptor assembly intermediates. J Biol Chem 276: 16024-16032.

Klausberger T, Sarto I, Ehya N, Fuchs K, Furtmuller R, Mayer B, Huck S, Sieghart W (2001b) Alternate use of distinct intersubunit contacts controls $GABA_A$ receptor assembly and stoichiometry. J Neurosci 21: 9124-9133.

Kneussel M, Brandstatter JH, Laube B, Stahl S, Muller U, Betz H (1999) Loss of postsynaptic GABA(A) receptor clustering in gephyrin-deficient mice. J Neurosci 19: 9289-9297.

Kornfeld R, Kornfeld S (1985) Assembly of asparagine-linked oligosaccharides. Annu Rev Biochem 54: 631-664.

Kowarik M, Young NM, Numao S, Schulz BL, Hug I, Callewaert N, Mills DC, Watson DC, Hernandez M, Kelly JF, Wacker M, Aebi M (2006) Definition of the bacterial N-glycosylation site consensus sequence. EMBO J 25: 1957-1966.

Krzywkowski K, Jensen AA, Connolly CN, Brauner-Osborne H (2007) Naturally occurring variations in the human 5-HT3A gene profoundly impact 5-HT3 receptor function and expression. Pharmacogenet Genomics 17: 255-266.

Kuhse J, Laube B, Magalei D, Betz H (1993) Assembly of the inhibitory glycine receptor: identification of amino acid sequence motifs governing subunit stoichiometry. Neuron 11: 1049-1056.

Le Novere N, Changeux JP (1999) The Ligand Gated Ion Channel Database. Nucleic Acids Res 27: 340-342.

Leite JF, Amoscato AA, Cascio M (2000) Coupled proteolytic and mass spectrometry studies indicate a novel topology for the glycine receptor. J Biol Chem 275: 13683-13689.

Liu Y, Choudhury P, Cabral CM, Sifers RN (1999) Oligosaccharide modification in the early secretory pathway directs the selection of a misfolded glycoprotein for degradation by the proteasome. J Biol Chem 274: 5861-5867.

Lo WY, Botzolakis EJ, Tang X, Macdonald RL (2008) A conserved Cys-loop receptor aspartate residue in the M3-M4 cytoplasmic loop is required for $GABA_A$ receptor assembly. J Biol Chem 283: 29740-29752.

Lu T, Rubio ME, Trussell LO (2008) Glycinergic transmission shaped by the corelease of GABA in a mammalian auditory synapse. Neuron 57: 524-535.

Lynch JW (2004) Molecular structure and function of the glycine receptor chloride channel. Physiol Rev 84: 1051-1095.

Macdonald RL, Gallagher MJ, Feng HJ, Kang J (2004) GABA(A) receptor epilepsy mutations. Biochem Pharmacol 68: 1497-1506.

Macdonald RL, Kang JQ, Gallagher MJ, Feng HJ (2006) GABA(A) receptor mutations associated with generalized epilepsies. Adv Pharmacol 54: 147-169.

Macdonald RL, Olsen RW (1994) $GABA_A$ receptor channels. Annu Rev Neurosci 17: 569-602.

Malizia AL, Cunningham VJ, Bell CJ, Liddle PF, Jones T, Nutt DJ (1998) Decreased brain GABA(A)-benzodiazepine receptor binding in panic disorder: preliminary results from a quantitative PET study. Arch Gen Psychiatry 55: 715-720.

Malosio ML, Marqueze-Pouey B, Kuhse J, Betz H (1991) Widespread expression of glycine receptor subunit mRNAs in the adult and developing rat brain. EMBO J 10: 2401-2409.

Maus AD, Pereira EF, Karachunski PI, Horton RM, Navaneetham D, Macklin K, Cortes WS, Albuquerque EX, Conti-Fine BM (1998) Human and rodent bronchial epithelial cells express functional nicotinic acetylcholine receptors. Mol Pharmacol 54: 779-788.

McKernan RM, Whiting PJ (1996) Which $GABA_A$-receptor subtypes really occur in the brain? Trends Neurosci 19: 139-143.

Meusser B, Hirsch C, Jarosch E, Sommer T (2005) ERAD: the long road to destruction. Nat Cell Biol 7: 766-772.

Michelsen K, Yuan H, Schwappach B (2005) Hide and run. Arginine-based endoplasmic-reticulum-sorting motifs in the assembly of heteromultimeric membrane proteins. EMBO Rep 6: 717-722.

Millar NS (2003) Assembly and subunit diversity of nicotinic acetylcholine receptors. Biochem Soc Trans 31: 869-874.

Millar NS, Harkness PC (2008) Assembly and trafficking of nicotinic acetylcholine receptors (Review). Mol Membr Biol 25: 279-292.

Milone M, Wang HL, Ohno K, Prince R, Fukudome T, Shen XM, Brengman JM, Griggs RC, Sine SM, Engel AG (1998) Mode switching kinetics produced by a naturally occurring mutation in the cytoplasmic loop of the human acetylcholine receptor epsilon subunit. Neuron 20: 575-588.

Miquel MC, Emerit MB, Nosjean A, Simon A, Rumajogee P, Brisorgueil MJ, Doucet E, Hamon M, Verge D (2002) Differential subcellular localization of the 5-HT3-As receptor subunit in the rat central nervous system. Eur J Neurosci 15: 449-457.

Mishina M, Takai T, Imoto K, Noda M, Takahashi T, Numa S, Methfessel C, Sakmann B (1986) Molecular distinction between fetal and adult forms of muscle acetylcholine receptor. Nature 321: 406-411.

Mohler H (2007) Molecular regulation of cognitive functions and developmental plasticity: impact of $GABA_A$ receptors. J Neurochem 102: 1-12.

Niesler B, Flohr T, Nothen MM, Fischer C, Rietschel M, Franzek E, Albus M, Propping P, Rappold GA (2001a) Association between the 5' UTR variant C178T of the serotonin receptor gene HTR3A and bipolar affective disorder. Pharmacogenetics 11: 471-475.

Niesler B, Kapeller J, Hammer C, Rappold G (2008) Serotonin type 3 receptor genes: HTR3A, B, C, D, E. Pharmacogenomics 9: 501-504.

Niesler B, Weiss B, Fischer C, Nothen MM, Propping P, Bondy B, Rietschel M, Maier W, Albus M, Franzek E, Rappold GA (2001b) Serotonin receptor gene HTR3A variants in schizophrenic and bipolar affective patients. Pharmacogenetics 11: 21-27.

Ning K, Li L, Liao M, Liu B, Mielke JG, Chen Y, Duan Y, El Hayek YH, Wan Q (2004) Circadian regulation of $GABA_A$ receptor function by CKI epsilon-CKI delta in the rat suprachiasmatic nuclei. Nat Neurosci 7: 489-490.

Noda M, Takahashi H, Tanabe T, Toyosato M, Furutani Y, Hirose T, Asai M, Inayama S, Miyata T, Numa S (1982) Primary structure of alpha-subunit precursor of Torpedo californica acetylcholine receptor deduced from cDNA sequence. Nature 299: 793-797.

Nymann-Andersen J, Wang H, Chen L, Kittler JT, Moss SJ, Olsen RW (2002) Subunit specificity and interaction domain between GABA(A) receptor-associated protein (GABARAP) and GABA(A) receptors. J Neurochem 80: 815-823.

Ohno K, Quiram PA, Milone M, Wang HL, Harper MC, Pruitt JN, Brengman JM, Pao L, Fischbeck KH, Crawford TO, Sine SM, Engel AG (1997) Congenital myasthenic syndromes due to heteroallelic nonsense/missense mutations in the acetylcholine receptor epsilon subunit gene: identification and functional characterization of six new mutations. Hum Mol Genet 6: 753-766.

Ohno K, Wang HL, Milone M, Bren N, Brengman JM, Nakano S, Quiram P, Pruitt JN, Sine SM, Engel AG (1996) Congenital myasthenic syndrome caused by decreased agonist binding affinity due to a mutation in the acetylcholine receptor epsilon subunit. Neuron 17: 157-170.

Ortells MO, Lunt GG (1995) Evolutionary history of the ligand-gated ion-channel superfamily of receptors. Trends Neurosci 18: 121-127.

Ou WJ, Bergeron JJ, Li Y, Kang CY, Thomas DY (1995) Conformational changes induced in the endoplasmic reticulum luminal domain of calnexin by Mg-ATP and Ca2+. J Biol Chem 270: 18051-18059.

Parodi AJ (2000) Protein glucosylation and its role in protein folding. Annu Rev Biochem 69: 69-93.

Paterson D, Nordberg A (2000) Neuronal nicotinic receptors in the human brain. Prog Neurobiol 61: 75-111.

Paulson HL, Ross AF, Green WN, Claudio T (1991) Analysis of early events in acetylcholine receptor assembly. J Cell Biol 113: 1371-1384.

Popot JL, Engelman DM (2000) Helical membrane protein folding, stability, and evolution. Annu Rev Biochem 69: 881-922.

Pratt MB, Husain SS, Miller KW, Cohen JB (2000) Identification of sites of incorporation in the nicotinic acetylcholine receptor of a photoactivatible general anesthetic. J Biol Chem 275: 29441-29451.

Quiram PA, Ohno K, Milone M, Patterson MC, Pruitt NJ, Brengman JM, Sine SM, Engel AG (1999) Mutation causing congenital myasthenia reveals acetylcholine receptor beta/delta subunit interaction essential for assembly. J Clin Invest 104: 1403-1410.

Rabow LE, Russek SJ, Farb DH (1995) From ion currents to genomic analysis: recent advances in $GABA_A$ receptor research. Synapse 21: 189-274.

Rea R, Tijssen MA, Herd C, Frants RR, Kullmann DM (2002) Functional characterization of compound heterozygosity for GlyRalpha1 mutations in the startle disease hyperekplexia. Eur J Neurosci 16: 186-196.

Reeves DC, Lummis SC (2002) The molecular basis of the structure and function of the 5-HT3 receptor: a model ligand-gated ion channel (review). Mol Membr Biol 19: 11-26.

Roccamo AM, Barrantes FJ (2007) Charged amino acid motifs flanking each extreme of the alphaM4 transmembrane domain are involved in assembly and cell-surface targeting of the muscle nicotinic acetylcholine receptor. J Neurosci Res 85: 285-293.

Ruddock LW, Molinari M (2006) N-glycan processing in ER quality control. J Cell Sci 119: 4373-4380.

Saliba RS, Pangalos M, Moss SJ (2008) The ubiquitin-like protein Plic-1 enhances the membrane insertion of $GABA_A$ receptors by increasing their stability within the endoplasmic reticulum. J Biol Chem 283: 18538-18544.

Sancar F, Czajkowski C (2004) A $GABA_A$ receptor mutation linked to human epilepsy (gamma2R43Q) impairs cell surface expression of alphabetagamma receptors. J Biol Chem 279: 47034-47039.

Schrag JD, Bergeron JJ, Li Y, Borisova S, Hahn M, Thomas DY, Cygler M (2001) The Structure of calnexin, an ER chaperone involved in quality control of protein folding. Mol Cell 8: 633-644.

Shen XM, Ohno K, Sine SM, Engel AG (2005) Subunit-specific contribution to agonist binding and channel gating revealed by inherited mutation in muscle acetylcholine receptor M3-M4 linker. Brain 128: 345-355.

Sieghart W, Sperk G (2002) Subunit composition, distribution and function of GABA(A) receptor subtypes. Curr Top Med Chem 2: 795-816.

Skok MV, Kalashnik EN, Koval LN, Tsetlin VI, Utkin YN, Changeux JP, Grailhe R (2003) Functional nicotinic acetylcholine receptors are expressed in B lymphocyte-derived cell lines. Mol Pharmacol 64: 885-889.

Smith MM, Lindstrom J, Merlie JP (1987) Formation of the alpha-bungarotoxin binding site and assembly of the nicotinic acetylcholine receptor subunits occur in the endoplasmic reticulum. J Biol Chem 262: 4367-4376.

Somogyi P, Tamas G, Lujan R, Buhl EH (1998) Salient features of synaptic organisation in the cerebral cortex. Brain Res Brain Res Rev 26: 113-135.

Sperk G, Furtinger S, Schwarzer C, Pirker S (2004) GABA and its receptors in epilepsy. Adv Exp Med Biol 548: 92-103.

Stein V, Nicoll RA (2003) GABA generates excitement. Neuron 37: 375-378.

Su K, Stoller T, Rocco J, Zemsky J, Green R (1993) Pre-Golgi degradation of yeast prepro-alpha-factor expressed in a mammalian cell. Influence of cell type-specific oligosaccharide processing on intracellular fate. J Biol Chem 268: 14301-14309.

Taylor PM, Connolly CN, Kittler JT, Gorrie GH, Hosie A, Smart TG, Moss SJ (2000) Identification of residues within GABA(A) receptor alpha subunits that mediate specific assembly with receptor beta subunits. J Neurosci 20: 1297-1306.

Taylor PM, Thomas P, Gorrie GH, Connolly CN, Smart TG, Moss SJ (1999) Identification of amino acid residues within GABA(A) receptor beta subunits that mediate both homomeric and heteromeric receptor expression. J Neurosci 19: 6360-6371.

Thompson JD, Higgins DG, Gibson TJ (1994) CLUSTAL W: improving the sensitivity of progressive multiple sequence alignment through sequence weighting, position-specific gap penalties and weight matrix choice. Nucleic Acids Res 22: 4673-4680.

Tretter V, Jacob TC, Mukherjee J, Fritschy JM, Pangalos MN, Moss SJ (2008) The clustering of GABA(A) receptor subtypes at inhibitory synapses is facilitated via the direct binding of receptor alpha 2 subunits to gephyrin. J Neurosci 28: 1356-1365.

Unwin N (2005) Refined structure of the nicotinic acetylcholine receptor at 4A resolution. J Mol Biol 346: 967-989.

Wanamaker CP, Christianson JC, Green WN (2003) Regulation of nicotinic acetylcholine receptor assembly. Ann N Y Acad Sci 998: 66-80.

Wanamaker CP, Green WN (2005) N-linked glycosylation is required for nicotinic receptor assembly but not for subunit associations with calnexin. J Biol Chem 280: 33800-33810.

Wanamaker CP, Green WN (2007) ER chaperones stabilize nicotinic receptor subunits and regulate receptor assembly. J Biol Chem.

Wang H, Bedford FK, Brandon NJ, Moss SJ, Olsen RW (1999) GABA(A)-receptor-associated protein links GABA(A) receptors and the cytoskeleton. Nature 397: 69-72.

Wang H, Olsen RW (2000) Binding of the GABA(A) receptor-associated protein (GABARAP) to microtubules and microfilaments suggests involvement of the cytoskeleton in GABARAPGABA(A) receptor interaction. J Neurochem 75: 644-655.

Wang JM, Zhang L, Yao Y, Viroonchatapan N, Rothe E, Wang ZZ (2002) A transmembrane motif governs the surface trafficking of nicotinic acetylcholine receptors. Nat Neurosci 5: 963-970.

Watson P, Forster R, Palmer KJ, Pepperkok R, Stephens DJ (2005) Coupling of ER exit to microtubules through direct interaction of COPII with dynactin. Nat Cell Biol 7: 48-55.

White SH, von Heijne G (2005) Transmembrane helices before, during, and after insertion. Curr Opin Struct Biol 15: 378-386.

Wu J, Kohno T, Georgiev SK, Ikoma M, Ishii H, Petrenko AB, Baba H (2008) Taurine activates glycine and gamma-aminobutyric acid A receptors in rat substantia gelatinosa neurons. Neuroreport 19: 333-337.

Wu Y, Swulius MT, Moremen KW, Sifers RN (2003) Elucidation of the molecular logic by which misfolded alpha 1-antitrypsin is preferentially selected for degradation. Proc Natl Acad Sci U S A 100: 8229-8234.